

**FUNCTIONAL ANALYSIS OF RESIDUES OF PROFILIN 1  
THAT ARE MODULATED BY  
WNT SIGNALING**

---

A Thesis  
Submitted to  
the Temple University Graduate Board

---

In Partial Fulfillment  
of the Requirements for the Degree  
DOCTOR OF PHILOSOPHY

---

by  
Mark L. Berns  
Diploma Date (August 2023)

Examining Committee Members:

Dr. Raymond Habas, Advisory Committee Chair, Department of Biology, Temple University

Dr. Darius Balciunas, Examining Committee Chair, Department of Biology, Temple University

Dr. Shohreh Amini, Department of Biology, Temple University

Dr. Bojana Gligorijevic, External Member – Department of Bioengineering, College of Engineering, Temple University

## ABSTRACT

The non-canonical Wnt signaling pathway regulates the actin cytoskeleton controlling cell migration, cell polarity, and cell survival. The protein Profilin1 is a downstream effector of the non-canonical Wnt pathway and directly binds to actin to facilitate cytoskeleton rearrangement. Profilin1 binds to monomeric actin and brings it to the FH1 (Formin Homology 1) domain of Daam1. The neighboring FH2 (Formin Homology 2) domain nucleates actin and caps the growing end of the completed actin filament. It is currently unknown which amino acids on Profilin1 facilitate binding to Daam1 and actin in non-canonical Wnt signaling. In this study, I identified two residues on the *Xenopus* protein Profilin1- Tyrosine 131 and Serine 135- that play a role in non-canonical Wnt signaling. In this study, I was able to show that non-canonical Wnt signaling leads to the phosphorylation of Tyrosine 131. Mutating Tyrosine 131 to Alanine (Tyr131Ala) causes a cytokinesis defect preventing gastrulation in *Xenopus* embryos. Additionally, overexpression of PFN1-Tyr131Ala prevents Wnt5a-mediated actin fiber formation and increases multinucleation in HeLa cells. Mutating Serine 135 to Alanine (PFN1- Ser135Ala) lowers the binding affinity of Profilin1 to the FH1 domain of Daam1 but does not affect cytokinesis. The evidence presented in this study suggests that Tyr131 regulates gastrulation, while Ser135 plays a role in modulating binding of Profilin1 to Daam1. Further research into the molecular mechanism of regulation of Tyr131 and Ser135 in non-canonical Wnt signaling would be a major step in uncovering the mechanism of

actin polymerization and a better understanding of cell signaling during vertebrate gastrulation.

# TABLE OF CONTENTS

	Page
ABSTRACT.....	ii
LIST OF FIGURES .....	iv
LIST OF TABLES .....	ix
LIST OF ACRONYMS .....	x
CHAPTER	
1. INTRODUCTION.....	1
1.1 Wnt Signaling .....	1
1.2 Canonical Wnt Signaling .....	4
1.3 Non-canonical Wnt Signaling.....	6
1.4 Vertebrate gastrulation and convergent extension .....	9
1.5 Neural tube closure .....	14
1.6 Formins and the Rho GTPases.....	18
1.7 Actin cytoskeleton and cell migration .....	26
1.8 Previous studies on Profilin .....	31
2. MATERIALS AND METHODS .....	36
2.1 Tissue culture and transfection .....	36
2.2 Generation of Profilin 1 mutant plasmids .....	37
2.3 Co-IP .....	37
2.4 Preparation of recombinant GST-fusion proteins .....	39
2.5 Extraction of GST fusion proteins .....	40

2.6 GST pulldown assay .....	40
2.7 Immunocytochemistry .....	40
2.8 mRNA overexpression in Xenopus embryos .....	41
2.9 Xenopus embryos.....	41
2.10 Src Assay.....	42
3. RESULTS.....	43
3.1 Generation of mutant PFN1 plasmids.....	43
3.2 The roles of Tyr131 and Ser131 in early embryonic development.....	45
3.3 Visualizing effects of PFN1 mutants on the actin cytoskeleton in HeLa cells .....	50
3.4 Ser135 has a role in binding of PFN1 to the FH1 domain of Daam1 .....	62
3.5 Wnt5a-mediated phosphorylation of Tyr129 is Src independent.....	74
4. DISCUSSION .....	78
BIBLIOGRAPHY.....	85

## LIST OF FIGURES

Figure	Page
1. Overview Of Canonical Wnt Signaling Pathway .....	5
2. PCP Core Proteins In Drosophila Are Asymmetrically Localized.....	7
3. Schematic Of Non-Canonical Wnt Signaling Pathway .....	9
4. Gastrulation In Xenopus Embryos.....	11
5. Morphogenetic Cell Movements During Gastrulation .....	13
6. Morphogenetic Cell Movements During Neurulation .....	14
7. Apical Constriction Occurs During Different Cellular Processes .....	16
8. Xenopus Laevis Life Cycle.....	18
9. Schematic Of Activation Of Formins .....	20
10. Mechanism Of Cycling Rho GTPases .....	21
11. Organization Of Domains Of Formins.....	23
12. Model of Diaphanous Related Formins Depicting Their Cellular Function And Localization .....	24
13. Different Types Of Filamentous Systems .....	26
14. Regulation Of Actin Treadmilling .....	28
15. Linear And Branched Actin Polymerization Require Different Actin Binding Proteins .....	29
16. Types Of Actin Structures In Cells .....	30
17. Amino Acid Alignment Of Human And Xenopus PFN1 .....	35
18. PFN1 Mutants Were Successfully Generated By QuikChange Mutagenesis .....	44
19. GFP-PFN1 And GFP Tagged PFN1 Mutants Express In Xenopus Embryos.....	45

20. Injected Xenopus Embryos Express Translated Mutant XPFN1 Proteins At The Correct Size .....	46
21. Dorsal Injection Of Tyr131Ala Causes Cytokinesis Defects .....	48
22. Quantification Of Phenotypes Of Dorsal mRNA Injections .....	49
23. Ventral Injection Of XPFN1 Mutants Produces No Effects .....	50
24. Wnt5a Increases Actin Fiber Formation And The Ratio Of Length/Width In HeLa Cells .....	54
25. Wnt5a Increases Actin Fiber Formation And The Ratio Of Length/Width In Cells Transfected With GFP XPFN1 .....	55
26. GFP-Ser135Ala Does Not Prevent Wnt5a-Mediated Actin Fiber Formation Nor The Increase In Cell Length/Width Ratio .....	56
27. Wnt5a Increases The Ratio Of Length/Width And Actin Fiber Formation In Cells Transfected With GFP-Ser135Glu.....	57
28. GFP-Tyr131Ala Prevents Wnt5a-Mediated Increases In Cell Length/Width Ratio And Actin Fiber Generation .....	58
29. GFP-Tyr131Ala;Ser135Ala Prevents Wnt5a-Mediated Increases In Cell Length/Width Ratio And Actin Fiber Generation .....	59
30. Visual Representation Of Multinucleation.....	60
31. GFP-Tyr131Ala Increases Multinucleation In Hela Cells, Compared To GFP- PFN1 .....	61
32. PFN1 And Daam1 Constructs Used In Binding Assays .....	63
33. Ser135Ala Lowers Binding Affinity Of PFN1 To FH1 .....	64
34. Quantification Of GST Pulldown Assays .....	66
35. Tyr131 And Ser135 Have No Effect On Binding Of PFN1 To Daam1 .....	67
36. Quantification Of Binding Of Mutant Pfn1 To Daam1 .....	68
37. Tyr131 And Ser135 Have No Effect On Binding Of PFN1 To Cdaam1 Gastrulation In Xenopus Embryos.....	69
38. Quantification Of Binding Of Mutant PFN1 To Cdaam1 .....	71
39. Ser135 Affects Binding Of PFN1 To FH1 Gastrulation In Xenopus Embryos .....	72

40. Ser135 Modulates Binding Of PFN1 To FH1.....	73
41. Wnt5a Induces Phosphorylation Of Tyr129 On HPFN1 And This Is Src Independent.....	77
42. Tyr131 Is Necessary For Proper Function Of PFN1 And Ser135 May Be One Of Several Residues That Regulate Binding To Daam1 .....	84

## LIST OF TABLES

Table	Page
1. Overview Of Canonical Wnt Signaling Pathway .....	37
2. PCP Core Proteins In Drosophila Are Asymmetrically Localized.....	75

## LIST OF ACRONYMS

ACK1	Activated cdc42 kinase
ALS	Amyotrophic lateral Sclerosis
Ala	Alanine
APC	Adenomatosis polyposis coli
BME	2-mercaptoethanol
BMP	Bone morphogenic protein
CamKII	Ca <sup>2+</sup> /calmodulin-dependent protein kinase II
CDC42	Cell division cycle 42
CK1 $\alpha$	Casein kinase 1 $\alpha$
Co-IP	co-immunoprecipitation
DAAM	Dvl-associated activator of morphogenesis
DID	Diaphanous inhibitor domain
Dia	Diaphanous
DIX	N-terminal Dishevelled and Axin domain
DRF	Diaphanous-related Formins
Dvl	Dishevelled
Eph	Ephrin kinase
EMA	epithelial-mesenchymal transition
ENA/VASP	Enabled/vasodilator-stimulated phosphoproteins
EV	Empty Vector
FH1	Formin homology 1 domain

FH2	Formin homology 2 domain
FHOD	formin homology domain-containing protein
FMNL	Formin-like proteins
Fz	Frizzled
G-Actin	Globular actin
GAP	GTPase activating protein
GBD	Rho GTPase binding domain
Glu	Glutamic acid
GPCR	G-protein coupled receptors
GPS 5.0	Group-based prediction system version 5.0
GSK3 $\beta$	Glycogen synthase kinase $\beta$
INSR	Insulin receptor tyrosine kinase
IP3	Inositol trisphosphate
JNK	c-Jun N terminal kinase
LEF1	Lymphoid enhancer-binding factor 1
LRP5/6	Low-density lipoprotein-related protein 5/6
NLK	Nemo-like kinase
N-WASP	Neural Wiskott-Aldrich Protein
NFAT	Nuclear factor of activated T-cells
PDZ	central postsynaptic density protein/Drosophila disc large tumor suppressor/zonula occludens-1 protein domain
PDE	Phosphodiesterase
PFN1	Profilin1

PFN2	Profilin 2
PFN3	Profilin 3
PFN4	Profilin 4
PK	Prickle
PK $\gamma$	Protein kinase gamma
PIP	polyphosphatidylinositol
PLC	Phospholipase C
PLP	Poly-L proline
PTK7	protein tyrosine kinase 7
ROR2	neurotrophic tyrosine kinase
ROCK	Rho-associated kinase
Ryk	Receptor tyrosine kinase
Ser	Serine
SH3	Src homology domain 3
TAK1	TGF $\beta$ -activated kinase
TCF	T-cell factor
TGF $\beta$	Tumor growth factor beta
Tyr	Tyrosine
Vangl	VanGogh-like
WH2	WASP-homology domain
WNT	Wingless/Integrated
WT	Wildtype
XPFN1	<i>Xenopus</i> Profilin1

# CHAPTER 1

## INTRODUCTION

### 1.1 Wnt signaling

Cell proliferation, polarity, motility, and lineage fate are regulated by a complex combination of growth factor signal transduction pathways during vertebrate embryonic development. Early studies in model systems identified and characterized various signaling pathways that are involved in early development<sup>1</sup>. These pathways are regulated by secreted ligands and are classified into five main classes: Wnt, fibroblast growth factor (FGF), Notch, Hedgehog, and tumor growth factor/ bone morphogenic protein (TGF $\beta$ /BMPs). Wnt signaling is an evolutionarily conserved pathway and one of the central signaling pathways required during early embryonic development. Defects associated with dysregulation of Wnt signaling include defects in cell fate determination, cell division, blastopore closure defects, neural tube closure defects, gastrulation defects, and malformed heads<sup>2</sup>.

Wnt signaling can be separated into a canonical or Wnt/ $\beta$ -catenin–dependent pathway and a non-canonical or  $\beta$ -catenin independent pathway. The canonical pathway regulates transcription of key developmental genes by regulating the amount of nuclear  $\beta$ -catenin.  $\beta$ -catenin functions as a transcriptional co-activator. The non-canonical pathway is crucial for the regulation of cell motility and polarity<sup>3,4</sup>.

Wnt proteins are glycoproteins, approximately 400 amino acids in length, and contain an N-terminal signal peptide for secretion<sup>5</sup>. The term *Wnt* is a fusion of the name of the *Drosophila* segment polarity gene *wingless* and the name of the vertebrate homologue, *integrated* or *int-1*<sup>6</sup>. Humans contain 19 different Wnt ligands that lead to activation of canonical Wnt signaling or non-canonical Wnt signaling<sup>7,8</sup>. Most Wnt ligands lead to activation of either canonical or non-canonical Wnt signaling. For example, Wnt1 exclusively activates canonical Wnt signaling, while Wnt5a activates non-canonical Wnt signaling<sup>9</sup>. Wnt3a, however, is an exception and can activate both Wnt pathways<sup>10</sup>.

Genetic analysis of the *Drosophila Wnt-1* gene comprises much of the early research into the role of Wnt signaling during development. Years of genetic study in *Drosophila* and biochemistry in *Xenopus* have contributed to our understanding of the molecular components and molecular mechanisms of the identified Wnt signaling components<sup>11,12</sup>. In *Drosophila*,  $\beta$ -catenin, known as *Armadillo*, was shown to be a transcriptional co-activator of canonical Wnt signaling<sup>13</sup>. Components of the Wnt pathway, including  $\beta$ -catenin, are localized to the Spemann-Mangold organizer on the dorsal side of the embryo<sup>13</sup>. Transplanting a piece of the organizer from the upper lip of the blastopore on the dorsal side to the ventral side of the embryos yielded a secondary axis. Axis duplication assays were used to characterize the roles of different components of the Wnt pathway in *Xenopus laevis*<sup>14</sup>.

Injection of Wnt1, Dishevelled (Dvl),  $\beta$ -catenin, dominant negative glycogen synthase kinase  $\beta$  (GSK3 $\beta$ ), or lymphoid enhancer-binding factor 1 (LEF1) mRNA into the ventral side of the developing embryo induced double axis formation<sup>15</sup>. The Wnt signaling pathway in the cytoplasm of cells has been elucidated through rigorous genetic and biochemical studies. A Wnt ligand binds to the Frizzled (Fz) receptor and (Low-density-lipoprotein-related protein 5/6) LRP5/6, and a signal is transduced to the cytoplasmic phosphoprotein Dvl. The Fz receptor is a seven-pass transmembrane protein and shares structural homology with G-Protein Coupled Receptors (GPCR). All three members of the Dvl family<sup>9</sup> have three conserved domains: the N-terminal Dishevelled and Axin (DIX) domain, a central postsynaptic density protein/Drosophila disc large tumor suppressor/zonula occludens-1 protein (PDZ) domain, and a carboxyl-terminal Dishevelled/ Egl-10/Pleckstrin (DEP) domain<sup>16,17</sup>.

Dvl, the cytoplasmic protein most immediately downstream of the transmembrane receptor/co-receptor complex, is important in both branches of Wnt signaling. The Wnt signaling pathway branches out to either the canonical or non-canonical pathway depending on where a protein binds to either the DIX or DEP domain on Dvl<sup>18</sup>. While most binding partners of Dvl bind to the PDZ domain, proteins that bind to the DIX domain leads to activation of canonical Wnt signaling while proteins that bind to the DEP domain leads to activation of non-canonical Wnt signaling<sup>18</sup>.

## 1.2 Canonical Wnt Signaling

Cytoplasmic accumulation and subsequent translocation of  $\beta$ -catenin into the nucleus is the identifying characteristic of canonical Wnt signaling. The canonical Wnt pathway was first identified from genetic screens in *Drosophila*. The fundamental molecular framework was then laid out through extensive studies in *Danio rerio*, *Xenopus*, *Drosophila*, and *C. elegans*<sup>19</sup>. Co-receptors and interactions between Wnt ligands and Fz receptors are necessary for transducing Wnt signaling. Low-density-lipoprotein-related protein 5/6 (LRP5/6) acts as a co-receptor in canonical Wnt signaling (Figure 1)<sup>7,20,21</sup>. The Wnt signal is transduced downstream to Dvl after a Wnt ligand binds to a receptor complex comprising of Fz and LRP5/6.  $\beta$ -catenin is primarily localized to E-Cadherins on the plasma membrane at adherens junctions, where it mediates cell-to-cell adhesion.  $\beta$ -catenin also exists in small concentrations in the cytoplasm through the rearrangement of adherens junctions. This causes  $\beta$ -catenin to diffuse into the cytoplasm, where its levels are regulated and kept low by a destruction complex [consisting of Axin, adenomatosis polyposis coli (APC), casein kinase 1 $\alpha$  (CK1 $\alpha$ ), and glycogen synthase kinase  $\beta$  (GSK3 $\beta$ )]. Wnt signaling inactivates the destruction complex leading to cytoplasmic accumulation of  $\beta$ -catenin and subsequent translocation into the nucleus. In the nucleus,  $\beta$ -catenin binds to TCF/LEF and displaces the repressor, Groucho leading to transcription of Wnt genes<sup>22-24</sup>.

Without an active Wnt signal, CK1 $\alpha$  and GSK3 $\beta$  regulate cytoplasmic  $\beta$ -catenin levels by phosphorylating  $\beta$ -catenin, targeting it for ubiquitination and subsequent

degradation by the proteasome<sup>7,25</sup>. In the presence of Wnt signaling, the cytosolic APC/Axin/GSK3 complex localizes to the plasma membrane, preventing the degradation of cytosolic  $\beta$ -catenin<sup>25</sup>. When Wnt binds to Fz, LRP5/6 co-receptors induce the binding of Dvl to Fz, leading to phosphorylation of LRP5/6 by CK1 $\alpha$  and GSK3 $\beta$  and the recruitment of Axin<sup>26,27</sup>. These events lead to the degradation of  $\beta$ -catenin, allowing for cytoplasmic accumulation and translocation of  $\beta$ -catenin into the nucleus. Custos, a protein localized to the nuclear membrane, adds an additional layer of regulatory control in canonical Wnt signaling by controlling the nuclear import of  $\beta$ -catenin<sup>28</sup>. Custos blocks secondary axis induction by inhibiting the formation of the Spemann-Mangold organizer on the dorsal side of the embryo. The canonical Wnt pathway is responsible for cell proliferation and primary axis formation during development<sup>29,30</sup>.

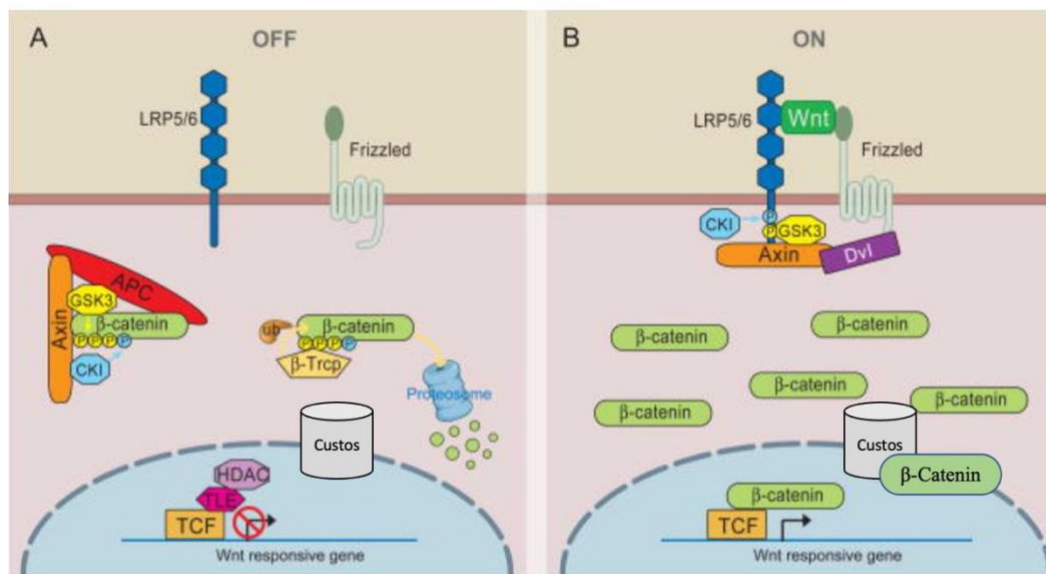


Figure 1. **Overview of the Canonical Wnt Signaling Pathway.** (A). In the absence of a Wnt ligand,  $\beta$ -catenin binds to Axin, GSK3, and CK1 forming a destruction complex.  $\beta$ -catenin is phosphorylated by CK1 and subsequently, GSK3. Phosphorylated  $\beta$ -catenin is targeted for proteasomal degradation. (B). In the presence of a Wnt ligand, Fz and LRP5/6 form a complex with Dvl. LRP5/6 is phosphorylated and recruits Axin away from the destruction complex. This results in disruption of the destruction complex and accumulation of  $\beta$ -catenin and nuclear translocation via Custos.  $\beta$ -catenin interacts with TCF and mediates Wnt target genes (adopted from MacDonald 2009).

### 1.3 Non-canonical Wnt signaling

The non-canonical Wnt pathway regulates ventral cell fate and mediates tissue separation and cell movements during gastrulation. In Wnt/Ca<sup>2+</sup> signaling, a branch of non-canonical Wnt signaling, Fz mediates the activation of Dvl by G-proteins. Dvl activates phosphodiesterase (PDE), inhibiting PK $\gamma$  (Protein Kinase gamma), in turn inhibiting the release of Ca<sup>2</sup>. Dvl activates (Inositol trisphosphate) IP3 through (Phospholipase C) PLC, leading to the release of intracellular Ca<sup>2</sup>, thereby activating (Ca<sup>2+</sup>/calmodulin-dependent protein kinase II) CamKII and calcineurin<sup>31</sup>. Calcineurin activates NFAT (nuclear factor of activated T-cells) to regulate ventral cell fates. Through PLC and PKC, DAG (diacylglycerol) activates cell division cycle 42 (CDC42) to mediate tissue separation and cell movements during gastrulation. CamKII activates (TGF $\beta$ -activated kinase) TAK1 and (Nemo-like kinase) NLK to antagonize  $\beta$ -catenin/TCF signaling<sup>19,32</sup>.

The PCP pathway is the most studied non-canonical Wnt pathway and regulates cell motility required for organogenesis. It coordinates the polarization of cells within a single tissue or epithelial plane that is perpendicular to the apical-basal axis<sup>2,33</sup>. This branch of Wnt signaling regulates the actin cytoskeleton via the organization of polarized structures such as those found in epithelial cells <sup>34</sup>. In *Xenopus* and *Danio*, the PCP

pathway regulates cell polarity and movement of mesodermal cells during convergent extension and neural tube closure during gastrulation<sup>4,35</sup>.

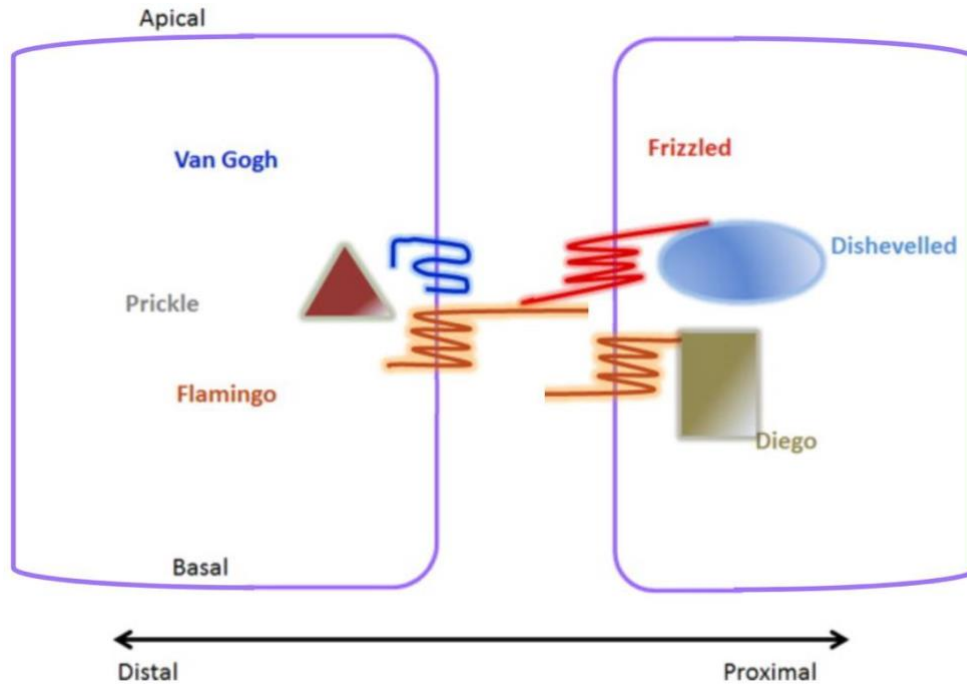


Figure 2. **PCP core proteins in drosophila are asymmetrically localized.** Frizzled, Dishevelled, and Diego localize to the proximal side of the cell. Van Gogh and Prickle localize to the distal side. Flamingo localizes to both ends of the cell<sup>31</sup>

The PCP pathway was first identified from genetic studies in *Drosophila*, similar to the canonical pathway<sup>34</sup>. Within vertebrate development, planar polarity functions at three distinct levels. First, at the organismal and tissue level, a gradient of morphogens coordinates morphogenetic movements, orients cell divisions, and organogenesis, and establishes embryonic axes. Second, at the cellular level, the core components of the PCP pathway mediate cell-to-cell communication by directing polarity in a single direction<sup>36</sup>.

Some core components of non-canonical Wnt signaling include Fz, Van Gogh-like (Vangl), Flamingo/Celsr, Dvl, Prickle (Pk), and an ankyrin-domain containing a

protein known as Diego or Diversin<sup>37</sup> (Figure 2). Lastly, at the subcellular level, components of the non-canonical Wnt signaling pathway are first uniformly recruited to the apical cell membrane and then asymmetrically distributed in polarized epithelia both between and within cells<sup>36</sup>. For example, in *Drosophila*, Fz, Dvl, and Diego (Diversin homolog) are localized at the proximal side; Van Gogh-like (Vangl) and Prickle (Pk) are localized to the distal side of the cell; and Flamingo (Celsr homolog) is localized at both the proximal and distal sides of the cell<sup>38</sup>.

In non-canonical Wnt signaling, the role of LRP5/6 as a co-receptor is unclear despite the Wnt signal being mediated through Fz in this pathway as well (Figure 3)<sup>7,39</sup>. Other potential co-receptors for non-canonical Wnt signaling have been identified, such as Ryk (Receptor Tyrosine Kinase)<sup>40</sup>, ROR2<sup>41,42</sup> (neurotrophic tyrosine kinase), and PTK7<sup>43</sup> (protein tyrosine kinase 7). Ryk is a Wnt co-receptor that is activated for neurite growth<sup>40</sup>. ROR2 is a tyrosine receptor kinase that, when activated through Wnt signaling, mediates filopodia formation for Wnt5a-mediated cell migration<sup>41</sup>. The PDZ and DEP domains of Dvl are necessary to activate two independent pathways, activating the small GTPases Rho and Rac<sup>18</sup>. The activation of Rho GTPase occurs through the binding of Daam1 to the PDZ domain of Dvl<sup>44</sup>. Activated Rho GTPase activates Rho-associated kinase (ROCK) and Myosin, resulting in modifications and rearrangements to the actin cytoskeleton<sup>45,46</sup>. The DEP domain of Dvl is required to activate Rac GTPase, which in

turn activates JNK and plays an important role in regulating convergent extension movements during vertebrate gastrulation<sup>47</sup>.

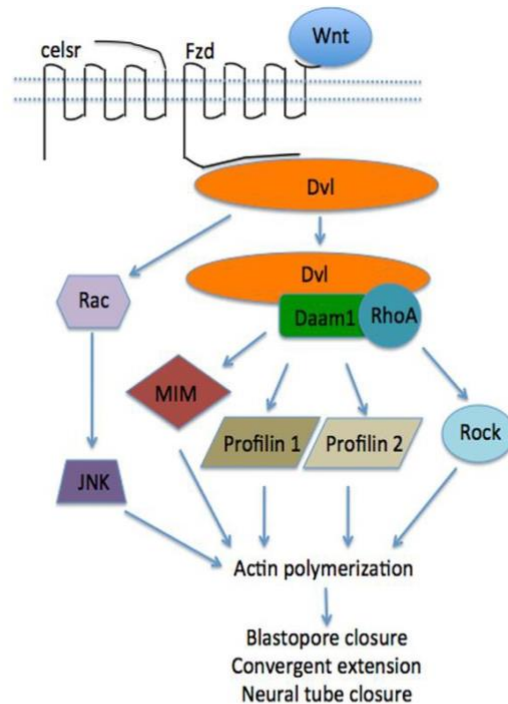


Figure 3. **Schematic of non-canonical Wnt signaling pathway.** When a Wnt ligand binds to Fzd, the signal is transduced downstream to Dvl. Dvl then accumulates at the cell membrane. Dvl activates Rho through interaction with Daam1 and activates Rac directly. The activation of Rho and Rac activates downstream targets that modulate the actin cytoskeleton by affecting actin polymerization.

#### 1.4 Vertebrate gastrulation and convergent extension

Before undergoing gastrulation, the embryo is known as a blastula. In *Xenopus* and mammalian development, a blastula is a ball of cells (blastomeres) containing a fluid-filled cavity, known as a blastocoel. In a blastula, the vegetal pole contains yolk cells and the animal pole contains rapidly dividing cells. The vegetal pole nourishes the rapidly dividing animal pole cells during development. At the beginning of gastrulation, mesodermal and endodermal progenitors internalize or move into the blastula via the

blastopore (involution). During the epithelial-mesenchymal transition (EMT), epithelial cells lose their polarity and transform into mesenchymal cells, which can later differentiate into fibroblasts, smooth muscle cells, chondrocytes, and osteoblasts<sup>48</sup>.

Vegetal rotation is the driving force of involution and occurs within the first two hours of gastrulation. This process distorts the endodermal vegetal cell mass and produces a rotation in the marginal zone towards the blastocoel<sup>49</sup>.

The hallmark of gastrulation is the establishment of the basic body plan and the formation of the three primordial germ layers: the ectoderm, endoderm, and mesoderm (Figure 4). Cell behaviors such as cell migration and cell polarity tightly regulate gastrulation<sup>46</sup>. Cells undergo tightly regulated polarization and rearrangement into new spatial positions, enabling the establishment of a complex body plan. Cell movement, the establishment of the anterior-posterior axis, and changes in cell fate are integral to gastrulation<sup>50</sup>. The process of gastrulation generates the ectoderm, endoderm, and mesoderm<sup>51</sup>. The ectoderm gives rise to the epithelial and neural tissues as well as hair and nails. The endoderm gives rise to the gastrointestinal tract, respiratory tract, and the endocrine, auditory, and urinary systems. Lastly, the mesoderm forms the connective

tissues, the endothelium of blood vessels, red and white blood cells, microglia, kidneys, and the heart<sup>52</sup>.

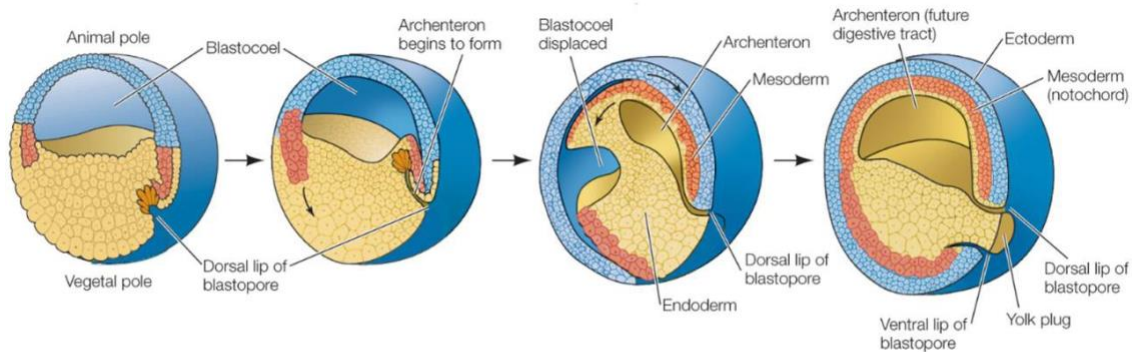


**Figure 4. Gastrulation in *Xenopus* embryos.** The blastocoel moves toward the animal pole in the blastula. The formation of the blastopore at the dorsal side of the blastula signals the beginning of gastrulation. As cells migrate through the blastopore, the blastocoel shrinks, and the archenteron begins to form. The archenteron will form the digestive cavity. Along with the archenteron, the three primary germ layers form by the end of gastrulation. Adapted from James Morris. *Biology: How Life Works* Fourth Edition MacMillan Publishing 2023.

At the beginning of involution, bottle cells, known for their distinctive, bottle-like shape, are located on the surface of the archenteron. The activation of myosin II causes the network of F-actin and myosin to contract, leading to constriction at the apical end. Apical constriction is required for gastrulation, neurulation, and organogenesis. Bottle cells constrict around the large yolk cells in the vegetal endoderm and invaginate to form the dorsal lip of the blastopore. Mesodermal precursors undergo involution under the roof of the blastocoel. Cells in the outer layer simultaneously extend around the embryo surface invoking a process known as epiboly. As the embryo undergoes gastrulation, a cavity known as the archenteron forms while the blastocoel contracts. Surrounded by endodermal tissue, the archenteron will form the primitive gut. In this stage, the cells in the inner layer of the roof of the cavity originated from outside of the

embryo. The ventral lip of the blastopore forms when bottle cells and other surface cells migrate into the embryo.

The cellular mechanisms involved in gastrulation are common to all animals. During gastrulation, cells undergo changes in cell shape, motility, and adhesion. There are several types of movements involved in gastrulation: invagination, ingression, involution, epiboly, intercalation, and convergent extension (Figure 5)<sup>53</sup>. Invagination is the process in which a sheet of epithelial cells bends inwards and forms a pocket. Ingression occurs when cells migrate from the epithelial sheet into mesenchymal cells. Involution is an inward movement of cells to form an underlying layer. Epiboly occurs when a sheet of cells spreads thinner. During intercalation, two or more rows of cells move between and create a longer but thinner series of cells. Convergent extension is the directional intercalation of cells<sup>54</sup>.

Convergent extension is one of the main driving forces of vertebrate gastrulation and consists of two separate movements: convergence and extension. During convergent extension, mesodermal cells intercalate between neighboring cells while migrating

toward the future dorsal side of the embryo. This results in a narrowing of the dorsal-ventral axis (*convergence*) and a lengthening of the anterior-posterior axis (*extension*)<sup>46</sup>.

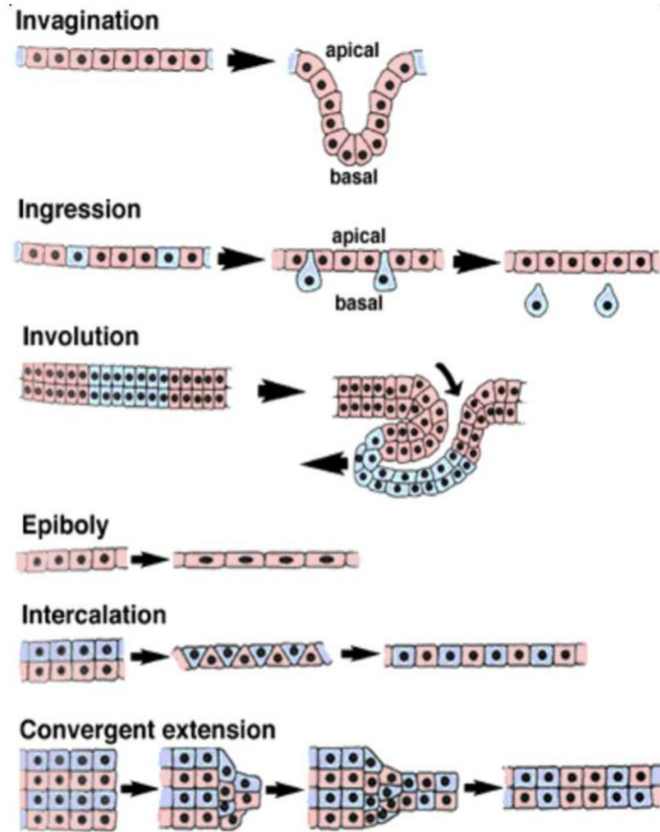


Figure 5. **Morphogenetic cell movements during gastrulation.** Cells employ different types of morphogenetic movements to achieve their objectives during gastrulation<sup>140</sup>

Convergent extension is not only a driving factor in gastrulation but also is involved in later morphogenetic movements, such as neural tube closure<sup>55</sup>. Convergent extension movements during vertebrate gastrulation and neurulation require the non-canonical Wnt pathway. Dvl controls the stability and polarity of lamellipodial protrusions that drive convergent extension<sup>56</sup>.

## 1.5 Neural tube closure

After gastrulation, the embryo forms its neural tube through a process known as *neurulation*. Neurulation in vertebrates involves a very precise set of orchestrated morphogenetic movements within the neural plate and the neighboring cells. A flat sheet of neuroepithelial cells, the neural plate, arises from the dorsal side of the blastoderm toward the end of gastrulation and forms the neural tube<sup>57,58</sup>. There are four steps to neurulation (Figure 6)<sup>55</sup>. First, the thickening of the ectoderm on the dorsal surface of the embryo forms the neural plate at the end of gastrulation<sup>59</sup>. Second, neuroepithelial cells are cuboidal in shape before neurulation, then become more columnar by elongating along the apical-basal axis<sup>57</sup>. The bending of the neural plate is the third step of neurulation.

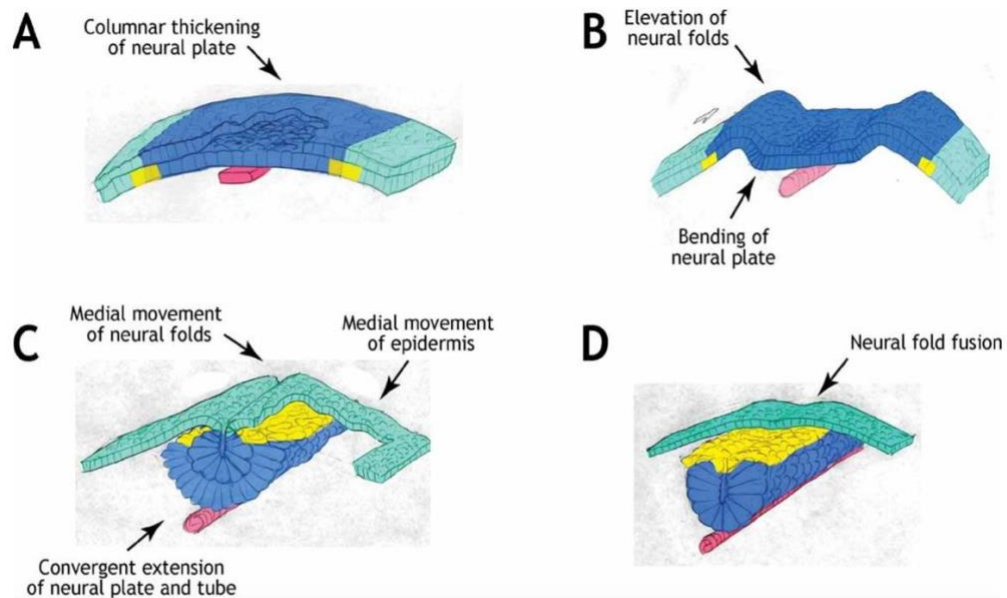


Figure 6. **Morphogenetic cell movements during neurulation.** Many types of cell movements and changes to cell shape are involved in neural tube closure. Panels A-D show changes in cell shape and cell movements associated with neurulation<sup>41</sup>

Neuroepithelial cells undergo apical constriction while the underlying mesodermal cells undergo convergent extension. The columnar cells undergo constriction at their apices to adopt a bottle-like shape. Columnar cells in the neural plate undergo apical constriction resulting in conversion to wedge-shaped cells and the bending of the neural epithelium<sup>55,57,58</sup>. In addition to apical constriction, the mesoderm undergoes convergent extension to push neural folds toward the midline<sup>60</sup>. During the fourth step of neurulation, the neural folds undergo fusion of epithelial tissue, forming the neural tube<sup>18</sup>.

The best supported hypothesis for the mechanism of apical constriction in the neural plate is the meshwork of F-actin and myosin located underneath the plasma membrane of neuroepithelial cells (Figure 7)<sup>61,62</sup>. In addition to its role in neural tube

closure, apical constriction occurs also in the removal of apoptotic cells and wound repair<sup>63-66</sup>.

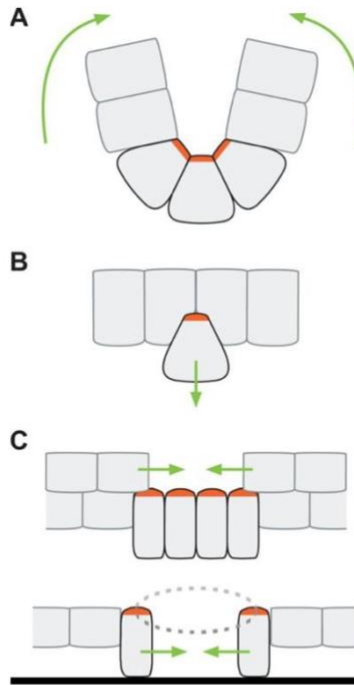


Figure 7. **Apical constriction occurs during different cellular processes.** Apical constriction is vital in many instances of cell motility in development. (A) During gastrulation and neurulation, tissue folding occurs. (B) Individual cells ingress EMT. (C) Embryonic tissue heals and seals off during wound healing by undergoing apical constriction <sup>141</sup>

Mediolateral cell intercalation drives convergent extension in the neural plate. The neural cells migrate along the mediolateral axis by projecting lamellipodia to one another resulting in a thinner and longer neural tube <sup>67</sup>. Neural tube closure and convergent extension both require non-canonical Wnt signaling. Dysfunction of non-canonical Wnt signaling causes failures in both processes<sup>3,4</sup>.

*Xenopus laevis* is an ideal model organism to study the protein function of non-canonical Wnt signaling components because of the abundance of proteins in the

relatively large embryo, compared to other model systems such as zebrafish or *Drosophila* which have much smaller embryos. They are easy to maintain and produce large numbers of eggs year-round. The injection of chorionic gonadotropin allows the production of eggs by a female frog to be controlled by the researcher. *Xenopus* embryos develop to the tadpole stage in about two days, allowing for quick experimental turnover and visualization of the effects of experimental interventions (Figure 8). Lastly, the development of *Xenopus* more closely mimics human development, as compared to *C. elegans* and *Drosophila*. This makes *Xenopus* an attractive model for investigating early developmental defects in humans. Using *Xenopus laevis*, researchers were able to identify the function of proteins within non-canonical Wnt signaling. Crucially, biochemical studies were able to link actin-nucleating proteins, known as *Formins*, to non-canonical Wnt signaling<sup>44</sup>.

## 1.6 Formins and Rho GTPases

Formins are evolutionarily conserved and are potent actin nucleating proteins (ANP)<sup>68</sup>. Formins control the rearrangement of the actin cytoskeleton and regulate cytokinesis and cell polarity<sup>69</sup>. The mammalian genome contains more than 15 Formin genes that can be grouped into eight different subcategories: Formins; Diaphanous formins (Dia); the Dvl-associated activators of morphogenesis (DAAM); inverted Formins (INF); Delphilin; the formin homology domain-containing protein (FHOD); Formin Formin-like proteins (FMNL); and WH2 domain containing Formin<sup>70</sup>.

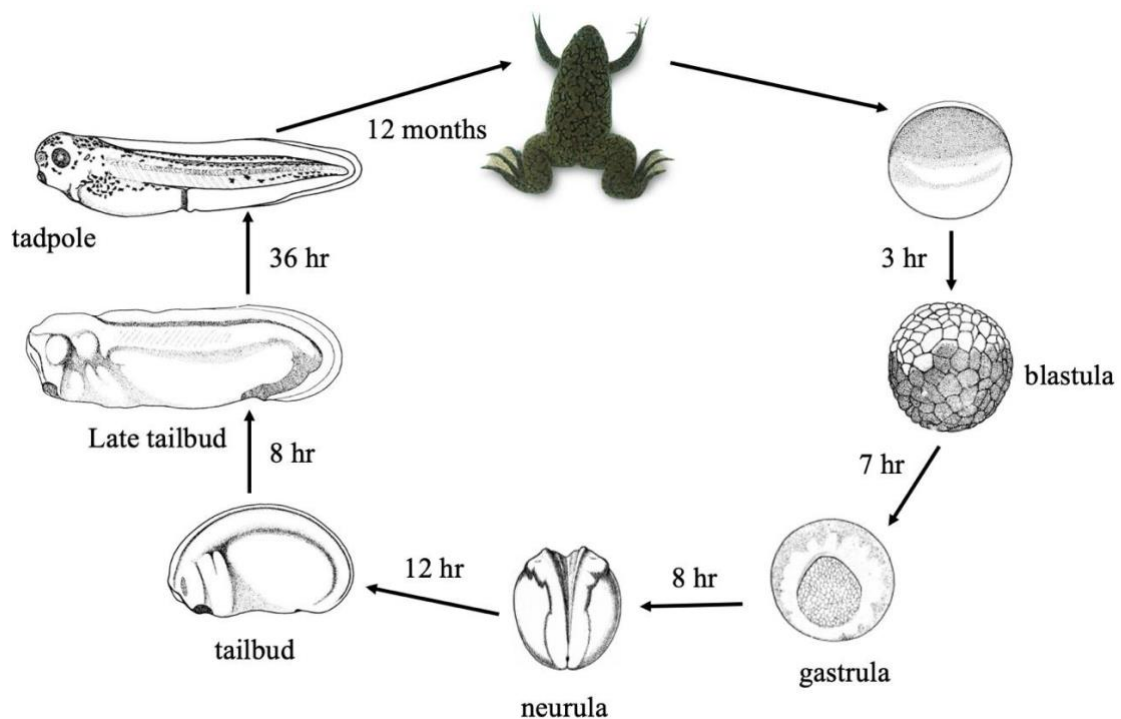


Figure 8. *Xenopus laevis* life cycle. Stages of embryonic development and time required between stages in *Xenopus laevis*. (Xenbase)

Formins are large (120-200 kDa) proteins containing multiple functional domains. Most Formins contain the Formin homology 1 (FH1) and Formin homology 2 (FH2) domains. The FH2 domain contains approximately 400 amino acids and is the actin nucleating domain of Formins. The structure of the FH2 domains in human Daam1, mouse mDia1, and yeast analog Bni1p were identified by crystallography. FH2 exists as a dimer and must be dimerized with itself to be active<sup>72-74</sup> (Figure 9). Loss of the ability to form dimers results in an inactive FH2 domain<sup>71</sup>. Located near the FH2 domain is the proline-rich FH1 domain. Some Formins contain a less conserved domain known as the diaphanous inhibitory domain (DID) located at the N-terminus within the GBD domain<sup>72</sup>. Also located in the N-terminus is the Rho GTPase binding domain (GBD). Formins that contain a GBD domain can be activated by the Rho family of GTPases<sup>73,74</sup>. Diaphanous-

related Formins (DRF) contain Dia, Daam1, and Formin-related (FRL) subcategories and are direct effectors of Rho GTPase<sup>75</sup>.

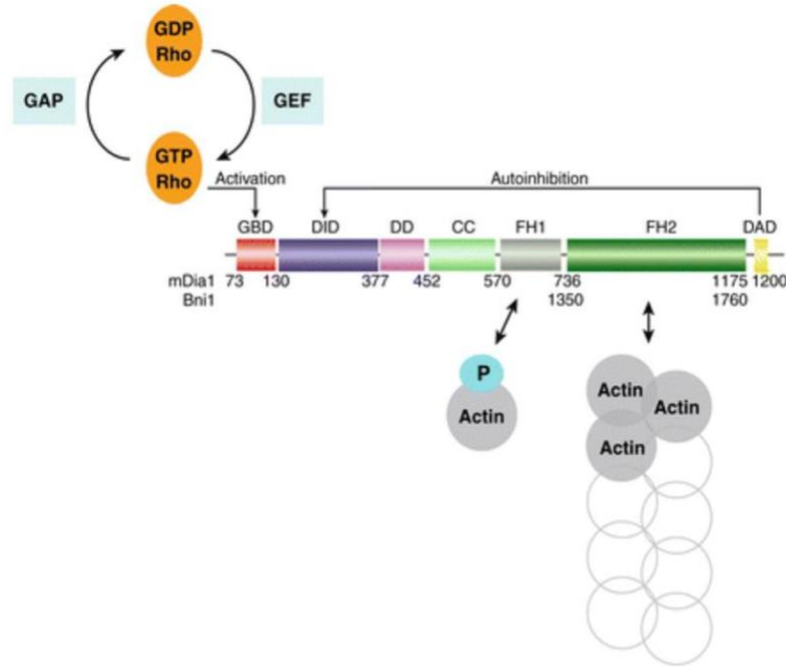


Figure 9. **Schematic of activation of Formins.** Formins are autoinhibited by intramolecular forces between the DAD and DID domains. Autoinhibition is released when GTP-bound Rho binds to the GBD domain. Actin bound Profilin 1 interacts with the FH1 domain to accelerate filament elongation. Actin binds to the FH2, which then nucleates actin to barbed end of the growing actin filament <sup>75</sup>.

All Formins exist in auto-inhibited states. All formins contain a DID on the N-terminus that binds to the diaphanous auto-regulatory domain (DAD) on the C-terminus, thereby auto-inhibiting the formin. The interaction between the DID and DAD domains is broken by Rho GTPase, thereby opening the FH1 and FH2 domains to actin binding and nucleation, respectively<sup>72-76,77</sup>. Removing either the DID or the DAD domain results in a constitutively active Formin<sup>73,78,79</sup>.

The Rho family of GTPases is classified under the superfamily, Ras-related GTPases. They function in nearly every cellular process. Rho GTPases act as bi-molecular switches that alternate between an active GTP-bound and an inactive GDP-bound states (Figure 10)<sup>80</sup>. Guanine exchange factors (GEFs) activate Rho GTPases on the plasma membrane by catalyzing the exchange of GDP for GTP. GTPase-activating protein (GAPs) inactivate Rho GTPases by increasing GTP hydrolysis to GDP. Lastly, guanine nucleotide-dissociation inhibitors (GDIs) sequester Rho GTPases in their GDP-bound form and modulate their cellular localization<sup>81</sup>. Over 80 GEFs and 70 GAPs have been reported in mammals, which suggests that regulation of Rho GTPases is highly complex and influenced by many signaling pathways<sup>39</sup>.

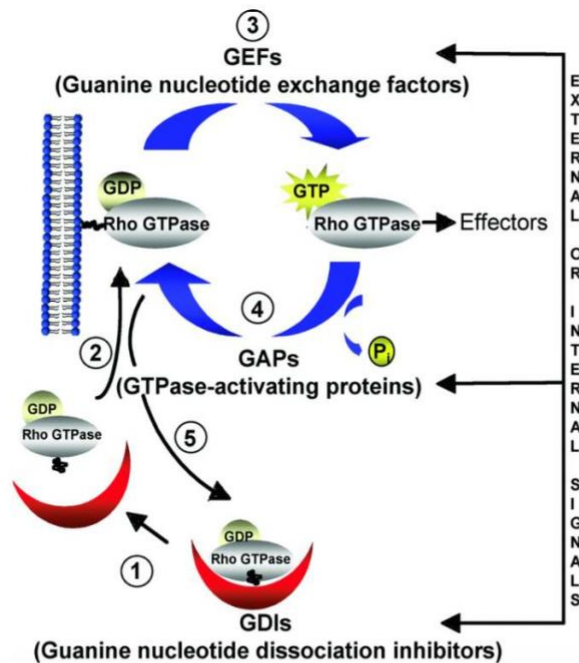


Figure 10. **Mechanism of cycling of Rho GTPases.** GDP bound Rho GTPase is the inactive form whereas GTP bound is the active form. The GDP-GTP cycle is tightly regulated by GEFs, GAPs, and GDIs. In the absence of a signal, GDIs maintain Rho GTPases in their inactive state. In the presence of an intracellular or extracellular signal, Rho GTPase is released from its inhibitory complex (1) and localize to the plasma membrane (2). Rho GTPase is activated by GEFs (3), enabling downstream effectors. Once the signal is removed, Rho GTPase are inactivated by GAPs (4), and stabilized and maintained by GDIs (5)<sup>142</sup>

RhoA, Rac, and Cdc42 are the best studied Rho GTPase family members.

Activation of Rho-associated kinase (ROCK) by RhoA leads to phosphorylation and inactivation of myosin light chain phosphatase and activation of myosin II<sup>82</sup>. Interaction between RhoA and a Formin promotes actin fiber formation and actin-myosin contractile filaments<sup>73</sup>. Rac1 releases WASP-family Verprolin homologous protein (WAVE) from an inhibitory complex and allows for activation of Arp2/3. This leads to branched actin filament growth around the plasma membrane and lamellipodia formation<sup>83</sup>. Lastly, Cdc42 stimulates filopodia and activates Arp2/3 through direct interaction with Neural Wiskott-Aldrich protein (N-WASP)<sup>84</sup>.

Whereas the types of Formins and their respective functions might vary between organisms and even cell types within organisms, all Formins influence the actin cytoskeleton<sup>76</sup>. Nucleation of actin structures becomes kinetically favorable in the presence of nucleating factors<sup>85</sup>. Formins enable the assembly of actin fibers by binding to proteins that carry actin, such as Profilin, to accelerate the elongation of the filament<sup>69</sup>. The FH1 and FH2 domains mediate interactions between Formins, actin, and the actin-binding protein (Figure 11). The FH1 domain allows actin binding proteins, such as Profilin carrying G-actin, to anchor to the Formin. The FH2 domain nucleates the nearby G-actin molecule to the actin fiber. Formins have been shown to nucleate actin during

mitosis, embryonic development, meiosis, vesicular trafficking, and cell polarity maintenance<sup>72</sup>.

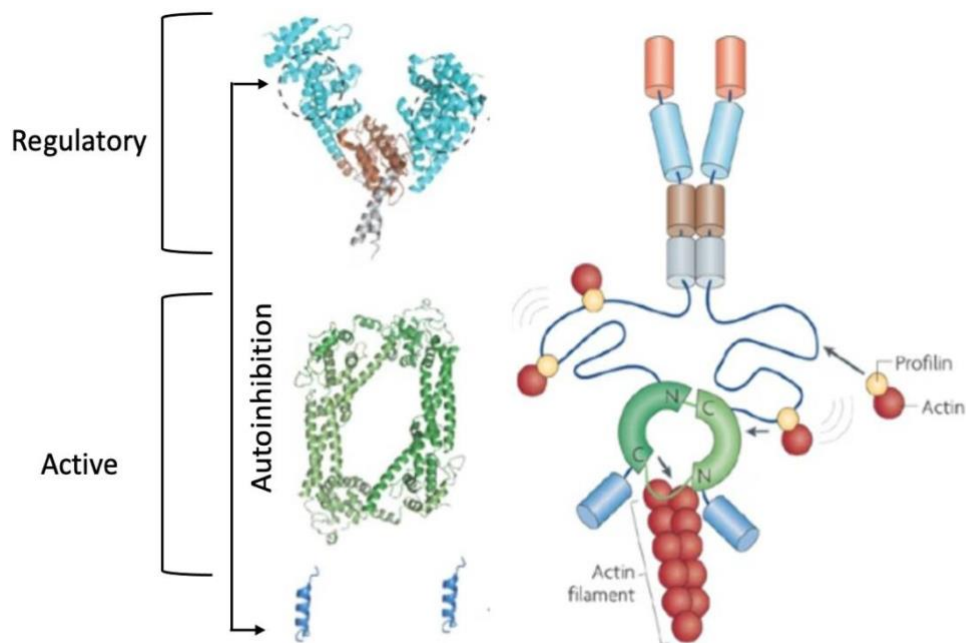


Figure 11. **Organization of domains of Formins.** The crystal structure depicts the DID domain, coiled coiled region in the N-terminus, FH2 domain in the middle of the protein, and the DAD in the C-terminus. The dimerization of FH2 is essential for the function of Formins. The FH2 domain alternates binding between itself and an actin subunit <sup>143</sup>

Formins trigger cellular motility and shape changes by modulating the actin cytoskeleton. Formins accomplish this feat by acting as downstream effectors of signal inputs and signaling through proteins containing Src Homology 3 (SH3) domains, such as Src kinase<sup>42,86</sup>. Formins have a wide variety of cellular functions, but their roles in embryonic development are less characterized. Knockdown and knockout studies have been crucial in characterizing the role of Formins in early embryonic development. mDia1, the most studied Formin, shows no effect on embryonic survivability or morphology but affects the ability of T-cells to migrate and adhere correctly (Figure 12).

Aging mDia1-deficient mice show myeloproliferative defects<sup>87-89</sup>. Formin1-deficient mice exhibit limb deformities attributable to improper BMP signaling, whereas Formin2-deficient mice survive into adulthood but exhibit age-dependent learning disabilities and are infertile<sup>90,91</sup>.

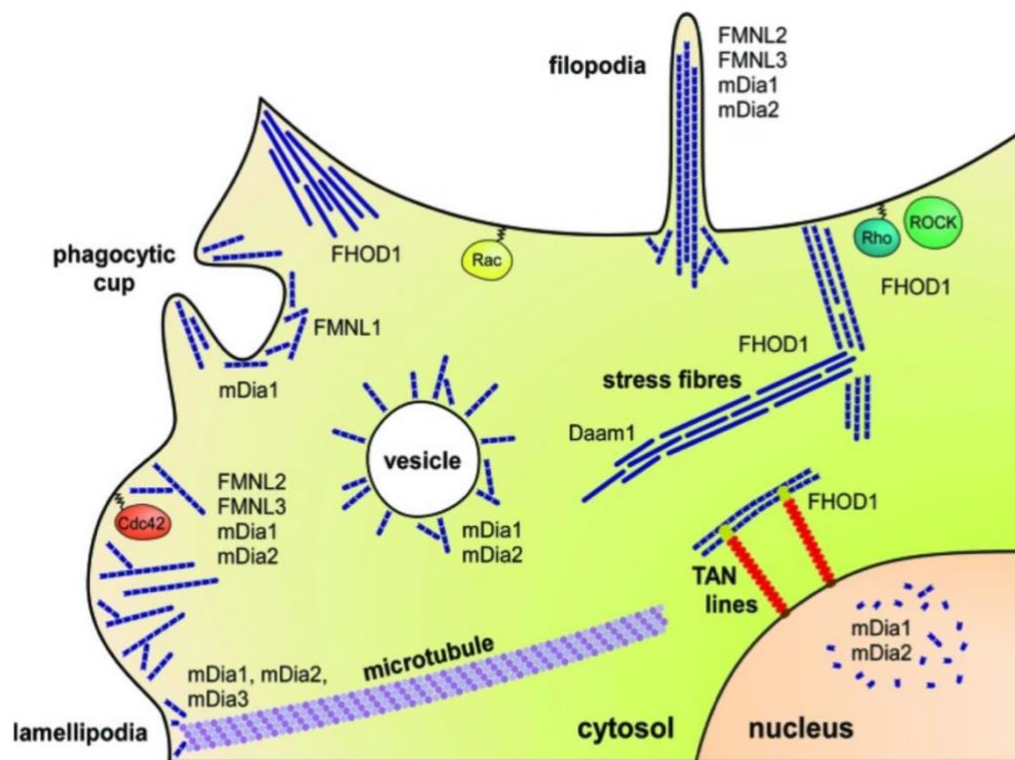


Figure 12. **Model of Diaphanous Related Formins depicting their cellular function and localization.** Formins are involved in the formation of filopodia and lamellipodia, stabilization of actin stress fibers, interaction of cytoskeletal structures, vesicle formation and trafficking<sup>143</sup>

Named after its binding partner in Wnt/PCP signaling, Daam1 plays a crucial role in gastrulation in *Xenopus*<sup>44</sup>. Daam1 exists in an auto-inhibited state because of the DID and DAD domains binding but is activated when the PDZ domain of Dvl binds to the DAD domain of Daam1<sup>79</sup>. Once activated, Daam1 activates RhoA, leading to actin polymerization<sup>44,79</sup>. In Zebrafish, knockdown of Daam1 results in brain asymmetry and lower neutrophil counts<sup>92</sup>. Lastly, Daam1-deficient mice demonstrate severe phenotypes.

They exhibit reduced fetal size, incorrect cytoskeletal structures, cardiac defects, and neonatal lethality<sup>93</sup>.

Daam2 (Dishevelled-associated-activator of morphogenesis 2) was first identified in chickens from a screen to identify Daam1 homologs<sup>94</sup>. Daam2 shares much domain homology with Daam1. Their GPD, FH1, FH2, and DAD domains share 77%, 64%, 66%, and 96% homology, respectively<sup>1</sup>. Like other Formins, Daam2 nucleates actin through its FH1 and FH2 domains. In Wnt signaling, Daam 2 binds to Dvl and is auto inhibited through the self-association of its DAD and DID domains. Daam2 localizes to actin fibers and regulates neural tube closure in early development. Daam 2 does not affect the formation of skeletal muscle nor does affect convergent extension<sup>1</sup>. Daam2 is not nearly as well studied as Daam1, but more recent studies link the former to heart and placental development<sup>95,96</sup>. The cascade of proteins activated by Wnt signaling that leads to the activation of Daam2 to affect the actin cytoskeleton requires further research.

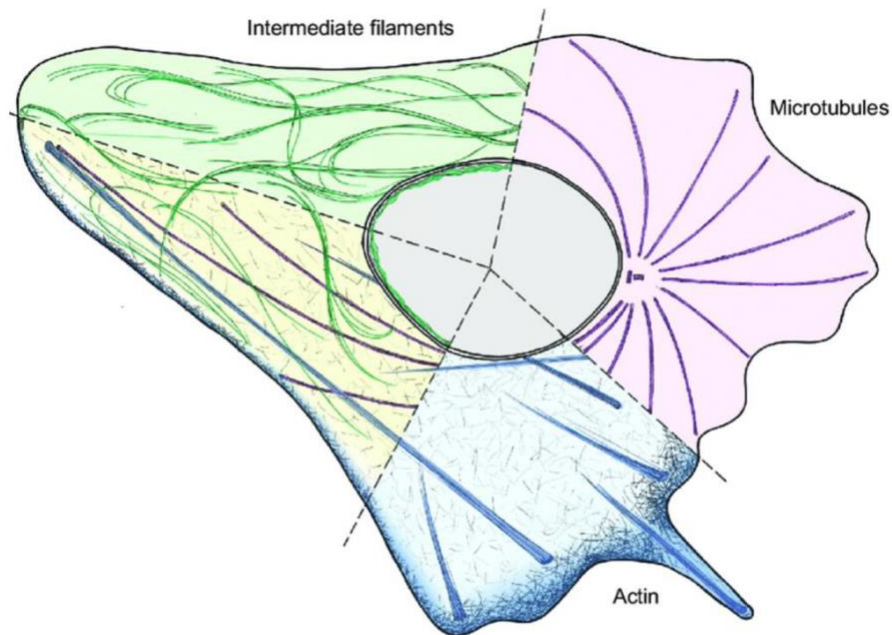


Figure 13. **Different types of filamentous systems.** Intermediate filaments are depicted in green, microtubules originating from centromeres in purple, and actin filaments are depicted in blue. All three filamentous systems function together <sup>144</sup>

## 1.7 Actin cytoskeleton and cell migration

Eukaryotic cytoskeletons are comprised of filamentous proteins to maintain cell rigidity and internal organization, and to carry out essential cellular functions such as cell division and movement. Animal cell cytoskeletons consist of microtubules, intermediate filaments, and actin microfilaments (Figure 13). Microtubules radiate from centrosomes to provide support for the cytoplasm and facilitate protein transport<sup>97</sup>. The strongest yet least dynamic fiber is the intermediary filament, which provides mechanical strength to cells and tissue<sup>97</sup>. Lastly, the highly dynamic actin cytoskeleton consists of actin microfilaments and many actin-binding and associated proteins. The actin cytoskeleton

undergoes complex reorganization to facilitate organelle positioning, cell movement and division, vesicular trafficking, and muscle contractility<sup>98</sup>.

Actin is a highly conserved and abundant protein 42 kDa in mass. It participates in more protein-protein interactions than any other known protein and is necessary for eukaryotic cell survival<sup>99,100</sup>. It exists as either free monomeric globular actin (G-actin) or as part of a linear polymer microfilament, known as filamentous actin (F-actin). G-actin and F-actin exist in a state of transitional equilibrium via ATP hydrolysis (Figure 14). Actin binds to and is under the control of many ABPs. Nucleotide hydrolysis by F-actin is one of the primary factors regulating the transition between G-actin and F-actin. *In vitro*, actin monomers join the fast-growing barbed (+) end of the filament in the ATP state. Hydrolysis then takes place in the filament, and ADP-actin monomers dissociate

faster from the pointed (-) end. The addition and removal of actin monomers are known as actin filament treadmilling and are regulated by ABPs<sup>101</sup>.

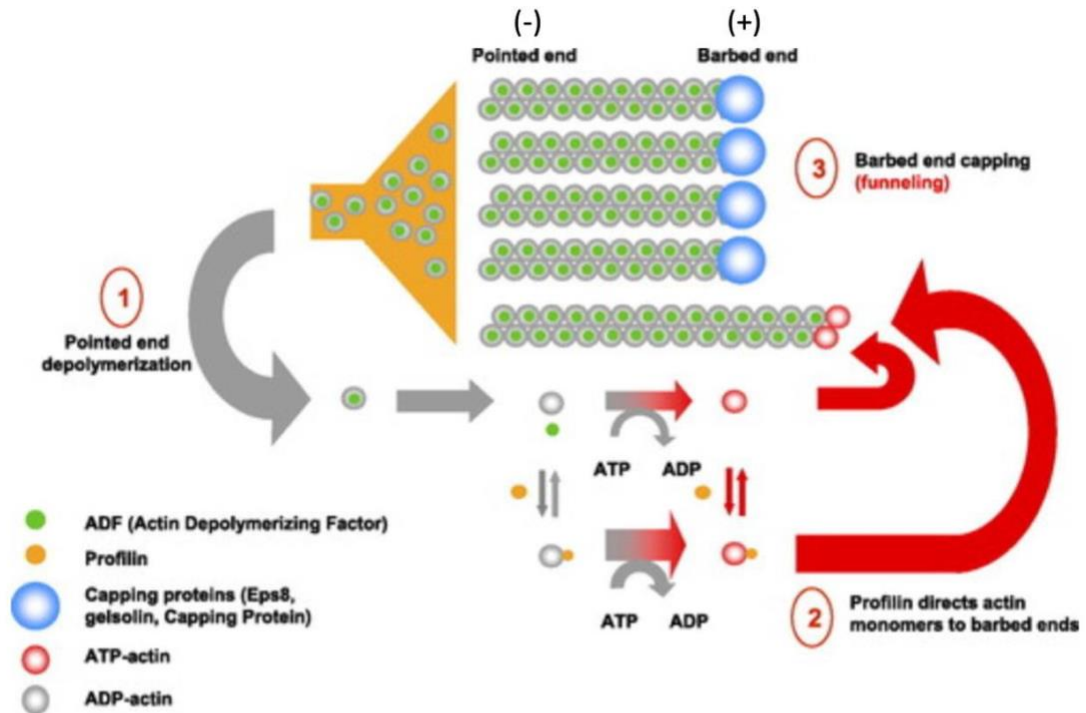
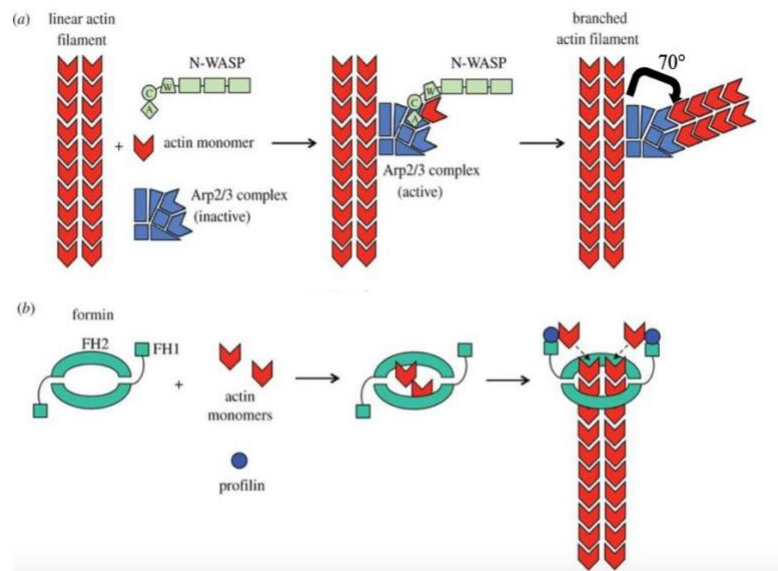


Figure 14. **Regulation of actin treadmilling.** (1) ADF binds to the pointed (-) end to increase depolymerization as well as the concentration of monomeric actin. (2) Profilin increases the rate of exchange of ADP to ATP actin, which increases the rate of actin polymerization. (3) Capping proteins bind to the the barbed (+) end and block additional actin polymerization. <sup>110</sup>

Polymerization of actin can be triggered in a variety of ways, including increasing the rate of addition of G-actin to the barbed end, nucleation of new filaments, and slowing depolymerization<sup>76</sup>. Because actin nucleation is not spontaneous, certain proteins are required to overcome this kinetic barrier. These factors include the Arp2/3 complex and its associated proteins, the Formins, and the WH2 (WASP-homology domain 2)-containing nucleators (Figure 15)<sup>85, 102-104</sup>. In addition to nucleating factors, proteins such as Profilin regulate intracellular concentrations of monomeric actin. Profilin is a key exchange factor that regulates the conversion of ADP-bound actin to active ATP-bound

actin. It also aids in actin polymerization and prevents incorrect polymerization by sterically hindering the addition of monomers to the barbed end<sup>105,106</sup>. The importance of Profilin in early embryonic development and adult cell processes is discussed in more depth in the next section.



**Figure 15. Linear and branched actin polymerization require different actin binding proteins.** (A) N-WASP carries an actin monomer to the Arp2/3 complex which nucleates new actin filaments from the side of existing actin chains at approximately a 70° angle. (B) Profilin carrying an actin monomer binds to an FH1 domain on a Formin protein. The FH2 domain binds to the actin monomer and elongates the actin filament at the barbed end of linear actin filaments<sup>145</sup>

Cell migration is vital for morphogenetic processes such as gastrulation and neurulation in embryogenesis<sup>107,108</sup>. Cell migration requires generating protrusions known as lamellipodia and filopodia to create the required force to migrate (Figure 16). Cells form new adhesions and retract their lagging edges to inch forward toward their intended locations<sup>109</sup>. Formed by the Arp2/3 complex, lamellipodia are composed of a dense network of short, branched actin fibers<sup>99,110</sup>. Conversely, filopodia are temporary, thin, hair-like protrusions composed of parallel actin fibers<sup>111</sup>. Whereas filopodia direct cell migration based on sensory cues from the environment such as food or a toxin, lamellipodia remain constant on the cell surface<sup>112</sup>.

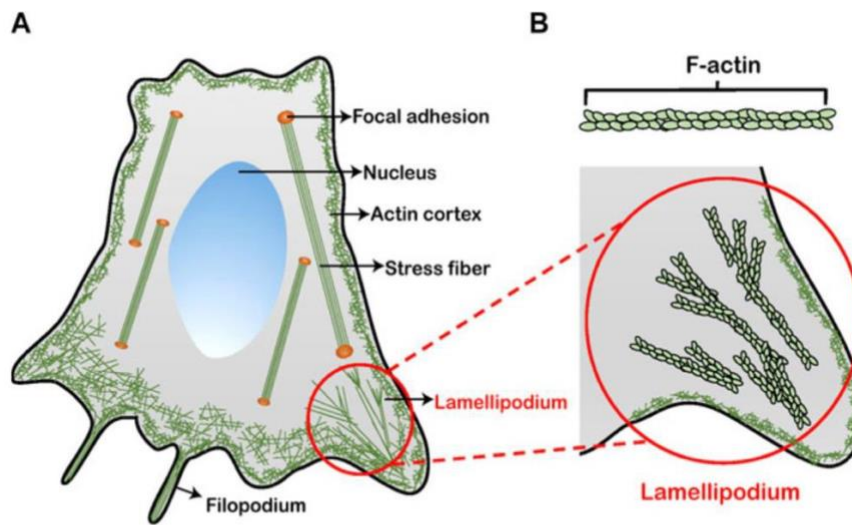


Figure 16. **Types of actin structures in cells.** (A) The formation of the three types of actin structures (stress fibers, filopodium, and lamellipodium) is crucial for proper tissue organization. Stress fibers are formed when individual actin filaments and myosin-II bind and span the length of the cell. Stress fibers are anchored by focal adhesions. Lamellipodium are formed when actin bundling occurs at the cell's leading. Filopodium are long, linear projections of actin filaments. (B) Actin bundling that creates lamellipodium form large net-like structures to promote cellular motility<sup>83</sup>

## 1.8 Previous studies on Profilin

There are four identified Profilin genes reported to date. Profilin1 (PFN1) is expressed ubiquitously in humans and mice, whereas the other isoforms are tissue specific. Profilin 2 (PFN2) is brain-specific and required for early neuronal development<sup>113</sup>. Profilin 3 (PFN3) is expressed in the testis, kidney, and in developing spermatids<sup>114</sup>. Profilin 3 and Profilin 4 (PFN4) show only about a 30% amino acid conservation to the much more heavily conserved Profilin1 and Profilin 2. This suggests that PFN3 and PFN4 are more evolutionary divergent from the much older PFN1 and PFN2 genes<sup>115</sup>. All Profilins are 15-kDa, structurally conserved proteins containing seven  $\beta$ -sheets and four  $\alpha$ -helices<sup>115,116</sup>. In addition to their many kinase and phosphatase binding partners, Profilins bind to two other types of ligands: actin and proteins containing proline repeat motifs (PLP).

PFN1 has a five-fold higher affinity for actin than PFN2<sup>117</sup>. PFN1 enables eukaryotic cells to undergo actin cytoskeletal reorganization in a coordinated manner<sup>118</sup>. PFN1 accomplishes its cellular functions by maintaining a pool of ATP-bound G-actin for polymerization and delivering it to actin nucleating proteins<sup>119</sup>. Interactions between Profilin and its many binding proteins dictate the type of F-actin network formed (linear or branched) and the development of different cellular projections (lamellipodia, filopodia). Ultimately, these intricate series of events will direct cell motility<sup>120</sup>.

PFN1 sequesters ATP-bound G-actin for polymerization by accelerating the exchange of ADP to ATP 1000-fold<sup>121</sup>. PFN1 carrying an ATP-bound actin monomer interacts with the fast growing, barbed end (+) of the actin filament to release the actin monomer, adding it to the filament. Due to the ATPase activity of actin, the ATP bound to the actin molecule is hydrolyzed into ADP in the older sections of the filament. This releases ADP bound actin from the pointed (-) end by depolymerization<sup>122</sup>.

PFN1 is required for cytokinesis during embryogenesis. Despite the cellular importance of PFN1 and a plethora of *in vitro* data, its role in development is less understood. A genetic knockout of Profilin1 in mice is embryonically lethal due to the inability of dividing cells to undergo cytokinesis<sup>113</sup>. In *Drosophila*, the Chickadee gene encodes Profilin1. Genomic deletions of the Chickadee locus result in embryonic lethality after the maternal deposition of PFN1 mRNA is exhausted<sup>123</sup>. In addition, binucleated cells, stalled cell migration, abnormal regulation of mitosis, and improper actin filament formation were detected in *Drosophila*<sup>123</sup>. In *Xenopus*, either overexpression or depletion of PFN1 results in the inhibition of blastopore closure, but tissue separation, convergent extension, and neural tube closure remain unaffected<sup>124</sup>.

Poly-L Proline (PLP) sites are strings of three or more proline residues that were shown to mediate binding to actin, Profilin, and the Src homology 3 domain<sup>125-127</sup>. Many proteins contain PLP sites, but two of the most studied families are the enabled/vasodilator-stimulated phosphoproteins (Ena/VASPs) and the Formins<sup>77,93,128</sup>. Ena/VASP localizes to the plasma membrane and through its interaction with PFN1,

forms branched networks of actin filaments to modulate filopodia formation and cell-to-cell adhesions<sup>129,130</sup>.

PFN1 binds to Formins at the PLP region between the FH1 and FH2 domains<sup>77</sup>. Profilin1 is a component of non-canonical Wnt signaling that co-localizes with Daam1 to actin fibers in response to Wnt stimulation. The kinases that regulate Profilin1 during cytoskeletal rearrangement via Daam1 during embryogenesis and in adult organisms remain unknown. However, several studies identify both serine and tyrosine kinases that phosphorylate Profilin on its C-terminus<sup>131,132</sup>. The residues that enable the binding of PFN1 to PLP sites have not yet been elucidated.

Tyrosine 129 (Tyr) and Serine 137 (Ser) are two residues that appear to regulate the function of HPFN1. *In vitro* assays show Src kinase phosphorylates Tyr129 under VEGF-A treatment in mice endothelial cells<sup>132</sup>. A conditional mouse mutant expressing Tyr129Phe shows severely decreased angiogenesis and greatly delayed wound closure, suggesting phosphorylation of Tyr129 is critical for cell motility and proliferation<sup>132</sup>. Hyperphosphorylation of Tyr129 correlates with increased tumor aggressiveness in glioblastoma<sup>133</sup>. ROCK phosphorylates Ser137 and is dephosphorylated by protein phosphatase 1 (PP1)<sup>131,134</sup>. Dysregulation of Ser137 does not impact PFN1's ability to bind to actin but may interfere with PFN1's ability to bind to PLP sites<sup>135</sup>. Moreover, phosphorylation of Ser137 shows an increase in tumorigenesis, suggesting it may play a role in regulating mitosis.

Dysregulation of Profilin has been implicated in several disease pathogenesises, ranging from solid tumor cancers to amyotrophic lateral sclerosis (ALS)<sup>115</sup>. Overexpression of Profilin1 is associated with increased aggressiveness of breast and renal carcinoma<sup>136,137</sup>. Moreover, due to its many binding partners, there is a high possibility of crosstalk between signaling pathways, adding an extra layer of complexity. In non-canonical Wnt signaling, for example, it is unknown which residues on Profilin1 facilitate interaction with Daam1. Even though Src and ROCK kinase phosphorylate Tyr129 and Ser137 respectively, the ANPs that interact with Profilin through these residues are unknown and individual residues functions have not been elucidated. The residues that facilitate Profilin1's function as a downstream effector of non-canonical Wnt signaling and its crucial role in early embryonic development are also unknown. Tyr129 and Ser137 are highly conserved in humans, mice, *Xenopus*, and chickens. In *Xenopus*, they correspond to Tyr131 and Ser135 (Figure 17). As yet, no research has been published on the roles of Tyr131 and Ser135 in *Xenopus* Profilin1 despite their conservation with Tyr129 and Ser137. Identifying whether Tyr131 and Ser135 confer the function of Profilin1 in non-canonical Wnt signaling would be an important step forward in understanding and controlling actin filament assembly.



## **CHAPTER 2**

### **MATERIALS AND METHODS**

#### **2.1 Tissue culture and transfection**

HEK293T and HeLa cell lines (ATCC) were grown in DMEM, high glucose, GlutaMAX supplement (Life Technologies); 10% fetal bovine serum (FBS; Fisher Scientific); and 1% penicillin-streptomycin (ThermoFisher) and split every 2-3 days to 40-50% confluency. Cells were cultured in 10cm tissue culture dishes (VWR). Cells were grown in 6-well tissue culture dishes (VWR) and transfected with appropriate plasmid(s) using Polyfect (Qiagen).

## 2.2 Generation of Profilin mutant plasmids

GFP-Profilin1 previously cloned into the CS2+ vector was used as template and mutated with QuikChange XL2 (Agilent) using the following sets of primers from IDT:

Plasmid Name	Forward Primer 5`to 3`	Reverse Primer 5`to 3`
GFP-P1 S135A	TACCTGAGATGTGCAGGCTACTGACTCGA GCCT	AGGCTCGAGTCAGTAGCCTGCACATC TCAGGTA
GFP-P1 S135E	TACCTGAGATGTGAGGGCTACTGACTCGA GCCT	AGGCTCGAGTCAGTAGCCCTCACATC TCAGGTA
GFP-P1 Y131A	GACATGGGCAAGGCCCTGAGATGTTCT	AGAACATCTCAGGGCCTTGCCCATGT C
GFP-P1 Y131A; S135A	GACATGGGCAAGGCCCTGAGATGTGCA	TGCACATCTCAGGGCCTTGCCCATGTC

Table 1. Primers used for generation of Profilin Mutants

## 2.3 Co-IP

HEK293T (ATCC) cells were seeded 24 hours before transfection at a density of  $6 \times 10^5$  cells. The cells were co-transfected with 2ug of each plasmid. After 48 hours, cells were treated with 50ng/mL Wnt5a (R&D Sciences) for 1 hour. Cells were then collected in PBS and lysed in 1% NP-40 lysis buffer (50 mM Tris-HCl pH 8.0, 150mM NaCl, 1% NP-40) containing Complete Mini Protease Inhibitor Cocktail (Sigma Millipore).

Samples were poured over a 50ul bed of Protein A agarose beads coupled to either Myc

or GFP antibodies and incubated for 1 hr at 4°C. The beads were then washed 5x with

RIPA buffer (150mM NaCl, 1% NP40, 0.5% sodium deoxycholate, 0.1% SDS, 50mM Tris pH 7.4). 50ul of loading buffer containing 2-mercaptoethanol (BME) was then added to each sample and incubated for 5 mins at 95°C before Western Blotting.

Pulldowns were tested by Western Blotting. Samples were run on 12% SDS-PAGE gel and transferred onto nitrocellulose membranes (Biorad). Membranes were washed with 3x for 5 mins in TBST (20mM Tris, 150mM NaCl and Tween 20 0.1% w/v), then blocked for 1 hour in 5% BSA in TBST (Fisher Scientific). The antibodies used were anti-c myc 9E10 (Santa Cruz), anti GFP (Abcam), Goat Anti-Mouse IgG HRP (Abcam), and Goat Anti-Rabbit IgG HRP (Abcam). Agarose Protein A beads (SCBT) were used for Co-IP pulldowns.

## **2.4 Preparation of Recombinant GST-Fusion Proteins**

GST-fusion plasmids (GST-cDaam1, GST-FH1, and GST-6PEG empty vector), were transformed into BL21 bacterial cells and plated onto LB-amp (100mg/L) petri dishes at 30°C. Single colonies were then picked and grown overnight in 20ml LB-amp (100mg/L) at 30°C. The culture was then diluted into 1L of LB-amp (100mg/L) and grown at 30°C until the optical density at 600nm reached 1.0, approximately 5-7 hours depending on starting optical density. Bacterial cultures were induced with 1mL of 1M IPTG and incubated at 30°C for 3 hours. Cells were sonicated in 1mL PBS containing

cComplete Mini Protease Inhibitor Cocktail (Sigma Millipore). The lysate was pelleted at 15,000 rpm for 15 mins at 4°C.

## **2.5 Extraction of GST Fusion Proteins**

Glutathione sepharose beads (Fisher Scientific) were prepared by swelling with 100ul of Wash Buffer (1x PBS/10mM DTT/1% Triton-X 100) for 1 hour on ice, then washed three times with 500uL Wash Buffer (1x PBS/10mM DTT/1% Triton-X 100). After the final wash, one aliquot of frozen GST Fusion Protein was added to preswollen beads and incubated on a nutator at 4°C for 45 mins. The beads were then washed five times with wash buffer.

## **2.6 GST Pulldown Assay**

50ul of whole cell lysates containing GFP-Profilin1 mutants were incubated with a 50ul bed of GST-cDaam1, GST-FH1, or GST empty vector coupled beads for 1 hour at 4°C on a nutator. Samples were then washed five times with wash buffer. 50ul of loading buffer containing 2-mercaptoethanol (BME) was then added to each sample and incubated for 5 mins at 95°C before Western Blotting.

## **2.7 Immunocytochemistry**

HeLa cells (ATCC) were seeded 24 hours prior to transfection at a density of  $4 \times 10^5$  cells into a 6-well tissue culture dish containing a fibronectin treated coverslip (Corning). Before transfection, full growth media was replaced with DMEM. Cells were transfected with 1 $\mu$ g of plasmid. After 24 hours, cell media was replaced with Opti-MEM reduced FBS serum (Fisher) to induce serum starvation. 24 hours later, cells were treated with 100ng/uL Wnt5a for 2 hours (R&D Sciences). The cells were then washed three times in cold PBS for 5 mins on low agitation and fixed in 5% PFA solution for 5 mins at -20°C. Actin was stained with Phalloidin-Alexa Fluor 555 (Fisher Scientific) and DAPI stain was used to visualize DNA (ThermoScientific).

## **2.8 mRNA overexpression in *Xenopus* embryos**

Cs2+GFP-Profilin1 and mutants were linearized with Not1 (NEB) and *in vitro* transcribed using mMessenger mMachine SP6 Transcription Kit (ThermoFisher).

## **2.9 *Xenopus* embryos**

*Xenopus* embryos were *in vitro* fertilized and de-jellied using L-Cysteine in 0.1x MMR (1M NaCl, 20mM KCl, 20mM CaCl<sub>2</sub>, 10mM MgCl<sub>2</sub>, 50mM Hepes) at pH 8. *Xenopus* embryos were then injected with mRNA at the 4-cell stage into the two dorsal cells or into the two ventral cells in 3% Ficoll in 0.5x MMR. Two hours after injection, embryos were changed into 0.1x MMR and cultured to approximately stage 35. Embryos

were fixed in MEMFA (1M MOPS, 20mM EGTA, and 10mM MgSO<sub>4</sub>) in pH 7.4 and stored in 4°C.

## **2.10 Src Assay**

HEK293T cells were seeded 24 hours before transfection at a density of  $6 \times 10^5$  cells. Cells were co-transfected with GFP-xPFN1 and control siRNA or siRNA targeting human Src kinase using Dharmafect Duo (Dharmacon) and allowed to express for 48 hours. Cells were then treated with 100ng/uL Wnt5a for 2 hours. Cells were then collected in PBS and lysed in 1% NP-40 lysis buffer (50 mM Tris-HCl pH 8.0, 150mM NaCl, 1% NP-40) containing cOmplete Mini Protease Inhibitor Cocktail (Sigma Millipore). Samples were run on 12% SDS-PAGE gel and transferred onto nitrocellulose membranes (Biorad). Membranes were washed with 3x for 5 mins in TBST (20mM Tris, 150mM NaCl and Tween 20 0.1% w/v), then blocked for 1 hour in 5% BSA in TBST (Fisher Scientific). The antibodies used were anti-GFP (Abcam), anti-Profilin 1 (CST), anti-Actin (CST), and anti-phospho Tyr129 (ECM). The secondary antibodies used were Goat Anti-Mouse IgG HRP (Abcam), and Goat Anti-Rabbit IgG HRP (Abcam).

## CHAPTER 3

### RESULTS

#### 3.1 Generation of mutant PFN1 constructs

I chose to investigate the functions of Tyr131 and Ser135 because Tyr131 is orthologous to Tyr129 on HPFN1 and Ser135 is conserved in HPFN1. Whether Tyr131 or Ser135 have a role in non-canonical Wnt signaling and whether they can regulate development in *Xenopus* is unknown. To answer this question, I generated various mutants of Tyr131 and Ser135 by PCR to investigate the functions of these residues. EGFP CS2+XPFN1 plasmid expression vector was used as a template to generate Tyrosine131Alanine (PFN1-Tyr131Ala), Serine135Alanine (PFN1-Ser135Ala), Ser135Glutamic acid (PFN1-Ser135Glu) single mutants, and PFN1-Tyr131Ala;Ser135Ala double mutant (Figure 18). Alanine was chosen because it is a neutral amino acid and mimics a protein that mimics an unphosphorylated state. Conversely, glutamic acid is negatively charged and acts as a phosphomimetic form of PFN1 at Ser135.

I generated mutants of Tyr131 and Ser135 using the QuikChange PCR method to investigate the potential functional role of these residues (Figure 18). All generated constructs were sequenced to ensure the mutations were present in the correct position and no additional mutants were detected anywhere else in the coding sequence.



Figure 18. *PFN1* mutants were successfully generated by QuikChange mutagenesis. GFP-XPFN1 was used as a template for a PCR based mutagenesis of Tyr131 and Ser135. The regions on PFN1 1 that were targeted for mutagenesis are highlighted in blue. Confirmed mutations are highlighted in green.

### 3.2 The roles of Tyr131 and Ser135 in early embryonic development

Having successfully cloned the mutant constructs, I first tested their effects when expressed during early *Xenopus* development. Previous studies have shown that overexpression or knockdown of PFN1 mRNA in *Xenopus* results in a blastopore closure defect<sup>124</sup>. mRNA was transcribed *in vitro*, injected into four-cell-stage *Xenopus laevis* embryos dorsally or ventrally, and injected embryos were allowed to develop for approximately 72 hrs before fixation. Images were taken using a fluorescent microscope to confirm the successful translation of mRNA (Figure 19). Injected embryos were collected, lysed, and a Western blot was performed to confirm the sizes of mutant XPFN1 proteins (Figure 20.)

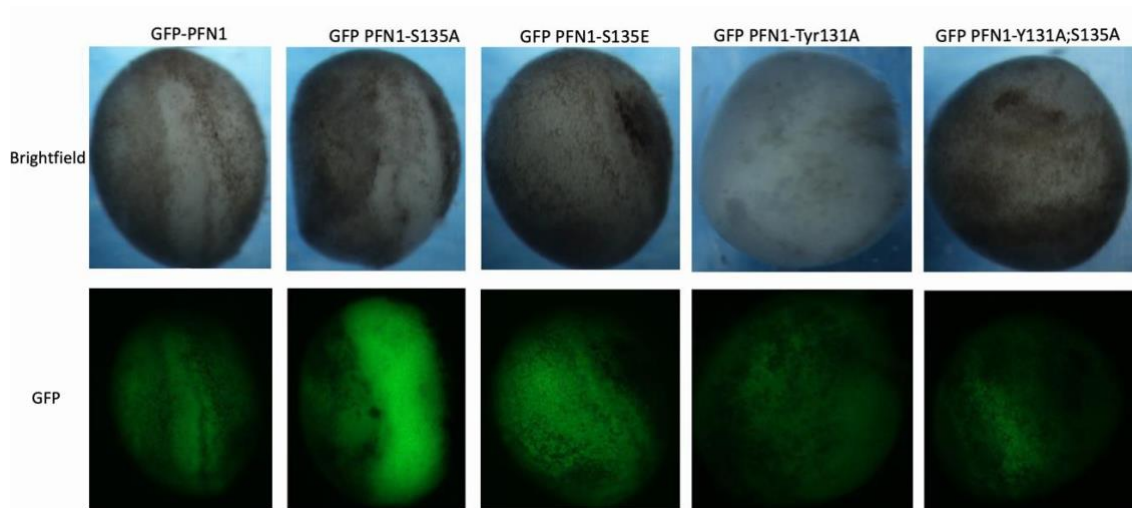


Figure 19. *GFP-PFN1 and GFP tagged PFN1 mutants express in Xenopus embryos.* Embryos were injected with 250pg of GFP-PFN1, GFP PFN1-Ser135Ala, GFP PFN1-Ser135Glu, GFP PFN1-Tyr131Ala, and GFP PFN1-Tyr131Ala; Ser135Ala mRNA at the four-cell stage. Images were taken 24 hours after injection on a fluorescent microscope. Visual confirmation of GFP signal shows that injected mRNA was successfully translated into protein.

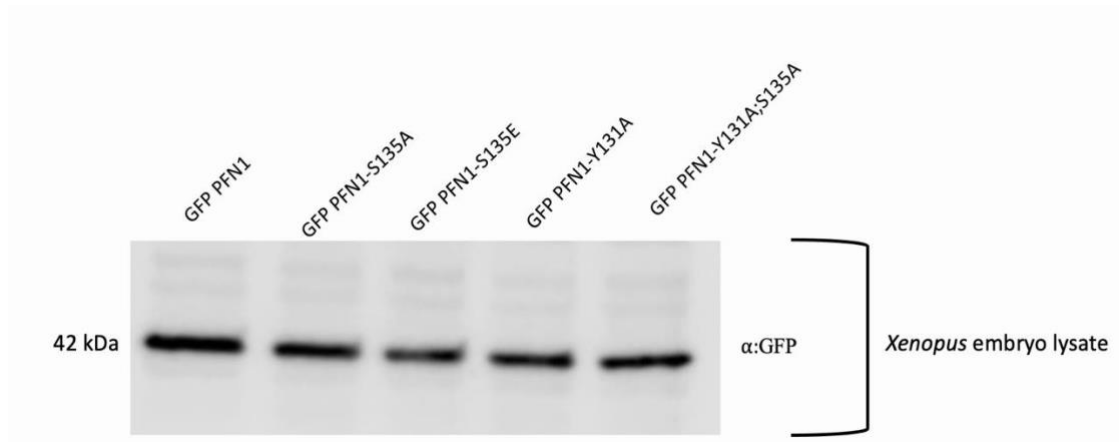


Figure 20. *Injected Xenopus embryos express mutant XPFN1 proteins at the correct size.* 250pg of each mRNA was injected into *Xenopus* embryos and lysed after 48 hours. Samples were run on a western blot to confirm the size of the translated proteins. The membrane was blotted with a GFP polyclonal antibody.

I next injected embryos with XPFN1 and XPFN1 mutant mRNAs test the roles of Tyr131 and Ser135 in gastrulation. Embryos were scored for severity in gastrulation defects. Embryos that displayed a small open blastopore were scored as having a mild gastrulation defect. Embryos that had a large open blastopore were scored as having a severe gastrulation defect. Embryos that arrested prior to gastrulation were scored as did not gastrulate. Overexpression and knockdown of PFN1 has been shown to cause an open blastopore<sup>124</sup>. Overexpression of PFN1-Ser135Ala has no effect on gastrulation while PFN1-Ser135Glu produces an open blastopore phenotype, as compared to XPFN1 (Figure 21). Overexpression of PFN1-Ser135Glu, however, shows a 20% increase in penetrance of the phenotypes at both 250pg and 500pg compared to PFN1. Approximately 40% of embryos injected with 250pg of either mRNA demonstrate severe gastrulation defects. At 500pg, approximately 50% of injected embryos show a severe gastrulation defect.

PFN1-Tyr131Ala produces a higher frequency of open blastopore defects in a dose-dependent manner. At 250pg, 65% of embryos show severe gastrulation defects while almost 90% of embryos display severe gastrulation defects in embryos injected with 500pg of mRNA. Embryos injected with the double-mutant PFN1-Tyr131Ala; Ser135Ala display a cytokinesis defect: embryos arrest before gastrulation occurs. In addition to the 80% of embryos injected that failed to gastrulate between stages 9 and 10, 15% display an open blastopore. Statistical analysis on total number of phenotypes in embryos injected with 250pg and 500pg shows that PFN1-Ser135Ala, PFN1-Ser135Glu, PFN1-Tyr131Ala, and PFN1-Tyr131Ala;Ser135Ala are statistically different from PFN1. At 250pg, embryos injected with PFN1-Ser135Ala display 35% fewer phenotypes, compared to PFN1. Embryos injected with PFN1-Ser135Glu display a 5% increase in phenotypes, compared to PFN1. Embryos injected with PFN1-Tyr131Ala and PFN1-Tyr131Ala;Ser135Ala both show an almost two fold increase in phenotypes, compared to PFN1 (88% and 93%, respectively). At 500pg, embryos injected with PFN1-Ser135Ala display 47% fewer phenotypes, compared to PFN1. Embryos injected with PFN1-Ser135Glu display a 12% increase in phenotypes, compared to PFN1. Embryos injected with PFN1-Tyr131Ala and PFN1-Tyr131Ala;Ser135Ala show an increase in phenotypes, compared to PFN1 (95% and 99%, respectively) (Figure 22).

Embryos injected ventrally displayed no phenotype and developed the same as wild-type embryos. (Figure 23).

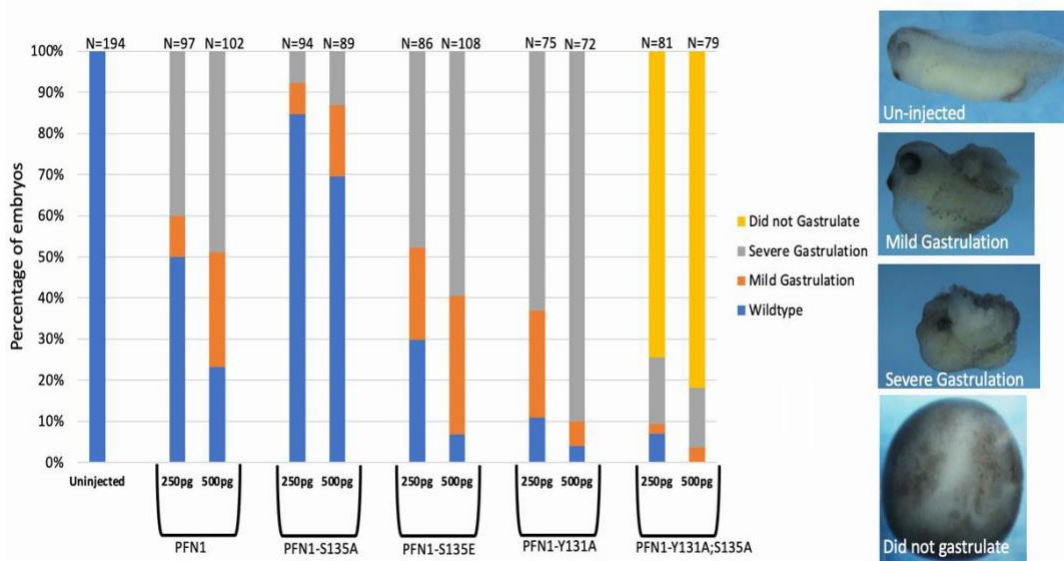


Figure 21. *Dorsal injection of Tyr131Ala causes cytokinesis defects.* Embryos were injected at the 4-cell stage with mRNA expressing XPFN1 and each mutant at 250pg or 500pg. Embryos were then scored based on the phenotypes observed. Embryos with a small open blastopore and a curved axis with scored as mild gastrulation. Embryos with a large open blastopore were scored as severe gastrulation. Developing embryos that arrested before gastrulation occurred were scored as did not gastrulate. This experiment was done in biological and technical triplicates.

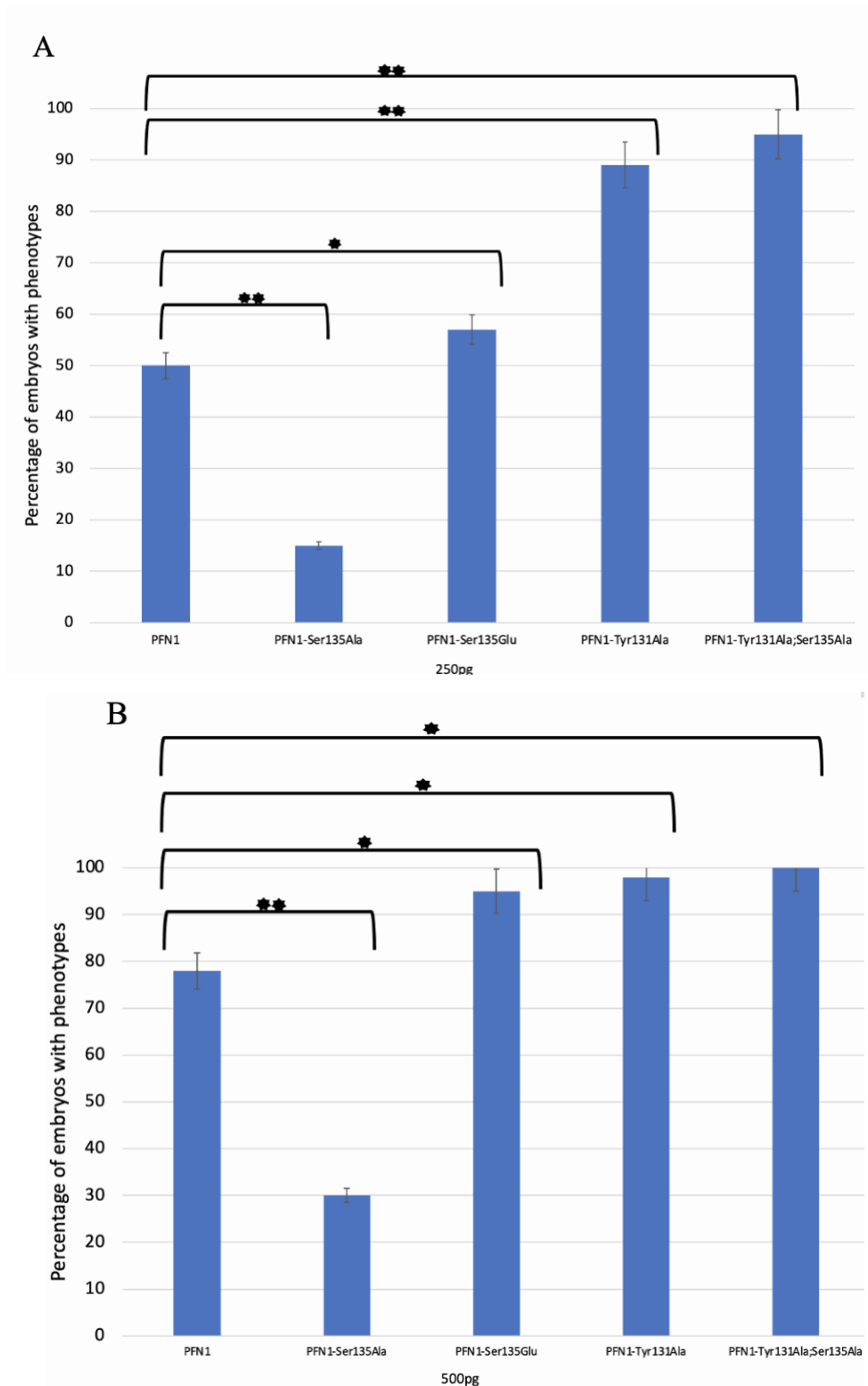


Figure 22. *Quantification of phenotypes of dorsal mRNA injections.* A) Total phenotypes of embryos injected with 250pg of each mRNA mutant were quantified and tested for statistical difference from PFN1 using T-test. B) Total phenotypes of embryos injected with 500pg of each mRNA mutant were quantified and tested for statistical difference from PFN1 using T-test.

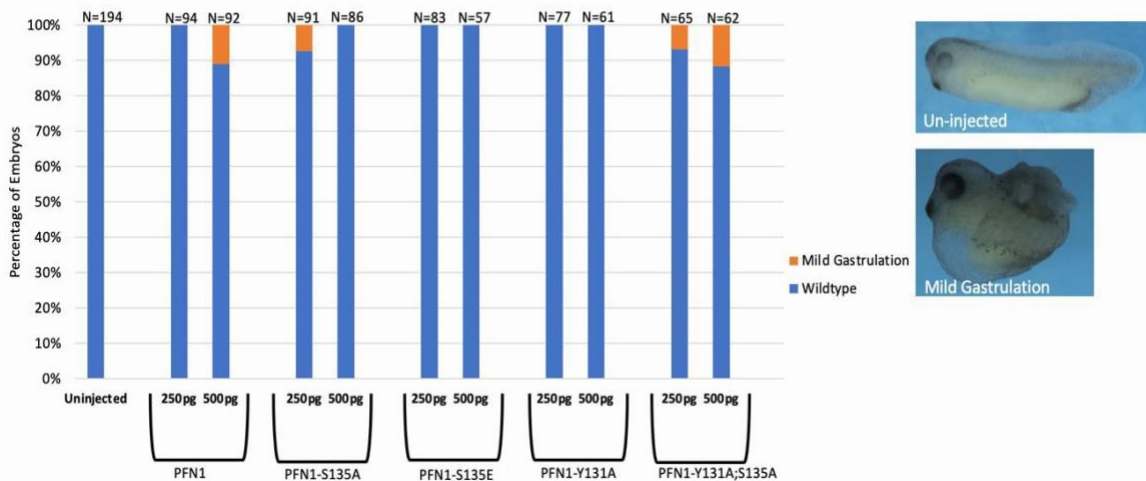


Figure 23. *Ventral injection of XPFN1 mutants produces no effects.* Embryos were injected at the 4-cell stage with mRNA expressing XPFN1 and each mutant at 250pg or 500pg. Embryos were then scored based on the phenotypes observed. Embryos with a small open blastopore and a curved axis with scored as mild gastrulation. This experiment was done in biological and technical triplicates.

### 3.3 Visualizing the effects of PFN1 mutants on the actin cytoskeleton in HeLa cells

To investigate the roles of Tyr131 and Ser135 on the actin cytoskeleton, PFN1 plasmids expressing mutant PFN1 protein were transfected into HeLa cells. Cells were serum starved in Opti-Mem low serum media to visualize changes in actin fibers without negatively affecting cell health or morphology. Wnt5a was used to activate non-canonical Wnt signaling. 1ug of GFP-empty vector was transfected into HeLa cells and allowed to express for 48 hours before being treated with Wnt5a (Figure 23A). Cells were then fixed and stained with Alexa-555-conjugated Phalloidin to label F-actin. Actin fibers were counted to test whether each mutant interferes with Wnt5a mediated actin fiber

formation. HeLa cells have an average of 10 actin fibers. Cells with greater than 10 actin fibers in control media or those treated with Wnt5a were then quantified. The lengths and widths of images obtained by confocal microscopy were measured on imageJ<sup>138</sup>. The cell measurements were completed blinded. Wnt5a increased actin fiber formation, as shown by the 20% increase in percentage of cells with greater than 10 fibers (62% control and 82% in Wnt5a treated cells) (Figure 23B). Treatment of Wnt5a increases the length to width ratio in HeLa cells. The average length/width ratio is 2.25 in control media, and 2.75 in Wnt5a treatment, demonstrating a 22% increase in the ratio of length to width (Figure 23C).

1 $\mu$ g of pCS2+GFP-XPFN1 was transfected into HeLa cells and allowed to express for 48 hours before being treated with Wnt5a (Figure 24A). The average length/width ratio is 3.75 in control media, and 4.25 in Wnt5a treatment, demonstrating a 13% increase in the ratio of length to width (Figure 24B). GFP-XPFN1 increases Wnt5a mediated actin fiber formation, as shown by a 45% reduction in cells with fewer than 10 fibers in the Wnt5a treated condition (Figure 24C).

1 $\mu$ g of pCS2+GFP PFN1-Ser135Ala was transfected into HeLa cells and allowed to express for 48 hours before being treated with Wnt5a (Figure 25A). The average length/width ratio is 1.75 in control media, and 2.25 with Wnt5a treatment, demonstrating a 29% increase in the ratio of length to width (Figure 25B). GFP PFN1-Ser135Ala does not prevent Wnt5a mediated actin fiber formation, as shown by a 40% reduction in cells with fewer than 10 actin fibers in the Wnt5a treated condition (Figure 25C).

1 $\mu$ g of pCS2+GFP PFN1-Ser135Glu was transfected into HeLa cells and allowed to express for 48 hours before being treated with Wnt5a (Figure 26A). GFP PFN1-Ser135Glu does not prevent Wnt5a mediated actin fiber formation, as shown by a 44% reduction in cells with fewer than 10 actin fibers in the Wnt5a treated condition (Figure 26B). The average cell length/width ratio is 2.80 in control media, and 3.75 in Wnt5a treatment, demonstrating a 33% increase in the ratio of length to width (Figure 26C).

1 $\mu$ g of pCS2+GFP PFN1-Tyr131Ala was transfected into HeLa cells and allowed to express for 48 hours before being treated with Wnt5a (Figure 27A). GFP PFN1-Tyr131Ala also prevents Wnt5a mediated actin fiber formation, as shown by a 45% reduction in cells with greater than 10 actin fibers in the Wnt5a treated condition, compared to GFP-EV (Figure 27B). The average length/width ratio is 4.75 in control media, and 2.05 in Wnt5a treatment, demonstrating a 43% decrease in the ratio of length to width (Figure 27C).

1 $\mu$ g of pCS2+GFP PFN1-Tyr131Ala;Ser135Ala was transfected into HeLa cells and allowed to express for 48 hours before being treated with Wnt5a (Figure 28A). GFP PFN1-Tyr131Ala;Ser135Ala prevents Wnt5a mediated actin fiber formation, as shown by a 49% reduction in cells with greater than 10 actin fibers in the Wnt5a treated condition, compared to GFP-EV (Figure 28B). The average length/width ratio is 6.1 in control media, and 3.05 in Wnt5a treatment, demonstrating a 51% decrease in the ratio of cell length to width (Figure 28C).

To test the effects of Tyr131 and Ser135 on cytokinesis defects, I measured multinucleation in transfected HeLa cells. Multinucleation was defined as at least 2 nuclei. Multinucleation is associated with an inability to fully complete cytokinesis (Figure 29). Quantification of multinucleation shows that overexpression of GFP-PFN1 and the mutants increases the incidence of multinucleation. Overexpression of GFP-PFN1, GFP PFN1-Ser135Ala, and GFP PFN1-Ser135Glu produced a two-fold increase in incidence of multinucleation compared to GFP-EV. Incidence of multinucleation doubles in cells transfected with PFN1-Tyr131Ala and PFN1-Tyr131Ala;Ser135Ala, compared to GFP-PFN1 and the serine mutants (Figure 29). Treatment of Wnt5a increases the frequency of multinucleation in all conditions except GFP-empty vector by approximately 10%. Overexpression of PFN1-Tyr131Ala and PFN1-Tyr131Ala;Ser135Ala causes a 60% and 65% incidence of multinucleation, respectively.

I next compared the effects of the mutants to produce multinucleated cells to PFN1 using an independent samples T-test in control and Wnt5a treated samples. Incidences of multinucleation in PFN1-Ser135Ala and PFN1-Ser135Glu was not found to be statistically different from PFN1 in either control or Wnt5a treated cells (Figure 31). Incidences of multinucleation in PFN1-Tyr131Ala and PFN1-Tyr131Ala;Ser135Ala is statistically different from PFN1 in both control or Wnt5a treated cells. Overexpression of PFN1-Tyr131Ala and PFN1-Tyr131Ala;Ser135Ala result in a 25% and 27%, respectively increase in multinucleation compared to PFN1. The incidence of multinucleation in Wnt5a treated cells increased by 31% and 35% in PFN1-Tyr131Ala and PFN1-Tyr131Ala;Ser135Ala respectively, compared to PFN1 (Figure 31).

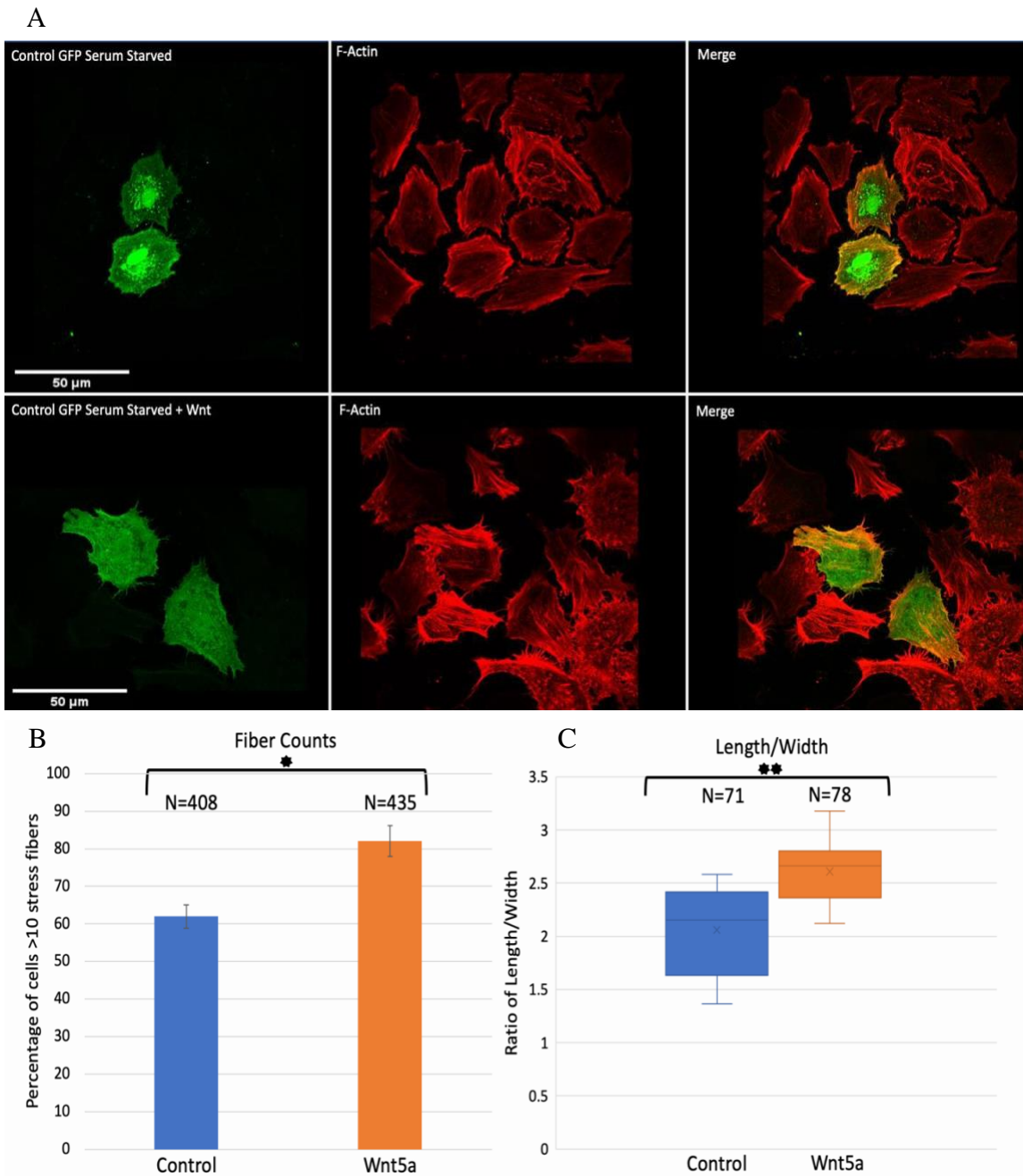


Figure 24. *Wnt5a* increases actin fiber formation and the ratio of length/width in *HeLa* cells. A) 1 $\mu$ g of GFP-empty vector was transfected into HeLa cells and treated with Wnt5a after 48 hours. Cells were fixed in 4%PFA and F-actin was labelled with an Alexa 555 conjugated Phalloidin stain. B) Images were taken and the lengths and widths of transfected cells were measured using ImageJ, according to Hassan 2019. The ratio of length to width was then plotted and a T-test was used to determine if the observed differences are statistically significant. C) Quantification of cells with fewer than 10 fibers shows that Wnt5 increases actin fiber formation. Number of cells evaluated is shown at the top of each bar. All experiments were done in biological and technical triplicates. Image quantifications were completed blinded. \* Signifies a p value of >0.05 and \*\* signifies a p value of >0.005.

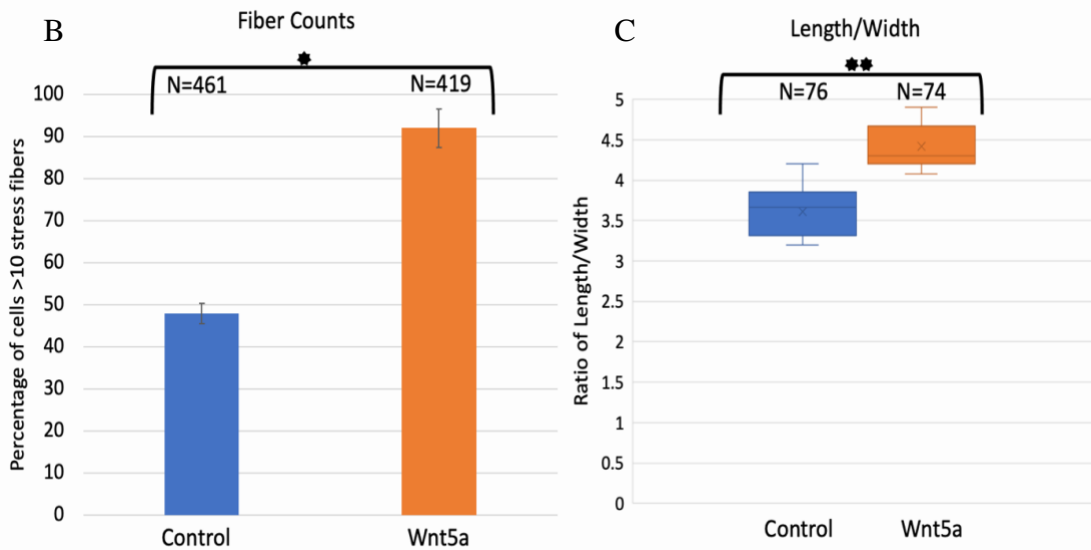
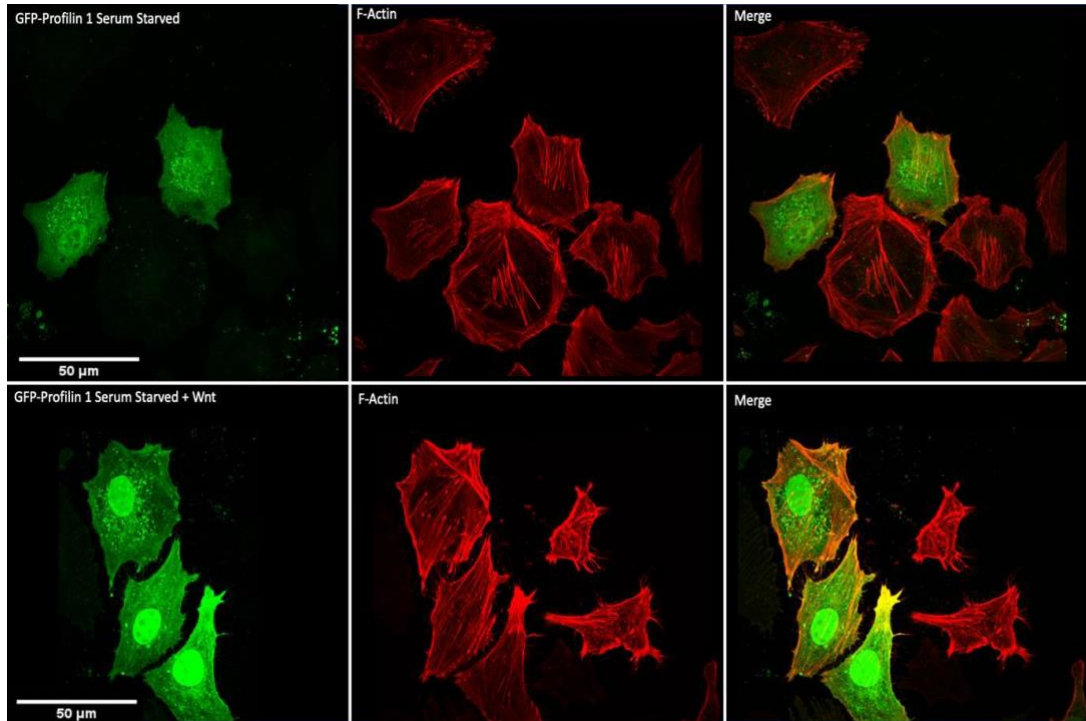


Figure 25. *Wnt5a* increases actin fiber formation and the ratio of length/width in cells transfected with GFP-XPFN1. A) 1 $\mu$ g of GFP-XPFN1 was transfected into HeLa cells and treated with Wnt5a after 48 hours. Cells were fixed in 4%PFA and F-actin was labelled with an Alexa 555 conjugated Phalloidin stain. B) Images were taken and the lengths and widths of transfected cells were measured using ImageJ, according to Hassan 2019. The ratio of length to width was then plotted and a T-test was used to determine if the observed differences are statistically significant. C) Quantification of cells with fewer than 10 fibers shows that GFP-XPFN1 increases Wnt5a-mediated actin fiber formation. Number of cells evaluated is shown at the top of each bar. All experiments were done in biological and technical triplicates. Image quantifications were completed blinded. \* Signifies a p value of >0.05 and \*\* signifies a p value of >0.005.

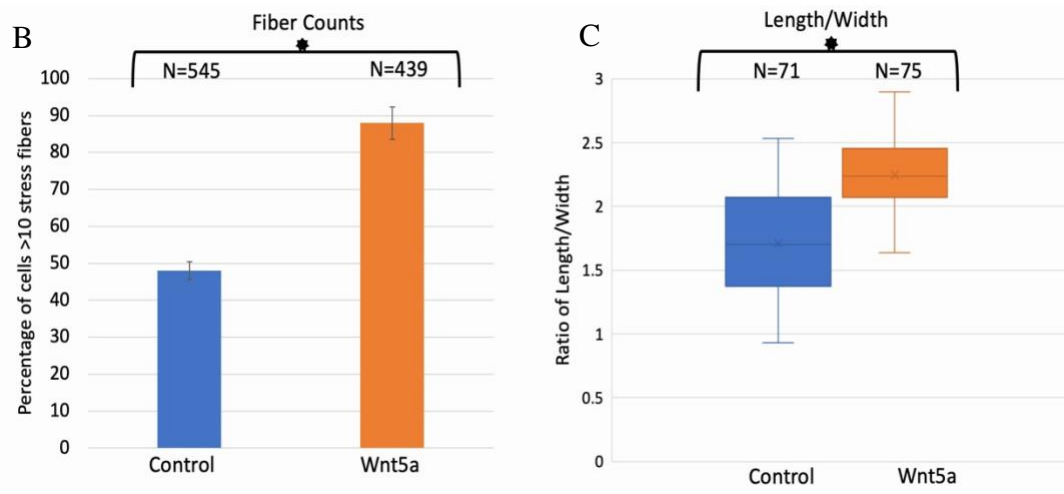
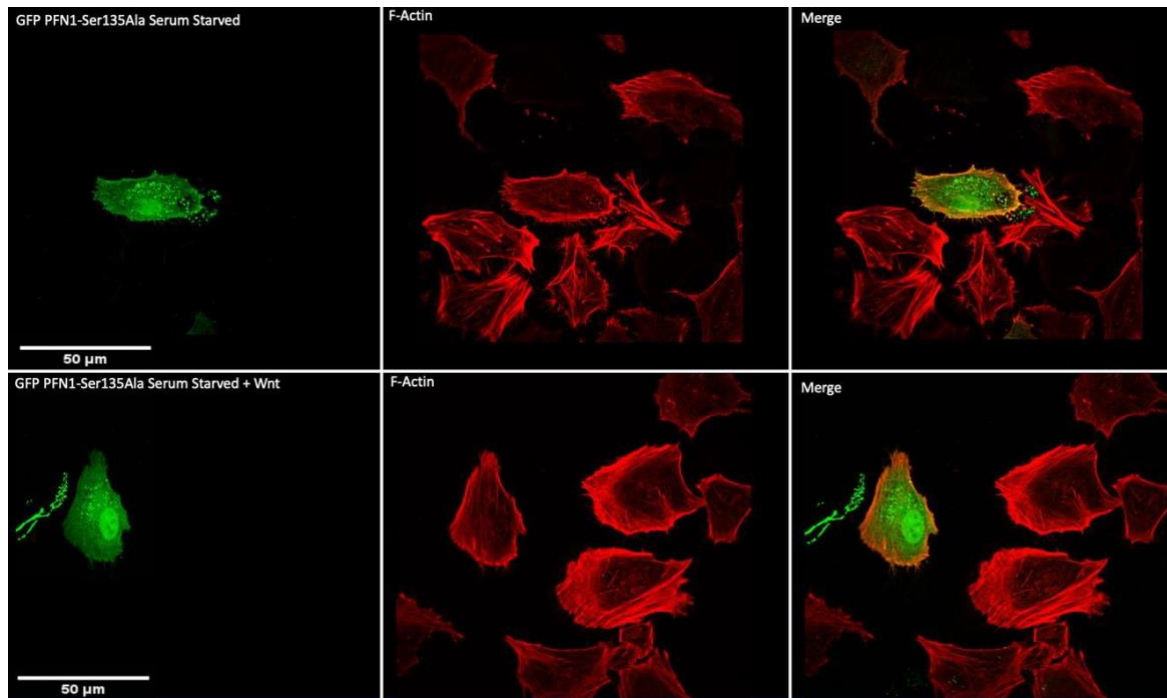


Figure 26. *GFP PFN1-Ser135Ala does not prevent Wnt5a-mediated actin fiber formation nor the increase in cell length/width ratio.* A) 1 $\mu$ g of GFP PFN1-Ser135Ala was transfected into HeLa cells and treated with Wnt5a after 48 hours. Cells were fixed in 4%PFA and F-actin was labelled with an Alexa 555 conjugated Phalloidin stain. B) Images were taken and the lengths and widths of transfected cells were measured using ImageJ, according to Hassan 2019. The ratio of length to width was then plotted and a T-test was used to determine if the observed differences are statistically significant. GFP PFN1-Ser135Ala does not prevent an increase in the cell length/width ratio associated with treatment Wnt5a. C) Quantification of cells with fewer than 10 actin fibers shows that GFP PFN1-Ser135Ala does not prevent Wnt5a-mediated actin fiber formation. Number of cells evaluated is shown at the top of each bar. All experiments were done in biological and technical triplicates. Image quantifications were completed blinded. \* Signifies a p value of >0.05 and \*\* signifies a p value of >0.005

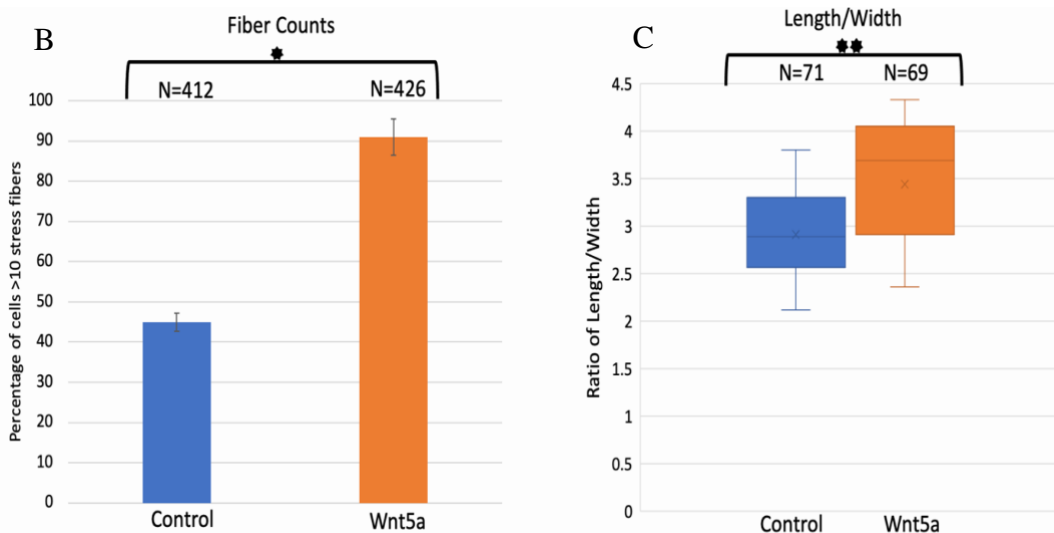
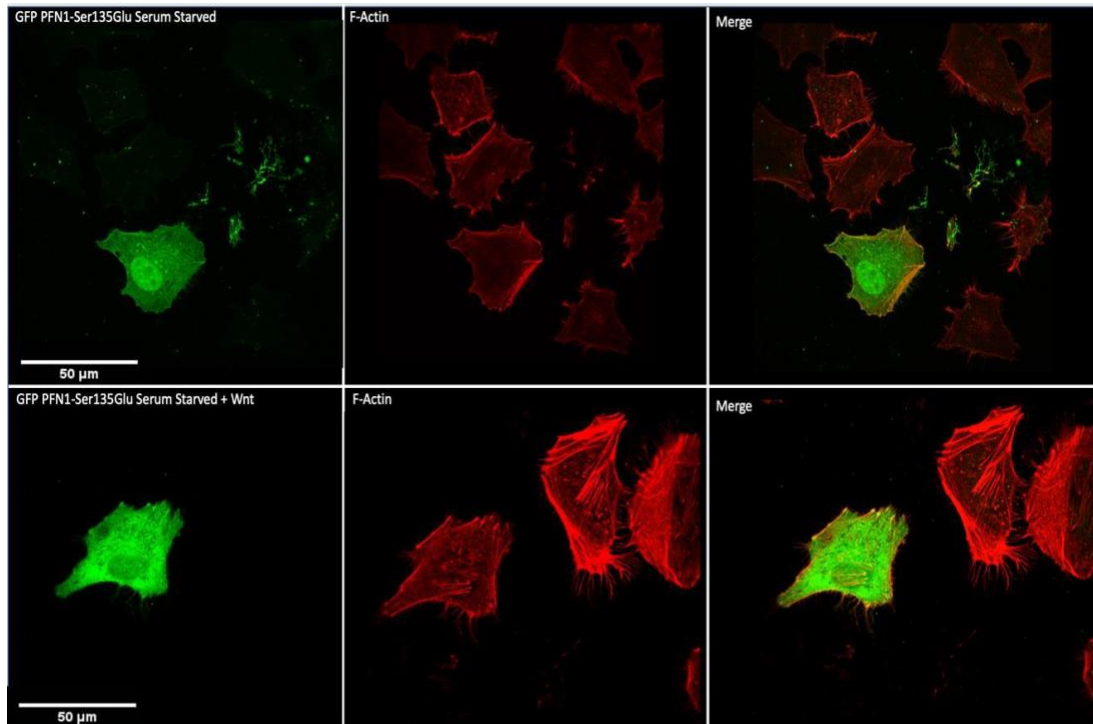


Figure 27. *Wnt5a* increases the ratio of length/width and actin fiber formation in cells transfected with GFP PFN1-Ser135Glu. A) 1 $\mu$ g of GFP PFN1-Ser135Glu was transfected into HeLa cells and treated with Wnt5a after 48 hours. Cells were fixed in 4% PFA and F-actin was labelled with an Alexa 555 conjugated Phalloidin stain. B) Images were taken and the lengths and widths of transfected cells were measured using ImageJ, according to Hassan 2019. The ratio of length to width was then plotted and a T-test was used to determine if the observed differences are statistically significant. GFP PFN1-Ser135Glu does not prevent an increase in the cell length/width ratio associated with treatment Wnt5a. C) Quantification of cells with fewer than 10 fibers shows that GFP PFN1-Ser135Glu does not prevent Wnt5a-mediated actin fiber formation. Number of cells evaluated is shown at the top of each bar. All experiments were done in biological and technical triplicates. Image quantifications were completed blinded. \* Signifies a p value of  $>0.05$  and \*\*

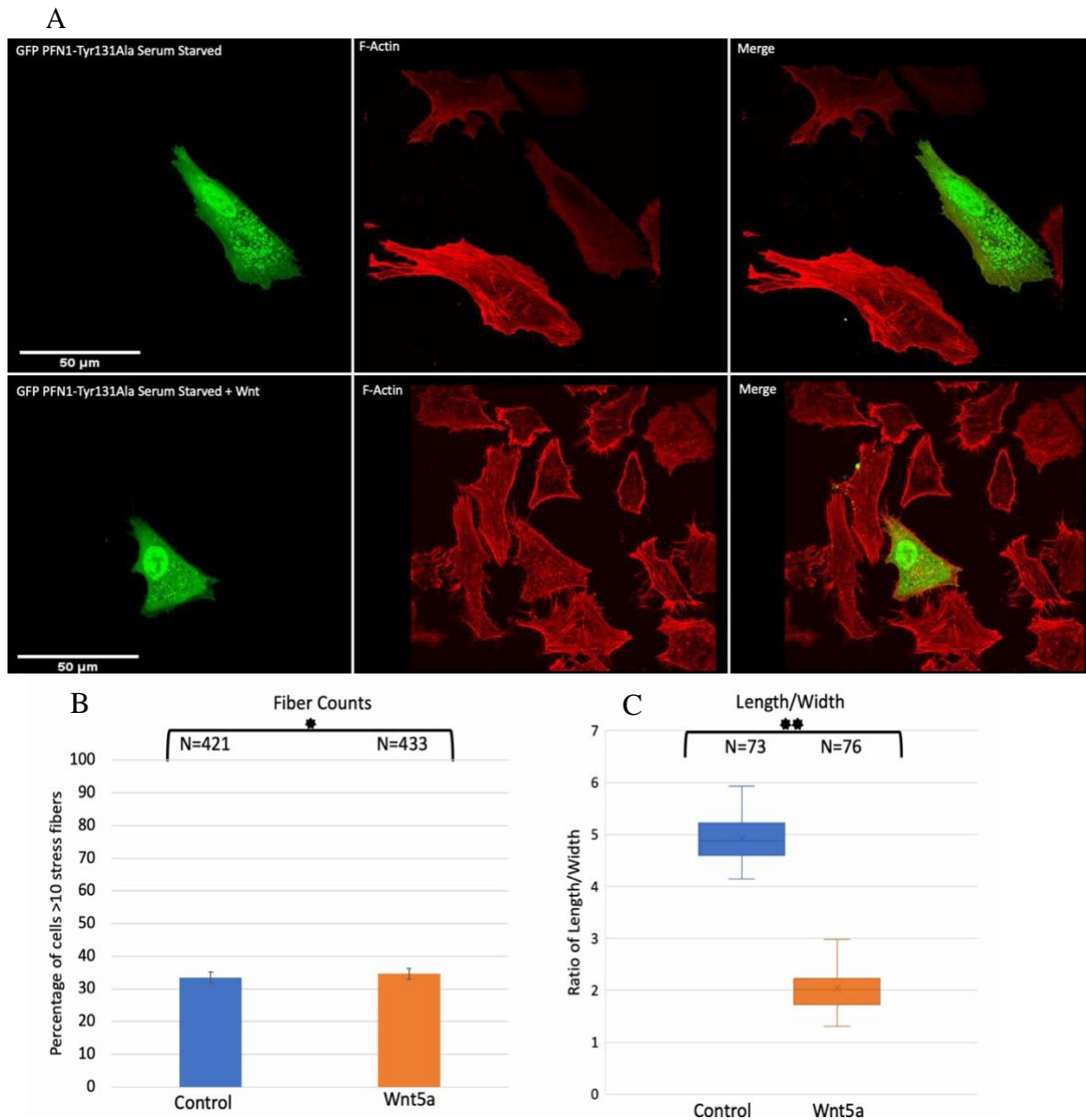


Figure 28. *GFP PFN1-Tyr131Ala prevents Wnt5a-mediated increases in cell length/width ratio and actin fiber formation.* A) 1 $\mu$ g of GFP PFN1-Tyr131Ala was transfected into HeLa cells and treated with Wnt5a after 48 hours. Cells were fixed in 4%PFA and F-actin was labelled with an Alexa 555 conjugated Phalloidin stain. B) Images were taken and the lengths and widths of transfected cells were measured using ImageJ, according to Hassan 2019. The ratio of length to width was then plotted and a T-test was used to determine if the observed differences are statistically significant. GFP PFN1-Tyr131Ala lowers the ratio of cell length to width and prevents Wnt5a mediated actin fiber formation. C) Quantification of cells with fewer than 10 fibers shows that GFP PFN1-Tyr131Ala prevents Wnt5a-mediated actin fiber formation. Number of cells evaluated is shown at the top of each bar. All experiments were done in biological and technical triplicates. Image quantifications were completed blinded. \* Signifies a p value of >0.05 and \*\* signifies a p value of >0.005.

A

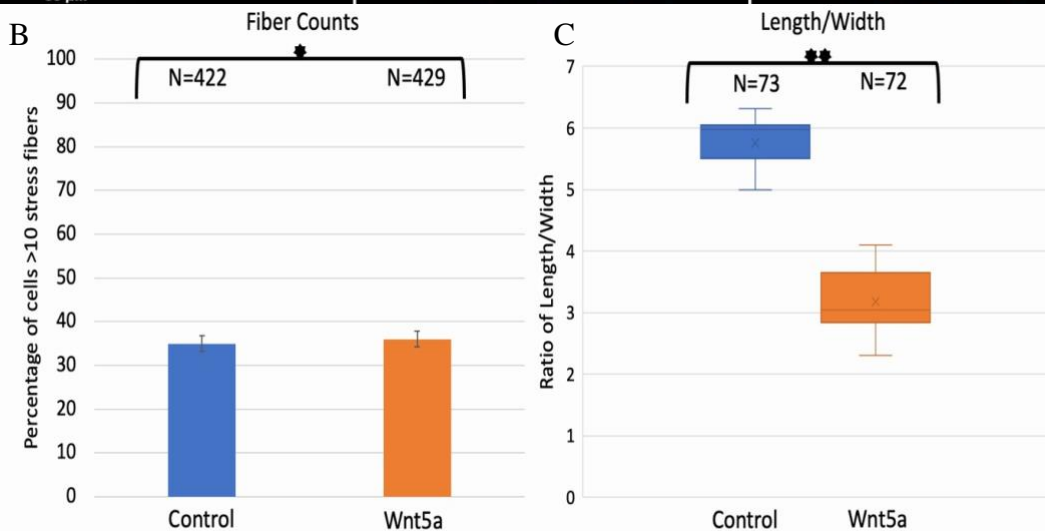
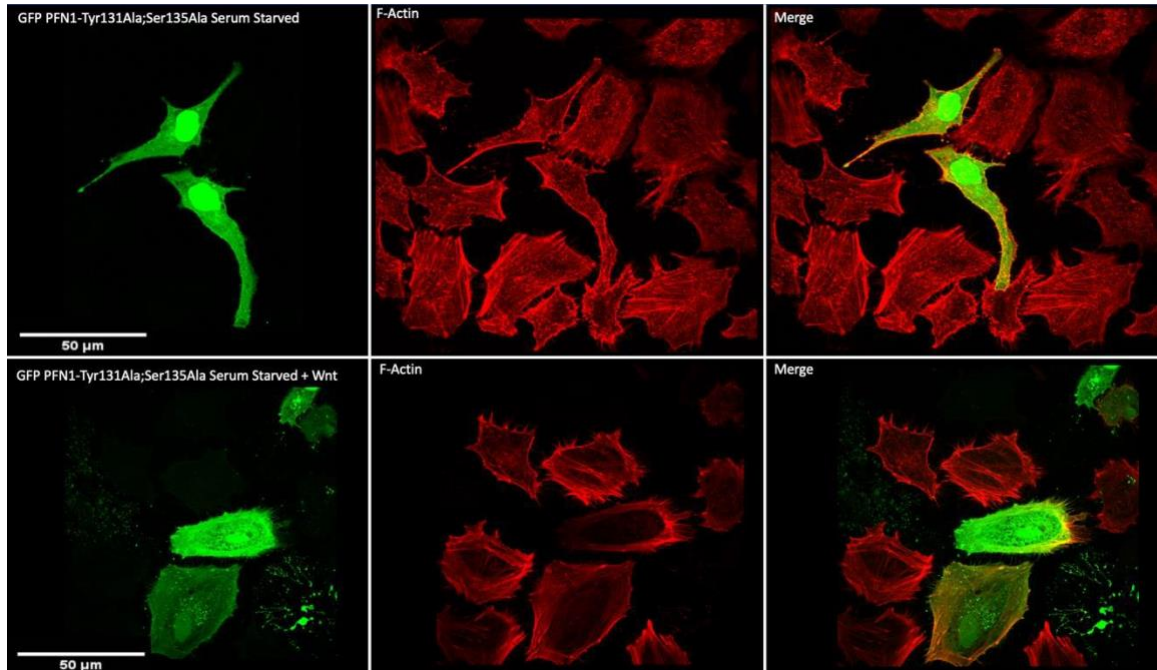


Figure 29. *GFP PFN1-Tyr131Ala; Ser135Ala prevents Wnt5a-mediated increases in cell length/width ratio and actin fiber formation.* A) 1 $\mu$ g of GFP PFN1-Tyr131Ala; Ser135Ala was transfected into HeLa cells and treated with Wnt5a after 48 hours. Cells were fixed in 4% PFA and F-actin was labelled with an Alexa 555 conjugated Phalloidin stain. B) Images were taken and the lengths and widths of transfected cells were measured using ImageJ, according to Hassan 2019. The ratio of length to width was then plotted and a T-test was used to determine if the observed differences are statistically significant. GFP PFN1-Tyr131Ala; Ser135Ala lowers the ratio of cell length to width and prevents Wnt5a mediated actin fiber formation. C) Quantification of cells with fewer than 10 fibers shows that GFP PFN1-Tyr131Ala; Ser135Ala prevents Wnt5a-mediated actin fiber formation. Number of cells evaluated is shown at the top of each bar. All experiments were done in biological and technical triplicates. Image quantifications were completed blinded. \* Signifies a p value of  $>0.05$  and \*\* signifies a p value of  $>0.005$ .

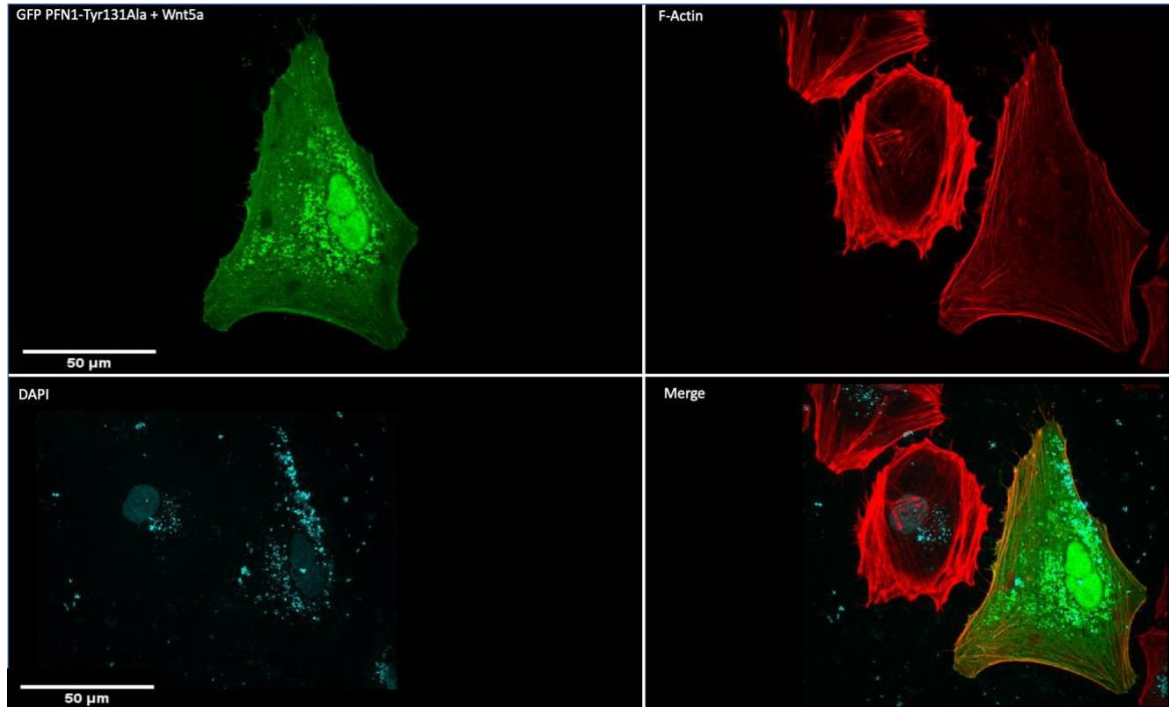


Figure 30. *Visual representation of multinucleation.* Multinucleation is defined as a large single cell with more than one nucleus. Multinucleation is associated with defects in cytokinesis. Cells were fixed in 4% PFA, F-actin was labelled with an Alexa 555 conjugated Phalloidin stain, and DAPI was used to label the nucleus. All experiments were done in biological and technical triplicates.

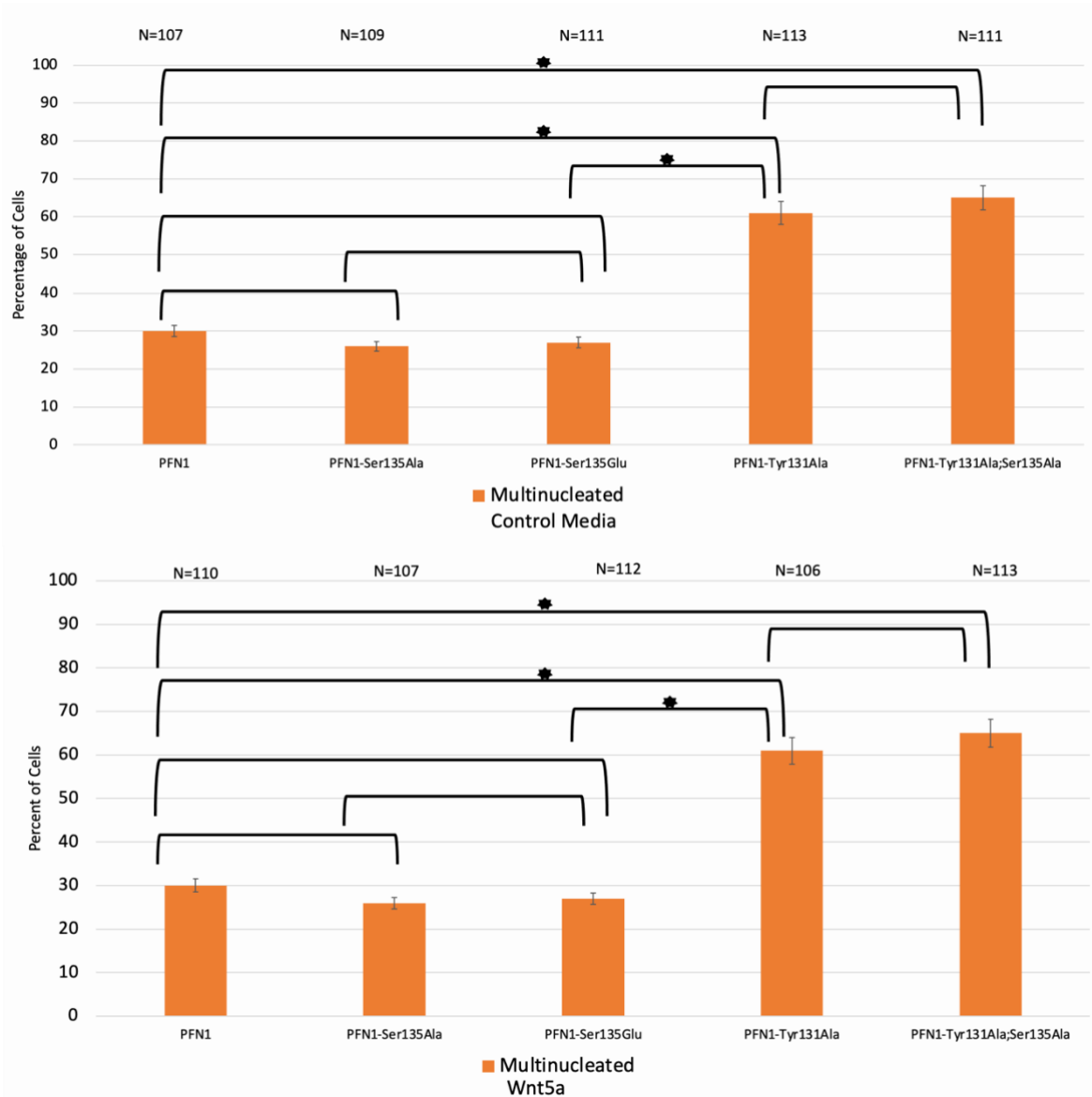


Figure 31. *GFP PFN1-Tyr131Ala increases multinucleation in HeLa cells, compared to GFP-PFN1.* A) 1 $\mu$ g of each plasmid was transfected into HeLa cells. They were fixed and scored for multinucleation. B) 1 $\mu$ g of each plasmid was transfected into HeLa cells and treated with Wnt5a. They were fixed and scored for multinucleation. Number of cells evaluated is shown at the top of each bar. \* Signifies a p value of >0.05 and \*\* signifies a p value of >0.005. This experiment was completed in biological and technical triplicates. Image quantifications were completed blinded.

### **3.4 Ser135 has a role in binding of PFN1 to the FH1 domain of Daam1**

Having shown that overexpression of PFN1 mutants produces different effects on the actin cytoskeleton in cultured cells, I next investigated whether the binding of PFN1 to Daam1 is regulated by Tyr131 or Ser135. I performed GST pulldown and co-immunoprecipitation binding assays to examine the binding of PFN1 and its mutants with Daam1. The plasmids used in this study are diagramed in Figure 32.

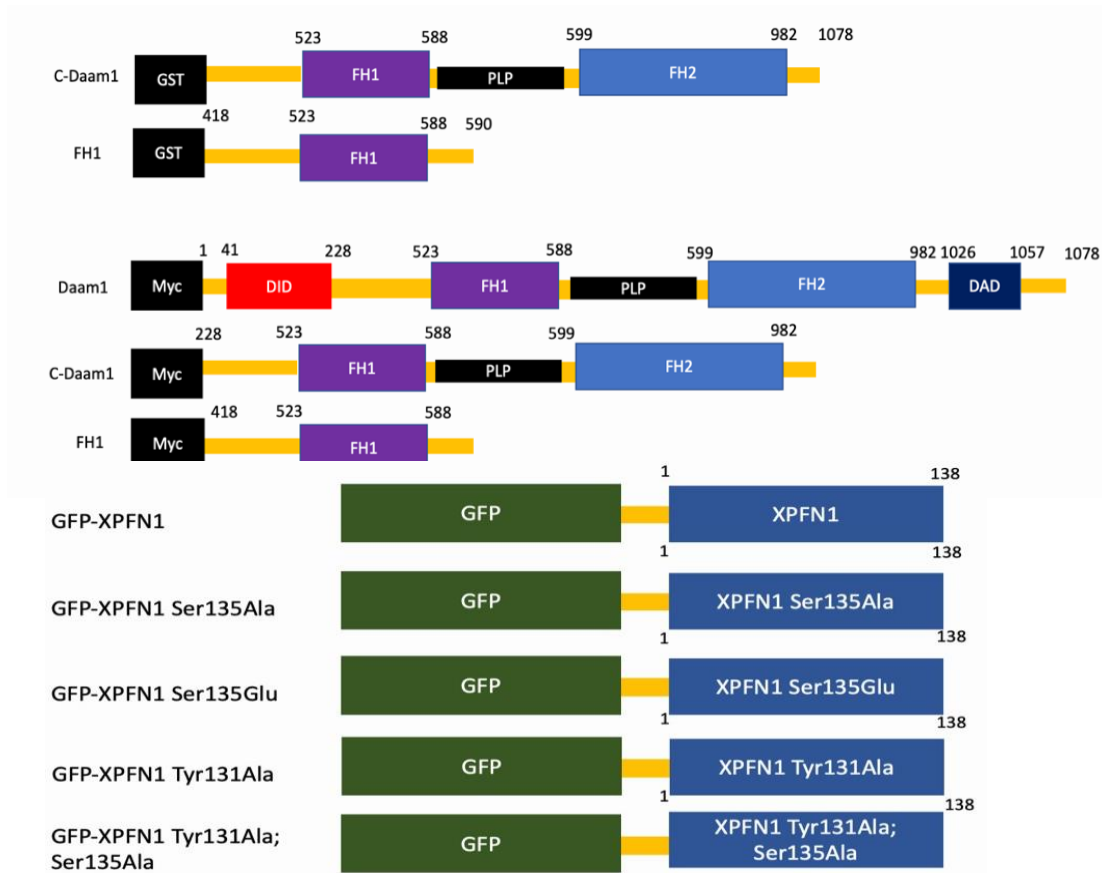


Figure 32. *PFN1* and *Daam1* constructs used in binding assays. GST-cDaam1 and Myc-cDaam1 both contain the FH1 and FH2 domains. PLP sites are present in between the two domains. GST-FH1 and Myc-FH1 contain only the FH1 domain. Myc-Daam1 is the full-length version of Daam1. It contains the DID, FH1, FH2, and DAD domains. The GFP tagged PFN1 constructs used in this study are displayed below. Numbers indicate the position of amino acids.

Previous studies show that PFN1 binds to the FH1 domain of Daam1 and this binding occurs within the c-Daam1 region. To test whether the binding of PFN1 to Daam1 is affected by Tyr131 or Ser135, I performed a GST-pulldown assay. GFP-tagged PFN1 mutants were transfected into HEK293T and samples were incubated with Glutathione agarose beads coupled to GST-cDaam1, GST-FH1, or GST-empty vector.

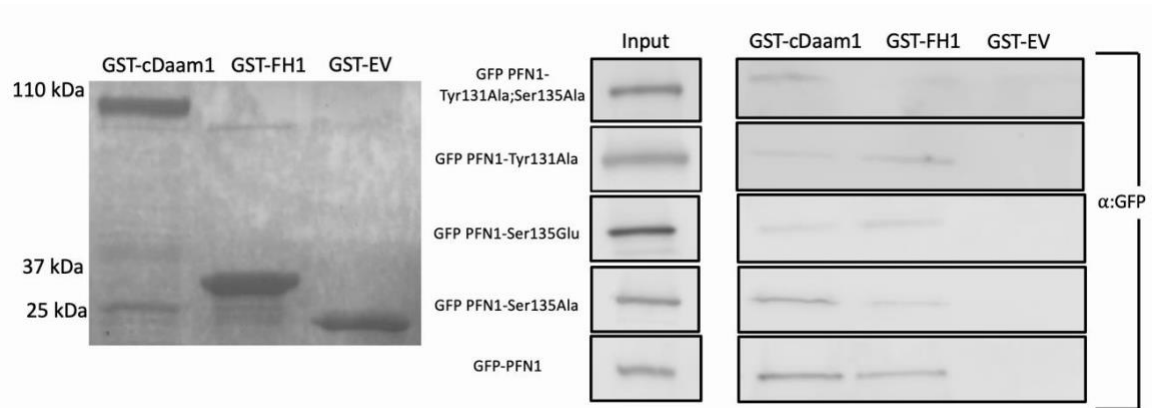


Figure 33. ***PFN1-Ser135Ala lowers binding affinity of PFN1 to FH1.*** GST-cDaam1, GST-FH1, and GST-EV were grown in *E.coli* cells, lysed, purified using GST beads, and visualized by Coomassie Staining to confirm correct protein sizes. GFP-PFN1 and mutants were then transfected into HEK293T cells and allowed to express for 48 hours before lysing. Lysates were incubated with beads coupled to each GST protein overnight, washed, and changes in binding were then evaluated by Western blotting. A polyclonal GFP antibody was used.

GST-cDaam1, GST-FH1, and GST-Empty Vector (EV) were grown and purified from *E.coli* cells and visualized by Coomassie staining (Figure 33) GFP PFN1 was shown to bind to GST-cDaam1 and FH1 equally, as does GFP PFN1-Ser135Glu. However, GFP PFN1-Ser135Ala does has a lower binding affinity to GST-FH1. GFP PFN1-Tyr131Ala binds equally to GST-cDaam1 and GST-FH1, while the double mutant binds weakly to GST-cDaam1 and loses binding to GST-FH1(Figure 33).

Quantification of GST pulldown binding assays shows GFP-PFN1 shows an almost equal binding affinity between GST-cDaam1 and GST-FH1 (Figure 34). GFP-PFN1-Ser135Ala has a 44% decrease in binding affinity to GST-FH1, compared with its binding to GST-cDaam1. The change in binding affinity between GFP-PFN1-Ser135Ala and GST-cDaam1 is not statistically significant from PFN1. However, the change in binding efficiency between GFP PFN1-Ser135Ala and GST-FH1 is statistically different from PFN1. The binding affinity of GFP-PFN1-Ser135Glu to GST-cDaam1 and GST-FH1 has no statistical difference from GFP-PFN1. The binding affinity of GFP-PFN1-Tyr131Ala to GST-cDaam1 and GST-FH1 has no statistical difference from GFP PFN1. Lastly, the double mutant displays a lower binding affinity to GST-FH1 than PFN1-Ser135Ala, 29% compared to 15%. This change is statistically significant when compared to PFN1. Like PFN1-Ser135Ala, the double mutant does not exhibit a statistically significant change in binding to GST-cDaam1.

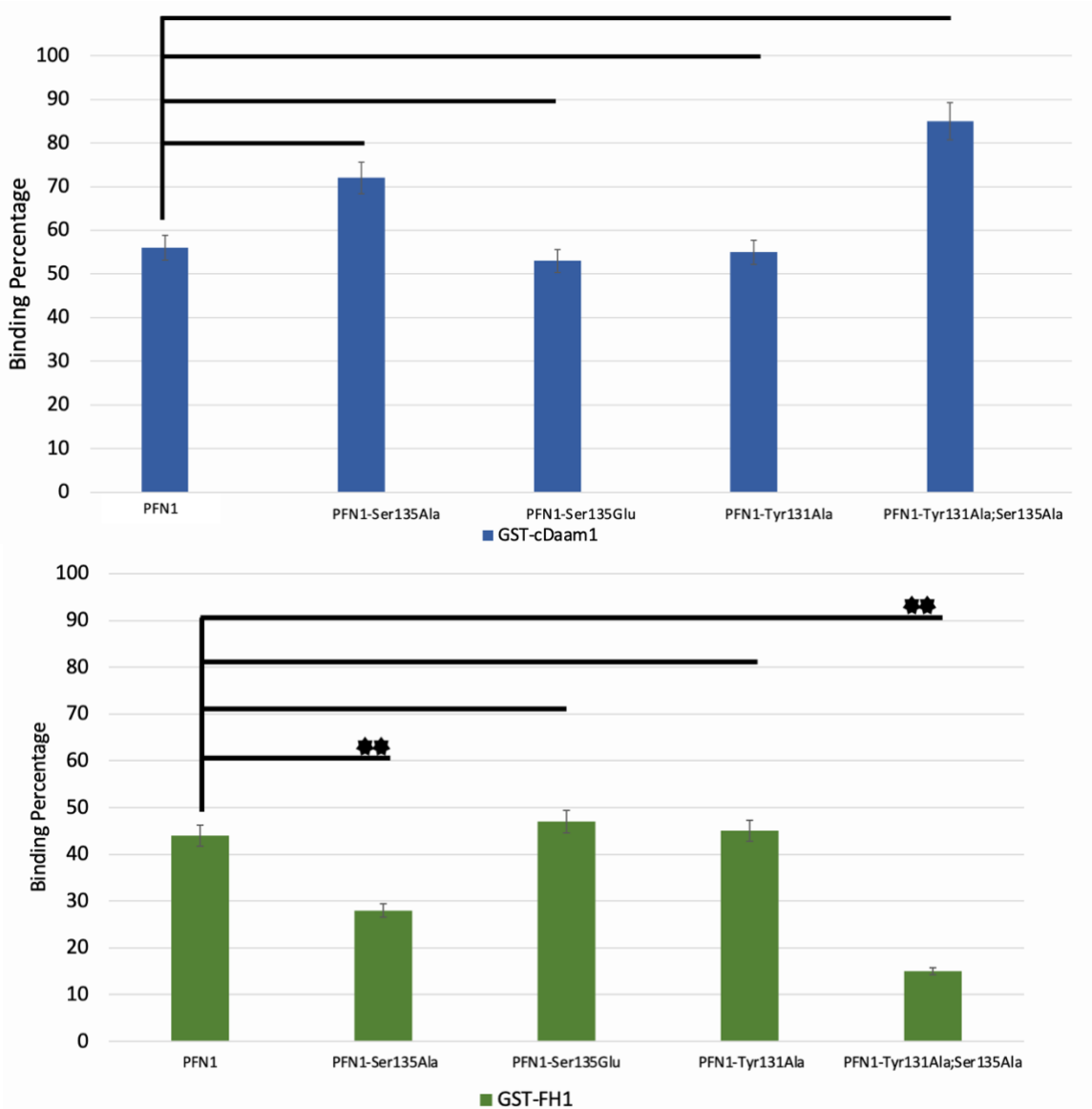


Figure 34. *Quantification of GST pulldown assays.* Average pixel intensities of GST-cDaam1 and GST-FH1 pulldowns was measured to quantify the effects of each mutant on their binding efficiencies to cDaam1 and FH1. The pixel intensities of bands from PFN1 and each mutant were compared using data from three technical and biological replicates. A T-test was performed comparing changes in pixel intensities between PFN1 and each mutant to GST-cDaam1 and GST-FH1. The resulting average pixel intensities were then plotted as a percentage.

To investigate whether Wnt signaling affects the binding of PFN1 to Daam1 through Tyr131 and Ser135, I conducted a co-immunoprecipitation assay (Co-IP). GFP-tagged PFN1 constructs were co-transfected with Myc-tagged Daam1, c-Daam1, or FH1 into HEK293T cells. Cells were treated with Wnt5a to induce activation of non-canonical Wnt signaling. Cells were then lysed, and a Co-IP was performed.

Myc-Daam1 binds to GFP-PFN1 and the mutants with equal intensity. Treatment of Wnt5a strengthens this interaction (Figure 35). Quantification of binding intensities shows no statistical differences between binding of PFN1 nor the mutants to Daam1 (Figure 36). Treatment of Wnt5a does strengthen the overall average binding affinity of each PFN1 to Daam1 but shows no difference between the populations. Daam1 interacts with GFP-PFN1 and the PFN1 mutants equally.

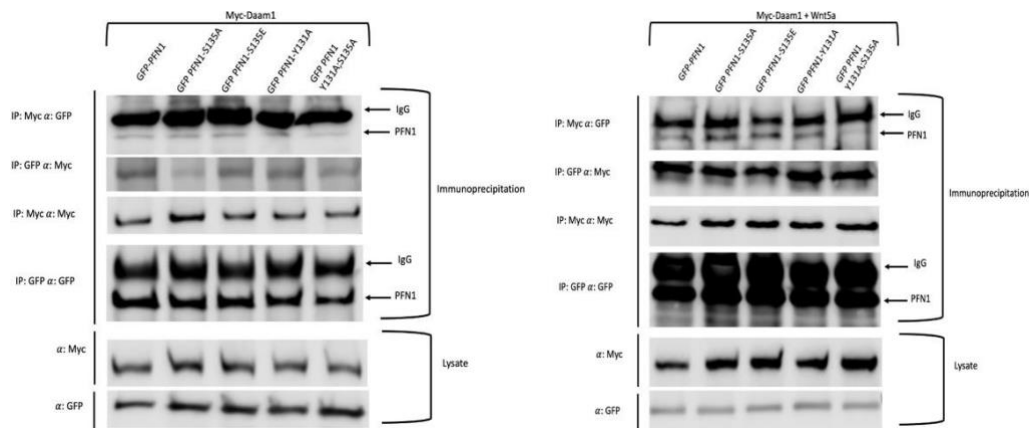


Figure 35. *Tyr131 and Ser135 have no effect on binding of PFN1 to Daam1.* 2ug of each PFN1 construct and 2ug of myc-Daam1 were co-transfected into HEK293T cells and treated with Wnt5a for 2 hours. Cells were lysed and samples were pulled down with Myc or GFP antibodies then run on a Western Blot.

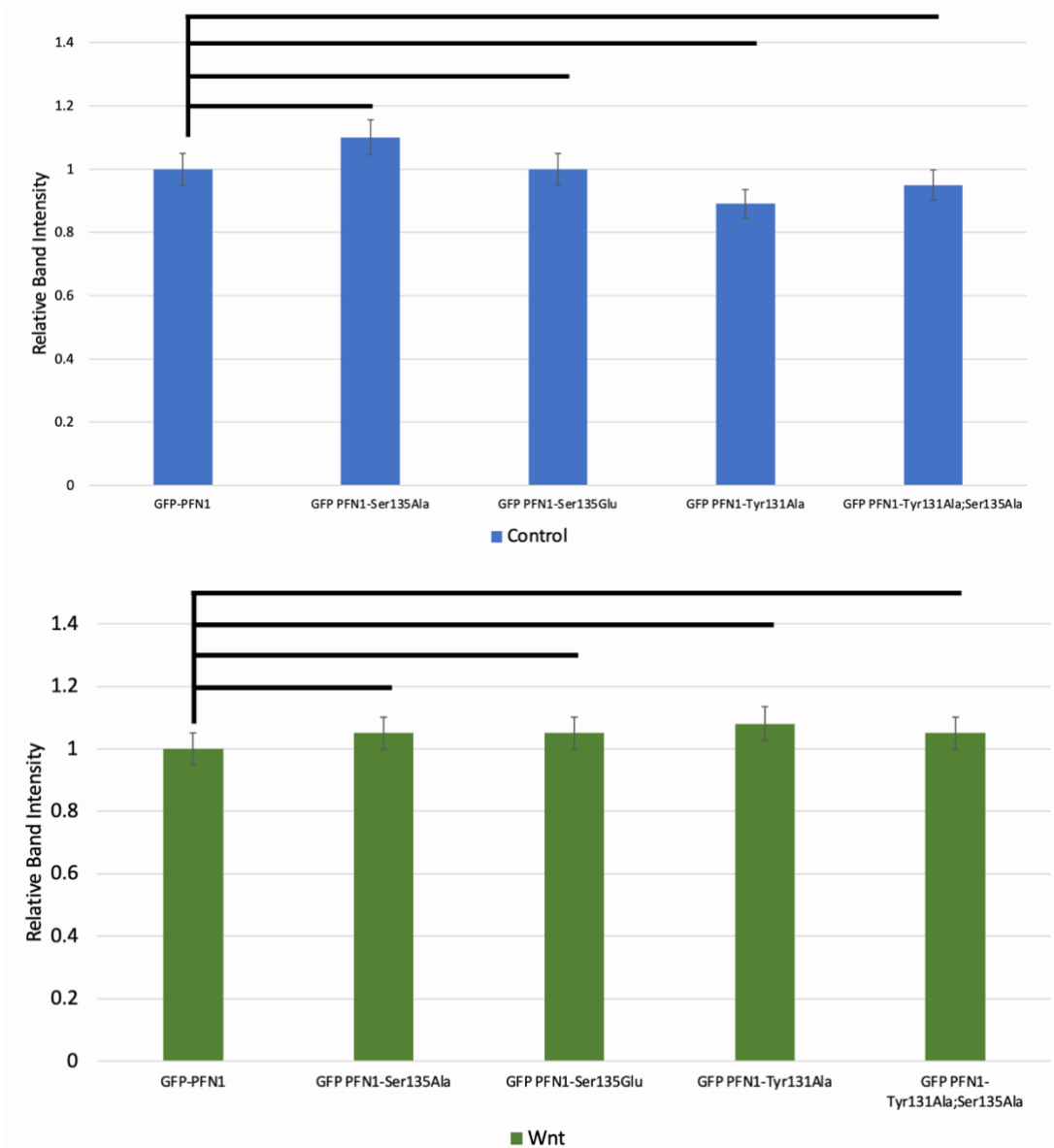


Figure 36. **Quantification of binding of mutant PFN1 to Daam1.** Average pixel intensities of each pulldown were measured to quantify the effects of each mutant on their binding efficiencies to Daam1 in control and Wnt5a treated samples. The pixel intensities of bands from PFN1 and each mutant were compared using data from three technical and biological replicates. A T-test was performed comparing changes in pixel intensities between PFN1 and each mutant to Daam1 in control and Wnt5a treated samples.

Myc-cDaam1 binds to GFP-PFN1 and the mutants with equal intensity. Treatment of Wnt5a strengthens this interaction (Figure 37). Quantification of binding intensities shows no statistical differences between binding of PFN1 nor the mutants to cDaam1 (Figure 38). Treatment of Wnt5a does strengthens the overall average binding affinity of each PFN1 to cDaam1 but shows no difference between the populations. cDaam1 interacts with GFP PFN1 and the PFN1 mutants equally.

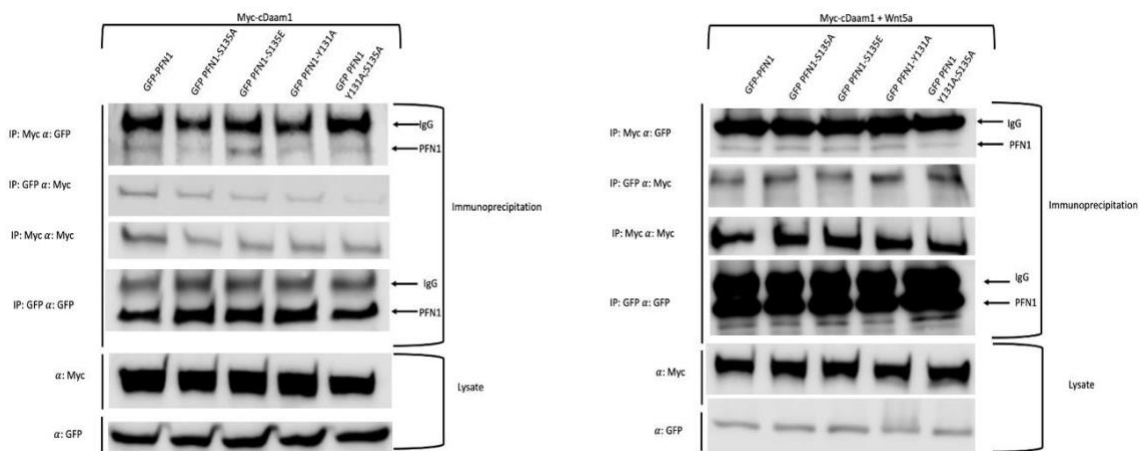


Figure 37. *Tyr131 and Ser135 have no effect on binding of PFN1 to cDaam1.* 2ug of each PFN1 construct and 2ug of myc-cDaam1 were co-transfected into HEK293T cells and treated with Wnt5a for 2 hours. Cells were lysed and samples were pulled down with Myc or GFP antibodies then run on a Western Blot.

PFN1-Ser135Ala and PFN1-Tyr131Ala;Ser135Ala lose binding affinity to Myc-FH1, while PFN1-Ser135Glu and PFN1-Tyr131Ala bind equally compared to PFN1. Treatment of Wnt5a rescues the loss in binding of PFN1-Ser135Ala and the double mutant to myc-FH1 (Figure 39). Quantification of binding intensities shows statistical differences between binding of PFN1-Ser135Ala and PFN1-Tyr131Ala;Ser135Ala to FH1 (Figure 40). Treatment of Wnt5a rescues the loss in binding of PFN1-Ser135Ala and PFN1-Tyr131Ala;Ser135Ala to FH1.

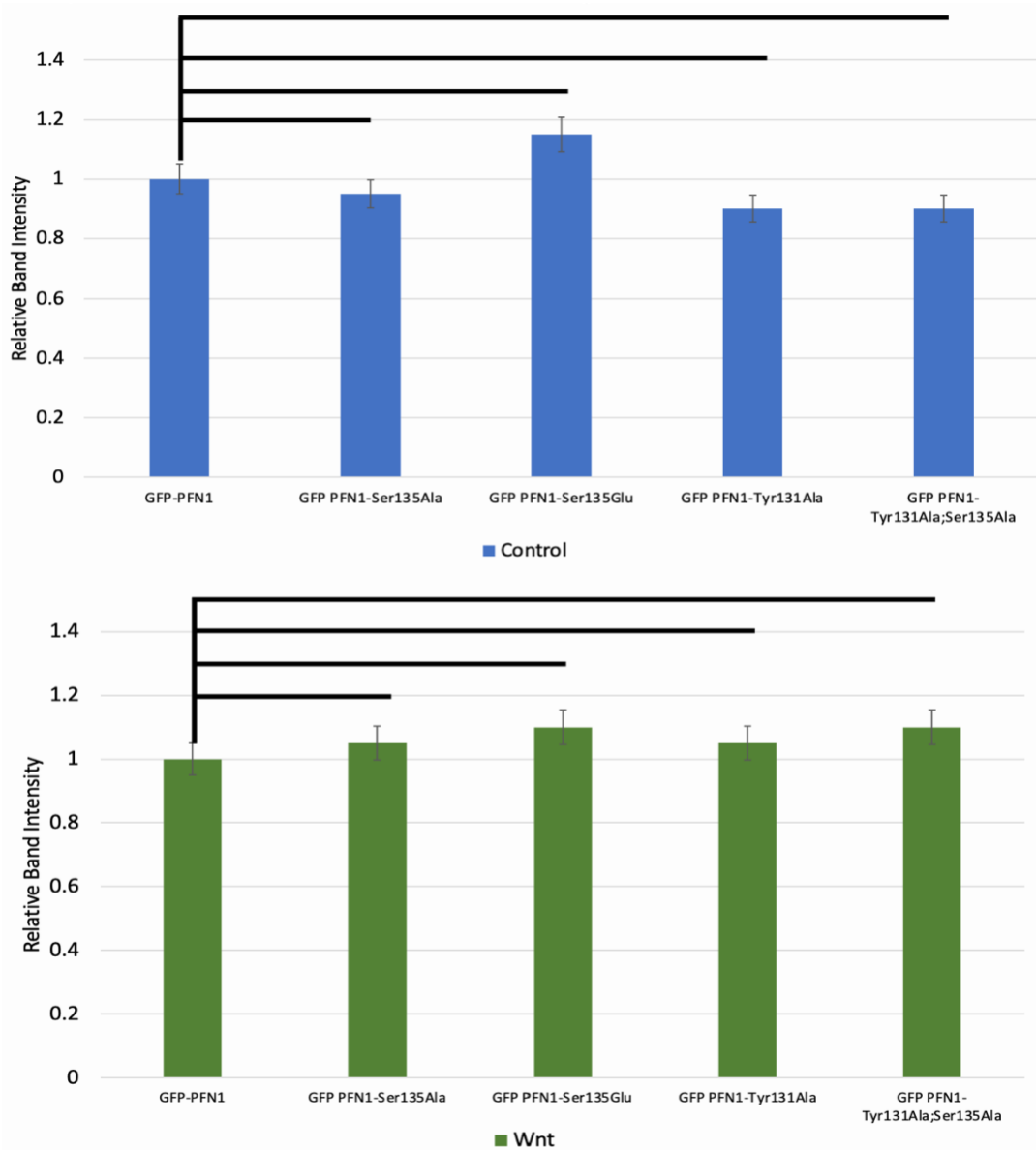


Figure 38. *Quantification of binding of mutant PFN1 to cDaam1.* Average pixel intensities of each pull-down were measured to quantify the effects of each mutant on their binding efficiencies to cDaam1 in control and Wnt5a treated samples. The pixel intensities of bands from PFN1 and each mutant were compared using data from three technical and biological replicates. A T-test was performed comparing changes in pixel intensities between PFN1 and each mutant to cDaam1 in control and Wnt5a treated samples.

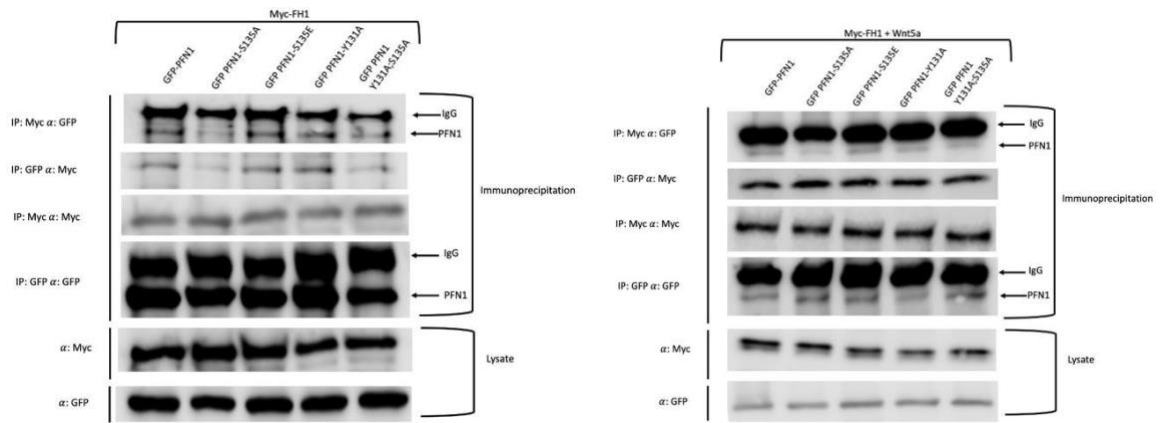


Figure 39. *Ser135 affects binding of PFN1 to FH1.* 2ug of each PFN1 construct and 2ug of myc-cDaam1 were co-transfected into HEK293T cells and treated with Wnt5a for 2 hours. Cells were lysed and samples were pulled down with Myc or GFP antibodies then run on a Western Blot.

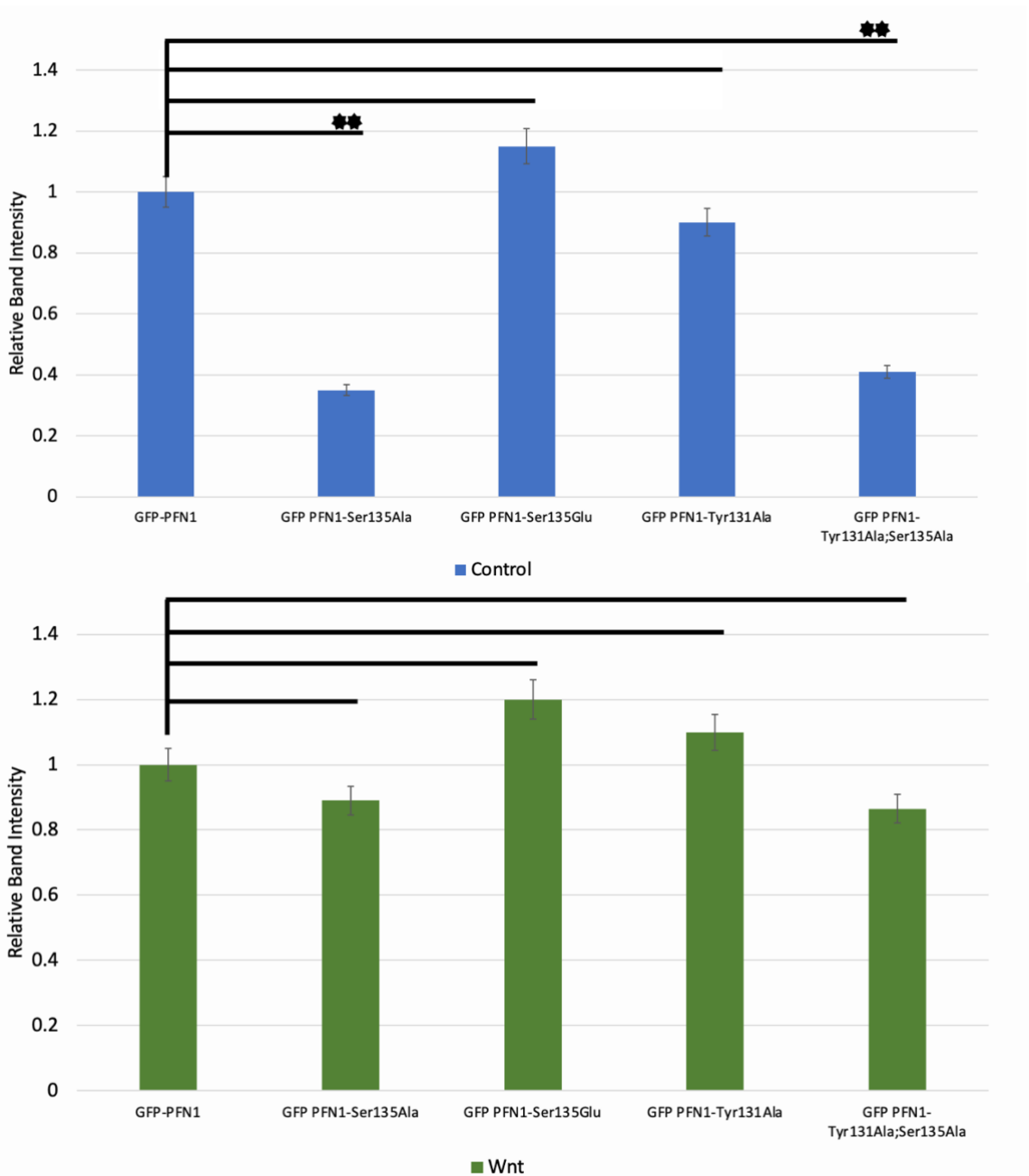


Figure 40. *Quantification of binding of mutant PFN1 to FH1.* Average pixel intensities of each pulldown were measured to quantify the effects of each mutant on their binding efficiencies to FH1 in control and Wnt5a treated samples. The pixel intensities of bands from PFN1 and each mutant were compared using data from three technical and biological replicates. A T-test was performed comparing changes in pixel intensities between PFN1 and each mutant to FH1 in control and Wnt5a treated samples.

### **3.5 Wnt5a-mediated phosphorylation of Tyr129 is Src independent**

Previous studies have identified several kinases that phosphorylate Tyr131 and Ser135 through different signaling pathways. However, the kinases that are recruited by non-canonical Wnt signaling to phosphorylate Tyr131 and Ser135 have not been explored. Using a predictive software that identifies the most likely kinase to phosphorylate a particular residue called Group-based prediction system v5 (GPS 5.0), I identified several kinases that may phosphorylate Tyr131 and Ser135 (Table 2). The software identifies the likelihood of a kinase phosphorylating a particular residue and generates a phosphorylation score. The higher the value, the more likely the residue is phosphorylated by the identified kinase. The most likely kinases identified to phosphorylate Tyr131 were activated cdc42 kinase (ACK1), Ephrin kinase (Eph), Insulin receptor tyrosine kinase (InsR), and Src kinase with similar predictive phosphorylation scores ranging from 21.512 to 18.525. The protein kinase A/G/C family (PK A/G/C), dystrophin myotonia protein kinase (DMPK), and ROCK were the most likely kinases to phosphorylate Ser135. The protein kinases family? and DMPK scored high predictive scores of 555.416, while ROCK scored a significantly lower 16.005.

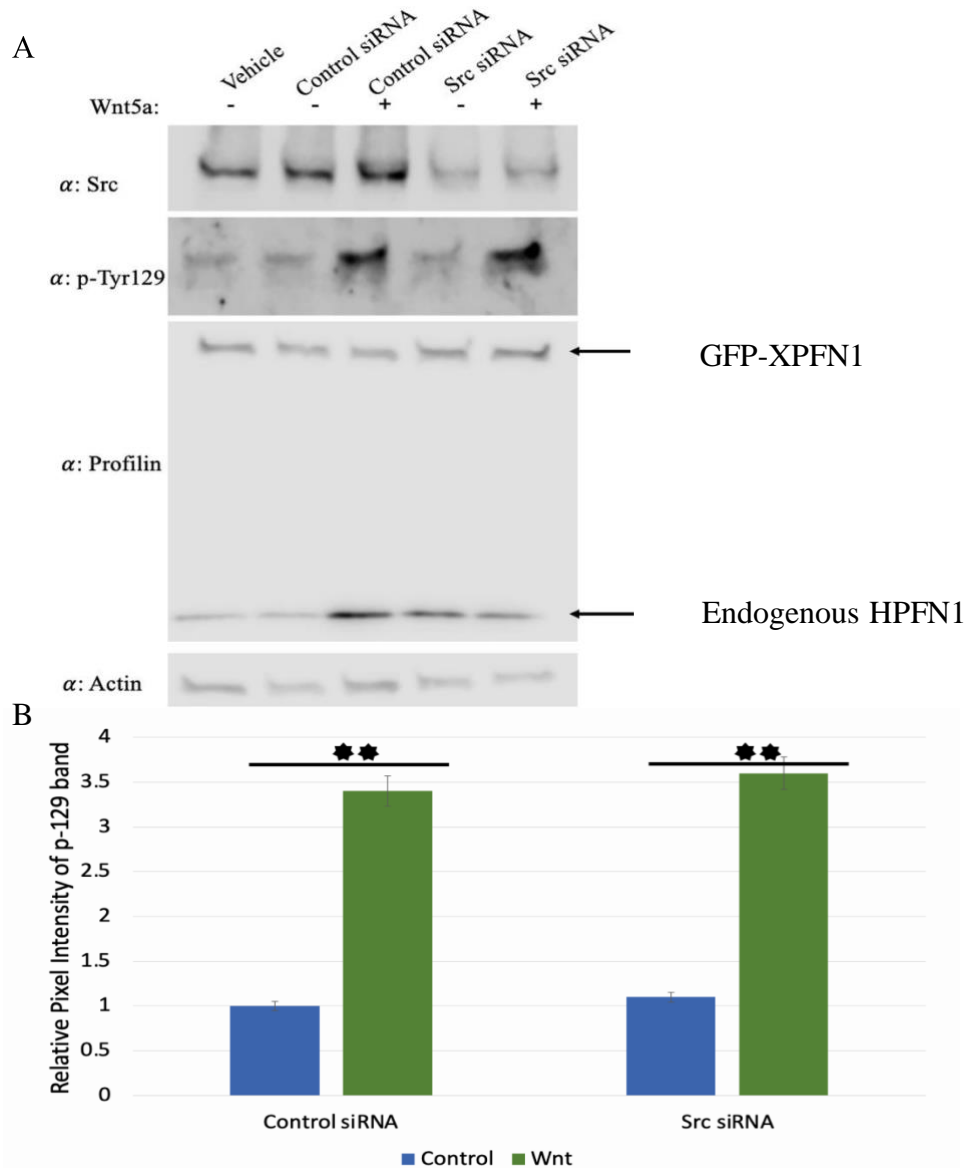
Position	Code	Kinase	Peptide	Score	Cutoff
131	Y	TK/Ack	KVFDMGKYLRCSGY	21.512	20.344
131	Y	TK/Eph	KVFDMGKYLRCSGY	20.237	15.808
131	Y	TK/InsR	KVFDMGKYLRCSGY	20.153	15.529
131	Y	Src/VEGFR	KVFDMGKYLRCSGY	18.525	17.626
135	S	AGC	MGKYLRCSGY*****	555.416	521.745
135	S	AGC/DMPK	MGKYLRCSGY*****	555.416	521.745
135	S	ROCK	MGKYLRCSGY*****	16.005	15.808

Table 2. *List of predicted kinases that may phosphorylate Tyr131 and Ser135.* The sequence of *Xenopus* PFN1 was scanned using GPS 5.0 to identify potential kinase targets.

Because Tyr131 effects gastrulation in *Xenopus* embryos and cytokinesis in HeLa cells, I decided to identify the kinase that is recruited through non-canonical Wnt signaling that phosphorylates Tyr131. Currently, only Src kinase has been shown to phosphorylate Tyr129 through VEGF signaling on HPFN1. I hypothesized that non-canonical Wnt signaling and VEGF signaling use Src to regulate PFN1.

To test this hypothesis, siRNA targeting Src was transfected into HEK293T cells and treated with Wnt5a. Cells were lysed and a western blot was performed using an antibody that detects phosphorylated Tyr129 in human cells. Actin was used as the loading control. Treatment of Wnt5a in cells transfected with control siRNA shows an increase in phosphorylation of Tyr129, compared to untreated cells. The p-Tyr129 antibody was unable to detect *Xenopus* PFN1. Cells that were transfected with Src siRNA and treated with Wnt5a show an increase in phosphorylation of Tyr129 compared to cells transfected with siRNA only (Figure 41). Cells treated with Wnt5a show an increase in

endogenous PFN1 despite both GFP-XPFN1 and actin levels remaining equal. This suggests that Wnt5a-mediated phosphorylation of Tyr129 is Src independent.



**Figure 41. *Wnt5a* induces phosphorylation of Tyr129 on HPFN1 and this is Src independent.** A) HEK293T cells were co-transfected with GFP-XPFN1 and Src siRNA or control siRNA and incubated for 48 hours. Cells were then treated with Wnt5a for 2 hours. Knockdown of Src was confirmed using an antibody that detects endogenous human Src. A phosphor-specific antibody that recognizes the phosphorylated form of Tyr129 in human, mouse, and rat was used to probe for phosphorylation of Tyr129. GFP-xPFN1 was used for visual confirmation of transfection and to test whether the phosphor-specific antibody detects Tyr131 in *Xenopus* PFN1 1. An antibody that detects PFN1 1 successfully recognizes endogenous hPFN1 and transfected GFP-xPFN1. Actin was used as the loading control. B) Quantification of phosphorylation of Tyr129 shows knockdown of Src does not prevent Wnt5a mediated phosphorylation of Tyr129. Average pixel intensity was measured using ImageJ. A T-Test was performed on the values to determine statistical significance. \* Denotes a statistical significance of  $>0.05$  and \*\* denotes a statistical significance of  $>0.005$ . This experiment was completed in biological and technical triplicates.

## CHAPTER 4

### DISCUSSION

How ligand based signaling pathways lead to downstream actin polymerization remains an essential question in non-canonical Wnt signaling and in developmental biology. Researchers have tackled this problem from different angles using genetic and biochemical approaches. Much research has been done characterizing the cellular effects of signaling cascades from different Wnt ligands, as well as identifying LRP5/6 as co-receptors to Fz. Researchers have identified Ryk, Vangl, and Celsr as crucial co-receptors in non-canonical Wnt signaling<sup>139</sup>. Years of research has led to identification of crucial signaling components and their roles in non-canonical Wnt signaling. However, less data exists on how the downstream effectors, such as PFN1, directly execute their primary function of actin cytoskeletal remodeling in response to ligand-based signaling pathways. In this study, I addressed this question by examining roles of two conserved amino acids on XPFN1, Tyr131 and Ser135, in regulating non-canonical Wnt signaling and in developmental biology.

PFN1 has been the focus of research since it was discovered in the 1970s<sup>121</sup>. Most of the research on PFN1 has been focused on its ability to affect actin polymerization, characterizing its many binding partners, and its role in early embryonic development. However, minimal research has been done on which ligand-based signaling pathways utilize PFN1 to affect the actin cytoskeleton and even fewer studies identify how phosphorylation of PFN1 affects its function. In response to VEGF signaling, Src

kinase phosphorylates Tyr129 on HPFN1 to regulate endothelial cell migration and angiogenesis during wound healing<sup>132</sup>. In this study, the researchers showed that substitution of Tyr129 for Ala prevents actin polymerization *in vitro*, slows wound healing, and prevents angiogenesis during tissue repair. In TGF- $\beta$  signaling, PFN1 regulates cardiac muscle development but no phosphorylation site for this function has yet been identified<sup>140</sup>. There is some evidence suggesting that phosphorylation of Ser137 on HPFN1 regulates binding of Profilin to PLP sites and may affect cytokinesis<sup>131</sup>. In non-canonical Wnt signaling, PFN1 and PFN2 were shown to have different roles during early development. XPFN1 regulates blastopore closure during gastrulation, while XPFN2 regulates convergent extension movement and axial extension during gastrulation<sup>124,141</sup>. PFN1 binds to the formin Daam1 to affect non-canonical Wnt-mediated actin cytoskeletal reorganization<sup>124</sup>. While PFN1 is a known downstream effector of non-canonical Wnt signaling, how PFN1 executes its function is unclear. Here, I provide evidence of the roles of Tyr131 and Ser135 on XPFN1, the analogous amino acids to Tyr129 and Ser137 on HPFN1, in non-canonical Wnt signaling and their roles in regulating development in *Xenopus*. It is worth noting that while Ser135 is conserved on XPFN1, Tyr131 is not. Tyr131 is likely orthologous to Tyr129 on HPFN1.

Extensive research has been done on the role of PFN1 during development in several animal models. Maternal knockout of PFN1 in mice prevents cell division at stage 2 resulting in embryo death<sup>113</sup>. In *Drosophila*, deletion of the Profilin locus, known as Chickadee, results in lethality due to cells being unable to divide<sup>123</sup>. In *C. elegans*,

PFN1 is necessary for PAR protein localization, centrosome formation, and mitotic spindle orientation, which are necessary for cell division and ultimately, development<sup>142</sup>.

In Zebrafish, knockdown of PFN1 prevents epiboly during gastrulation. Overexpression of PFN1 led to defects in cell migration in zebrafish embryos. This was evidenced by abnormal migration of cells in the developing brain and spinal cord, as well as defects in the formation of the neural crest<sup>143</sup>. Lastly, in *Xenopus*, morpholino knockdown or mRNA overexpression of PFN1 results in an open blastopore<sup>124</sup>. Despite the clear importance of PFN1 on development, no residues have yet been identified that regulate its function during development. In this study, I was able to show that an alanine substitution at Tyr131 arrests developing embryos preventing gastrulation from occurring. I further explored this effect at the cellular level in and provide some evidence of how a mutation Tyr131Ala may prevent gastrulation from occurring.

As mentioned earlier, only a small handful of studies have directly linked a ligand based signaling pathway to PFN1's downstream role in actin fiber formation. While this is not the first study to link non-canonical Wnt signaling to PFN1, it is the first to explore which residues on PFN1 play a role on the downstream cellular effects of activation of non-canonical Wnt signaling. Mutating Tyr131 to alanine, which mimics an unphosphorylated form of PFN1, prevents Wnt5a mediated actin cytoskeletal organization and interferes with cytokinesis while Ser135 has no such effect. Normally with Wnt5a stimulation, formation of actin fibers increases, and changes in cell morphology. Overexpression of PFN1-Tyr131Ala prevents these Wnt-mediated effects, suggesting that PFN1-Tyr131Ala prevents downstream cellular effects of non-canonical

Wnt signaling. Furthermore, I was able to show that PFN1-Tyr131Ala prevents gastrulation by causing a cytokinesis defect, a previously observed phenomenon in studies on PFN1 for which an explanation was never presented.

Previous studies have shown that mutations in PFN1 result in higher incidences of multinucleation in *C. elegans*, *Drosophila*, and cancer cells lines<sup>145,146,147</sup>. Multinucleation occurs in cells that are unable to complete cytokinesis. Multinucleation was noted as an effect of deletions of the C-terminus of PFN1 in an early *Drosophila* study of the *Chickadee* gene but no specific residues were ever implicated<sup>123</sup>. In this study, I observed similar incidences of multinucleation when the residues are changed in PFN1-Ser135Ala and PFN1-Ser135Glu. However, overexpression of PFN1-Tyr131Ala and PFN1-Tyr131Ala; Ser135Ala shows a two-fold increase in incidence of multinucleation compared to PFN1 in control and Wnt5a treated cells. This is the first study linking a specific amino acid to the known increase in incidence of multinucleation observed with mutations on PFN1.

PFN1 is known to bind to proteins containing PLP sites such as Formins and WASP. The binding regions on Formins and WASP that modulate binding to PFN1 have been identified. PFN1 binds to the FH1 domain on Formins and to the proline rich N-terminus of WASP<sup>115,144</sup>. In non-canonical Wnt signaling, PFN1 binds to the FH1 domain on the C-terminus of Daam1<sup>124</sup>. No studies have yet shown which residues on PFN1 regulate binding to ANPs although some evidence exists that phosphorylation of Ser137 on HPFN1 prevents binding of PFN1 to PLP-fused beads<sup>131</sup>. In this study, I present

contrary evidence suggesting that PFN1-Ser135Ala on XPFN1 prevents binding of PFN1 to the FH1 domain of Daam1, while Tyr131Ala has no such effect.

PFN1-Ser135Ala led to disruption of binding of PFN1 to the FH1 domain of Daam1, and this loss in binding was rescued by treatment of Wnt5a. This suggests that non-canonical Wnt signaling may phosphorylate other residues in addition to Ser135 to regulate binding of XPFN1 to FH1. In addition, it was surprising that PFN1-Ser135Ala binds to cDaam1 and Daam1 but not to FH1, as the FH1 domain is located on the C-terminus of Daam1. One possible explanation is that replacing Ser135 with a hydrophobic residue such as Alanine sterically prevents binding of PFN1 to FH1. This can be tested by mutating Ser135 to Threonine, a structurally similar amino to serine. This would test whether binding of PFN1 to FH1 is being disrupted by steric inhibition or regulation.

While Tyr131 on XPFN1 showed no role in regulating binding of PFN1 to Daam1, phosphorylation of Tyr129 on HPFN1 by Src kinase through VEGF signaling was shown to cause downstream actin polymerization during wound healing in what system<sup>132</sup>. A phospho-inactive version of Tyr129 shows decreased ability to polymerize G-actin *in vitro*, slow endothelial cell migration, and prevent wound healing<sup>132</sup>. Given the known roles of PFN1 in VEGF and non-canonical Wnt signaling, I hypothesized that these two ligand-based signaling pathways use Src kinase to regulate PFN1.

I was able to show that while Wnt5a leads to phosphorylation of Tyr129 on HPFN1, this phosphorylation event is Src-independent because siRNA knockdown of Src did not prevent Wnt5a-mediated phosphorylation of Tyr129. Two different ligand-based pathways, VEGF and non-canonical Wnt signaling, separately lead to phosphorylation of Tyr129 on HPFN1. As previously described, I identified several kinases that may phosphorylate Tyr131 and Ser135 on XPFN1 using GPS v5.0. The most likely kinases identified to phosphorylate Tyr131 were activated cdc42 kinase (ACK1), Ephrin kinase (Eph), Insulin receptor tyrosine kinase (InsR), and Src kinase with similar predictive phosphorylation scores ranging from 21.512 to 18.525. siRNA knockdown experiments could be used to test whether non-canonical Wnt signaling recruits ACK1, Eph, or InsR phosphorylate Tyr129 on HPFN1. Because Cdc42 is a known downstream effector of non-canonical Wnt signaling, it is the most sensible target to phosphorylate Tyr129.

This study presents evidence that Tyr131 and Ser135 have different roles on PFN1. Tyr131 regulates gastrulation, Wnt5a mediated actin fiber formation, cytokinesis, and cellular elongation while Ser135 regulates binding of XPFN1 to Daam1 but the molecular mechanism is unclear. These findings expand our understanding of non-canonical Wnt signaling and actin dynamics. Identification of the importance of Tyr131 on XPFN1, and by extension Tyr129 on HPFN1, is poised to expand our knowledge of non-canonical Wnt signaling and actin dynamics. Here, I propose a model whereby Tyr131 regulates PFN1's role in Wnt5a-mediated actin cytoskeletal reorganization and Ser135 regulates binding of PFN1 to Daam1.

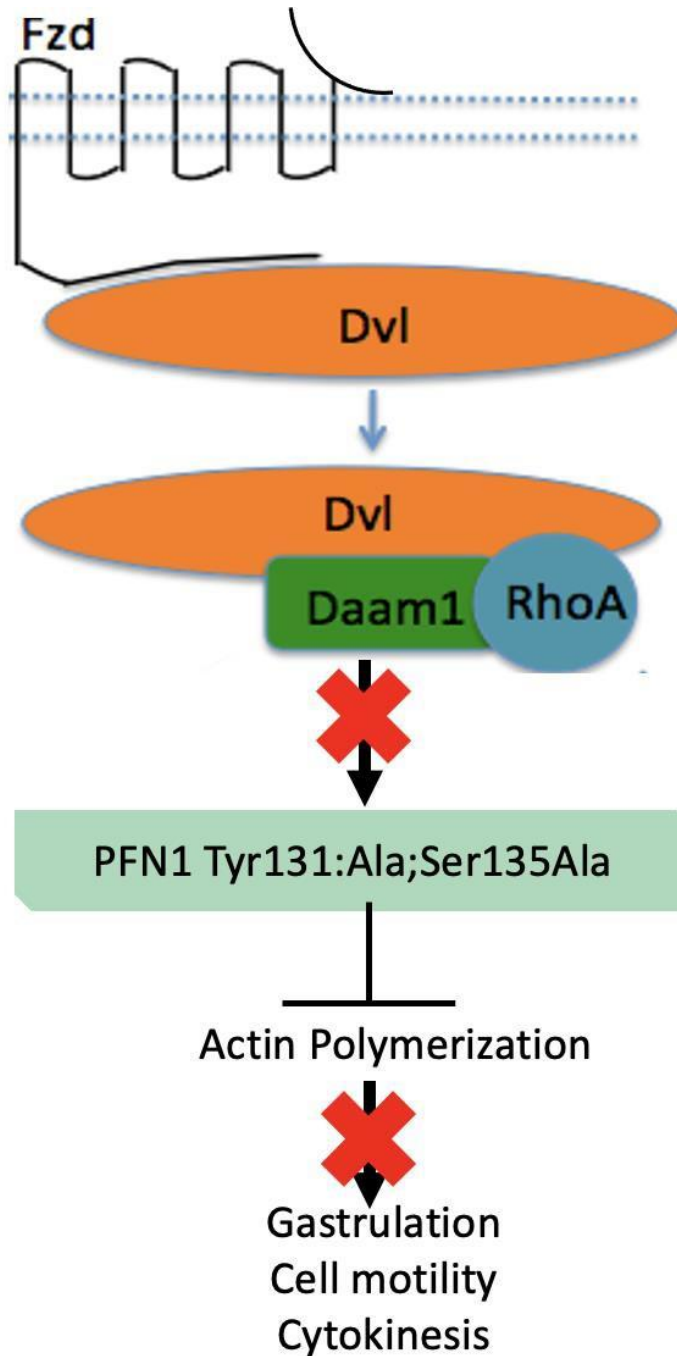


Figure 42. *Tyr131 is necessary for proper function of PFN1 and Ser135 may be one of several residues that regulate binding to Daam1.* Activation of non-canonical Wnt signaling by Wnt5a leads to phosphorylation of Tyr131 by an unknown kinase. Regulation of Tyr131 appears to be crucial for the role of PFN1 in actin fiber formation and gastrulation. Tyr131Ala prevents Wnt5a mediated actin fiber generation while Ser135 has no effect on the actin cytoskeleton. Ser135 may act in tandem with other residues to modulate binding of PFN1 to FH1 via PLP sites. Alanine substitutions of both Tyr131 and Ser135 prevents gastrulation and Wnt5a-mediated actin fiber formation.

## REFERENCES

- 1 Nama, K. *Characterization of Dishevelled Associated Activator of Morphogenesis 2 (Daam2) in Wnt Signaling During Early Embryonic Development*, Temple University. Libraries, (2015).
- 2 Sugimura, R. & Li, L. Noncanonical Wnt signaling in vertebrate development, stem cells, and diseases. *Birth Defects Research Part C: Embryo Today: Reviews* **90**, 243-256 (2010).
- 3 Keller, R. Shaping the vertebrate body plan by polarized embryonic cell movements. *Science* **298**, 1950-1954 (2002).
- 4 Wallingford, J. B. & Harland, R. M. Neural tube closure requires Dishevelled-dependent convergent extension of the midline. (2002).
- 5 MacDonald, B. T., Tamai, K. & He, X. Wnt/ $\beta$ -catenin signaling: components, mechanisms, and diseases. *Developmental cell* **17**, 9-26 (2009).
- 6 Wodarz, A. & Nusse, R. Mechanisms of Wnt signaling in development. *Annual review of cell and developmental biology* **14**, 59-88 (1998).
- 7 He, X. A wnt-wnt situation. *Developmental cell* **4**, 791-797 (2003).
- 8 Huelsken, J. & Birchmeier, W. New aspects of Wnt signaling pathways in higher vertebrates. *Current opinion in genetics & development* **11**, 547-553 (2001).
- 9 Sharma, M., Castro-Piedras, I., Simmons Jr, G. E. & Pruitt, K. Dishevelled: A masterful conductor of complex Wnt signals. *Cellular signalling* **47**, 52-64 (2018).
- 10 Grumolato, L. *et al.* Canonical and noncanonical Wnts use a common mechanism to activate completely unrelated coreceptors. *Genes Dev* **24**, 2517-2530 (2010). <https://doi.org:10.1101/gad.1957710>
- 11 Klingensmith, J. & Nusse, R. Signaling by wingless in Drosophila. *Developmental biology* **166**, 396-414 (1994).
- 12 Perrimon, N. The genetic basis of patterned baldness in Drosophila. *Cell* **76**, 781-784 (1994).
- 13 Waltzer, L. & Bienz, M. Drosophila CBP represses the transcription factor TCF to antagonize Wingless signalling. *Nature* **395**, 521-525 (1998).
- 14 Sokol, S., Christian, J. L., Moon, R. T. & Melton, D. A. Injected Wnt RNA induces a complete body axis in Xenopus embryos. *Cell* **67**, 741-752 (1991).

- 15 Klaus, A. & Birchmeier, W. Wnt signalling and its impact on development and cancer. *Nature Reviews Cancer* **8**, 387-398 (2008).
- 16 Wharton Jr, K. A. Runnin'with the Dvl: proteins that associate with Dsh/Dvl and their significance to Wnt signal transduction. *Developmental biology* **253**, 1-17 (2003).
- 17 Boutros, M. & Mlodzik, M. Dishevelled: at the crossroads of divergent intracellular signaling pathways. *Mechanisms of development* **83**, 27-37 (1999).
- 18 Wallingford, J. B. & Habas, R. The developmental biology of Dishevelled: an enigmatic protein governing cell fate and cell polarity. (2005).
- 19 Komiya, Y. & Habas, R. Wnt signal transduction pathways. *Organogenesis* **4**, 68-75 (2008).
- 20 MacDonald, B. T. & He, X. Frizzled and LRP5/6 receptors for Wnt/ $\beta$ -catenin signaling. *Cold Spring Harbor perspectives in biology* **4**, a007880 (2012).
- 21 MacDonald, B. T., Semenov, M. V., Huang, H. & He, X. Dissecting molecular differences between Wnt coreceptors LRP5 and LRP6. *PloS one* **6**, e23537 (2011).
- 22 Fan, M. J., Grüning, W., Walz, G. & Sokol, S. Y. Wnt signaling and transcriptional control of Siamois in *Xenopus* embryos. *Proceedings of the National Academy of Sciences* **95**, 5626-5631 (1998).
- 23 Kishida, S. *et al.* DIX domains of Dvl and Axin are necessary for protein interactions and their ability to regulate  $\beta$ -catenin stability. *Molecular and cellular biology* **19**, 4414-4422 (1999).
- 24 Wong, H.-C. *et al.* Direct binding of the PDZ domain of Dishevelled to a conserved internal sequence in the C-terminal region of Frizzled. *Molecular cell* **12**, 1251-1260 (2003).
- 25 Gordon, M. D. & Nusse, R. Wnt signaling: multiple pathways, multiple receptors, and multiple transcription factors. *Journal of Biological Chemistry* **281**, 22429-22433 (2006).
- 26 Mao, J. *et al.* Low-density lipoprotein receptor-related protein-5 binds to Axin and regulates the canonical Wnt signaling pathway. *Molecular cell* **7**, 801-809 (2001).
- 27 Zeng, X. *et al.* Initiation of Wnt signaling: control of Wnt coreceptor Lrp6 phosphorylation/activation via frizzled, dishevelled and axin functions. (2008).

- 28 Komiya, Y., Mandrekar, N., Sato, A., Dawid, I. B. & Habas, R. Custos controls  $\beta$ -catenin to regulate head development during vertebrate embryogenesis. *Proceedings of the National Academy of Sciences* **111**, 13099-13104 (2014).
- 29 Moon, R. T. & Kimelman, D. From cortical rotation to organizer gene expression: toward a molecular explanation of axis specification in *Xenopus*. *Bioessays* **20**, 536-546 (1998).
- 30 Harland, R. & Gerhart, J. Formation and function of Spemann's organizer. *Annual review of cell and developmental biology* **13**, 611-667 (1997).
- 31 Saneyoshi, T., Kume, S., Amasaki, Y. & Mikoshiba, K. The Wnt/calcium pathway activates NF-AT and promotes ventral cell fate in *Xenopus* embryos. *Nature* **417**, 295-299 (2002).
- 32 Ishitani, T. *et al.* The TAK1–NLK–MAPK-related pathway antagonizes signalling between  $\beta$ -catenin and transcription factor TCF. *Nature* **399**, 798-802 (1999).
- 33 Arbouzova, N. & McNeill, H. Visualization of PCP Defects in the Eye and Wing of *Drosophila melanogaster*. *Wnt Signaling*, 127-140 (2009).
- 34 Seifert, J. R. & Mlodzik, M. Frizzled/PCP signalling: a conserved mechanism regulating cell polarity and directed motility. *Nature Reviews Genetics* **8**, 126-138 (2007).
- 35 Veeman, M. T., Slusarski, D. C., Kaykas, A., Louie, S. H. & Moon, R. T. Zebrafish prickle, a modulator of noncanonical Wnt/Fz signaling, regulates gastrulation movements. *Current biology* **13**, 680-685 (2003).
- 36 Gray, R. S., Roszko, I. & Solnica-Krezel, L. Planar cell polarity: coordinating morphogenetic cell behaviors with embryonic polarity. *Developmental cell* **21**, 120-133 (2011).
- 37 Sokol, S. Y. in *Seminars in cell & developmental biology*. 78-85 (Elsevier).
- 38 Sebbagh, M. & Borg, J.-P. Insight into planar cell polarity. *Experimental cell research* **328**, 284-295 (2014).
- 39 Bryja, V. *et al.* The extracellular domain of Lrp5/6 inhibits noncanonical Wnt signaling in vivo. *Molecular biology of the cell* **20**, 924-936 (2009).
- 40 Lu, W., Yamamoto, V., Ortega, B. & Baltimore, D. Mammalian Ryk is a Wnt coreceptor required for stimulation of neurite outgrowth. *Cell* **119**, 97-108 (2004).

- 41 Nishita, M. *et al.* Filopodia formation mediated by receptor tyrosine kinase Ror2 is required for Wnt5a-induced cell migration. *The Journal of cell biology* **175**, 555-562 (2006).
- 42 Lai, S.-s. *et al.* Ror2-Src signaling in metastasis of mouse melanoma cells is inhibited by NRAGE. *Cancer genetics* **205**, 552-562 (2012).
- 43 Lu, X. *et al.* PTK7/CCK-4 is a novel regulator of planar cell polarity in vertebrates. *Nature* **430**, 93-98 (2004).
- 44 Habas, R., Kato, Y. & He, X. Wnt/Frizzled activation of Rho regulates vertebrate gastrulation and requires a novel Formin homology protein Daam1. *Cell* **107**, 843-854 (2001).
- 45 Marlow, F., Topczewski, J., Sepich, D. & Solnica-Krezel, L. Zebrafish Rho kinase 2 acts downstream of Wnt11 to mediate cell polarity and effective convergence and extension movements. *Current biology* **12**, 876-884 (2002).
- 46 Weiser, D. C., Pyati, U. J. & Kimelman, D. Gravin regulates mesodermal cell behavior changes required for axis elongation during zebrafish gastrulation. *Genes & development* **21**, 1559-1571 (2007).
- 47 Yamanaka, H. *et al.* JNK functions in the non-canonical Wnt pathway to regulate convergent extension movements in vertebrates. *EMBO reports* **3**, 69-75 (2002).
- 48 Keller, R. An experimental analysis of the role of bottle cells and the deep marginal zone in gastrulation of *Xenopus laevis*. *Journal of Experimental Zoology* **216**, 81-101 (1981).
- 49 Winklbauer, R. & Schurfeld, M. Vegetal rotation, a new gastrulation movement involved in the internalization of the mesoderm and endoderm in *Xenopus*. *Development* **126**, 3703-3713 (1999).
- 50 Stern, C. D. Vertebrate gastrulation. *Current opinion in genetics & development* **2**, 556-561 (1992).
- 51 Ewald, A. J., Peyrot, S. M., Tyszk, J. M., Fraser, S. E. & Wallingford, J. B. Regional requirements for Dishevelled signaling during *Xenopus* gastrulation: separable effects on blastopore closure, mesendoderm internalization and archenteron formation. (2004).
- 52 Solnica-Krezel, L. & Sepich, D. S. Gastrulation: making and shaping germ layers. *Annual review of cell and developmental biology* **28**, 687-717 (2012).

- 53 Davidson, L. A. Embryo mechanics: balancing force production with elastic resistance during morphogenesis. *Current topics in developmental biology* **95**, 215-241 (2011).
- 54 Gilbert, S. F. The generation of novelty: the province of developmental biology. (2006).
- 55 Wallingford, J. B. in *American Journal of Medical Genetics Part C: Seminars in Medical Genetics*. 59-68 (Wiley Online Library).
- 56 Wallingford, J. B. *et al.* Dishevelled controls cell polarity during *Xenopus* gastrulation. *Nature* **405**, 81-85 (2000).
- 57 Suzuki, M., Morita, H. & Ueno, N. Molecular mechanisms of cell shape changes that contribute to vertebrate neural tube closure. *Development, growth & differentiation* **54**, 266-276 (2012).
- 58 Smith, J. L. & Schoenwolf, G. C. Neurulation: coming to closure. *Trends in neurosciences* **20**, 510-517 (1997).
- 59 Kee, N. *et al.* Neogenin and RGMa control neural tube closure and neuroepithelial morphology by regulating cell polarity. *Journal of Neuroscience* **28**, 12643-12653 (2008).
- 60 Schroeder, T. E. Neurulation in *Xenopus laevis*. An analysis and model based upon light and electron microscopy. (1970).
- 61 Hildebrand, J. D. & Soriano, P. Shroom, a PDZ domain-containing actin-binding protein, is required for neural tube morphogenesis in mice. *Cell* **99**, 485-497 (1999).
- 62 Haigo, S. L., Hildebrand, J. D., Harland, R. M. & Wallingford, J. B. Shroom induces apical constriction and is required for hingepoint formation during neural tube closure. *Current biology* **13**, 2125-2137 (2003).
- 63 Toyama, Y., Peralta, X. G., Wells, A. R., Kiehart, D. P. & Edwards, G. S. Apoptotic force and tissue dynamics during *Drosophila* embryogenesis. *Science* **321**, 1683-1686 (2008).
- 64 Slattum, G., McGee, K. M. & Rosenblatt, J. P115 RhoGEF and microtubules decide the direction apoptotic cells extrude from an epithelium. *Journal of Cell Biology* **186**, 693-702 (2009).
- 65 Antunes, M., Pereira, T., Cordeiro, J. V., Almeida, L. & Jacinto, A. Coordinated waves of actomyosin flow and apical cell constriction immediately after wounding. *Journal of Cell Biology* **202**, 365-379 (2013).

- 66 Davidson, L. A., Ezin, A. M. & Keller, R. Embryonic wound healing by apical contraction and ingression in *Xenopus laevis*. *Cell motility and the cytoskeleton* **53**, 163-176 (2002).
- 67 Elul, T. & Keller, R. Monopolar protrusive activity: a new morphogenic cell behavior in the neural plate dependent on vertical interactions with the mesoderm in *Xenopus*. *Developmental biology* **224**, 3-19 (2000).
- 68 Higgs, H. N. Formin proteins: a domain-based approach. *Trends in biochemical sciences* **30**, 342-353 (2005).
- 69 Breitsprecher, D. & Goode, B. L. Formins at a glance. *Journal of cell science* **126**, 1-7 (2013).
- 70 Schönichen, A. & Geyer, M. Fifteen formins for an actin filament: a molecular view on the regulation of human formins. *Biochimica et Biophysica Acta (BBA)-Molecular Cell Research* **1803**, 152-163 (2010).
- 71 Yamashita, M. *et al.* Crystal structure of human DAAM1 formin homology 2 domain. *Genes to Cells* **12**, 1255-1265 (2007).
- 72 Wallar, B. J. & Alberts, A. S. The formins: active scaffolds that remodel the cytoskeleton. *Trends in cell biology* **13**, 435-446 (2003).
- 73 Watanabe, N., Kato, T., Fujita, A., Ishizaki, T. & Narumiya, S. Cooperation between mDia1 and ROCK in Rho-induced actin reorganization. *Nature cell biology* **1**, 136-143 (1999).
- 74 Watanabe, N. *et al.* p140mDia, a mammalian homolog of *Drosophila* diaphanous, is a target protein for Rho small GTPase and is a ligand for profilin. *The EMBO journal* **16**, 3044-3056 (1997).
- 75 Goode, B. L. & Eck, M. J. Mechanism and function of formins in the control of actin assembly. *Annu. Rev. Biochem.* **76**, 593-627 (2007).
- 76 Evangelista, M., Zigmond, S. & Boone, C. Formins: signaling effectors for assembly and polarization of actin filaments. *Journal of cell science* **116**, 2603-2611 (2003).
- 77 Li, F. & Higgs, H. N. The mouse Formin mDia1 is a potent actin nucleation factor regulated by autoinhibition. *Current biology* **13**, 1335-1340 (2003).
- 78 Alberts, A. S. Identification of a carboxyl-terminal diaphanous-related formin homology protein autoregulatory domain. *Journal of Biological Chemistry* **276**, 2824-2830 (2001).

- 79 Liu, W. *et al.* Mechanism of activation of the Formin protein Daam1. *Proceedings of the National Academy of Sciences* **105**, 210-215 (2008).
- 80 Selwood, T. & Jaffe, E. K. Dynamic dissociating homo-oligomers and the control of protein function. *Archives of Biochemistry and Biophysics* **519**, 131-143 (2012).
- 81 Ageberg, M., Drott, K., Olofsson, T., Gullberg, U. & Lindmark, A. Identification of a novel and myeloid specific role of the leukemia-associated fusion protein DEK-NUP214 leading to increased protein synthesis. *Genes, Chromosomes and Cancer* **47**, 276-287 (2008).
- 82 Kobayashi, H. *et al.* Increased Myosin light chain 9 expression during Kawasaki disease vasculitis. *Frontiers in Immunology* **13**, 1036672 (2023).
- 83 Chen, Z.-H. *et al.* LDHA maintains the growth and migration of vascular smooth muscle cells and promotes neointima formation via crosstalk between K5 crotonylation and K76 mono-ubiquitination. *bioRxiv*, 2023.2002. 2028.530389 (2023).
- 84 Rohatgi, R. *et al.* The interaction between N-WASP and the Arp2/3 complex links Cdc42-dependent signals to actin assembly. *Cell* **97**, 221-231 (1999).  
[https://doi.org/10.1016/s0092-8674\(00\)80732-1](https://doi.org/10.1016/s0092-8674(00)80732-1)
- 85 Pollard, T. D. Regulation of actin filament assembly by Arp2/3 complex and formins. *Annu Rev Biophys Biomol Struct* **36**, 451-477 (2007).  
<https://doi.org/10.1146/annurev.biophys.35.040405.101936>
- 86 Yamaguchi, Y. *et al.* Highly purified murine interleukin 5 (IL-5) stimulates eosinophil function and prolongs in vitro survival. IL-5 as an eosinophil chemotactic factor. *The Journal of experimental medicine* **167**, 1737-1742 (1988).
- 87 Peng, J. *et al.* Myeloproliferative defects following targeting of the Drf1 gene encoding the mammalian diaphanous related formin mDia1. *Cancer Res* **67**, 7565-7571 (2007). <https://doi.org/10.1158/0008-5472.Can-07-1467>
- 88 Eisenmann, K. M. *et al.* T cell responses in mammalian diaphanous-related formin mDia1 knock-out mice. *J Biol Chem* **282**, 25152-25158 (2007).  
<https://doi.org/10.1074/jbc.M703243200>
- 89 Sakata, D. *et al.* Impaired T lymphocyte trafficking in mice deficient in an actin-nucleating protein, mDia1. *J Exp Med* **204**, 2031-2038 (2007).  
<https://doi.org/10.1084/jem.20062647>

- 90 Leader, B. *et al.* Formin-2, polyploidy, hypofertility and positioning of the meiotic spindle in mouse oocytes. *Nature cell biology* **4**, 921-928 (2002).
- 91 Huang, X. *et al.* Structure and function of the two tandem WW domains of the pre-mRNA splicing factor FBP21 (formin-binding protein 21). *Journal of Biological Chemistry* **284**, 25375-25387 (2009).
- 92 Colombo, A. *et al.* Daam1a mediates asymmetric habenular morphogenesis by regulating dendritic and axonal outgrowth. *Development* **140**, 3997-4007 (2013). <https://doi.org/10.1242/dev.091934>
- 93 Nakaya, M. A. *et al.* Identification and comparative expression analyses of Daam genes in mouse and *Xenopus*. *Gene Expr Patterns* **5**, 97-105 (2004). <https://doi.org/10.1016/j.modgep.2004.06.001>
- 94 Kida, Y., Shiraishi, T. & Ogura, T. Identification of chick and mouse Daam1 and Daam2 genes and their expression patterns in the central nervous system. *Developmental brain research* **153**, 143-150 (2004).
- 95 Nakaya, M.-a. *et al.* Placental defects lead to embryonic lethality in mice lacking the Formin and PCP proteins Daam1 and Daam2. *PLoS One* **15**, e0232025 (2020).
- 96 de Alwis, N. *et al.* DAAM2 is elevated in the circulation and placenta in pregnancies complicated by fetal growth restriction and is regulated by hypoxia. *Scientific Reports* **11**, 5540 (2021).
- 97 Garcin, C. & Straube, A. Microtubules in cell migration. *Essays Biochem* **63**, 509-520 (2019). <https://doi.org/10.1042/ebc20190016>
- 98 Schmidt, J. M., Zhang, J., Lee, H.-S., Stromer, M. H. & Robson, R. M. Interaction of talin with actin: sensitive modulation of filament crosslinking activity. *Archives of Biochemistry and Biophysics* **366**, 139-150 (1999).
- 99 Pollard, T. D., Blanchoin, L. & Mullins, R. D. Molecular mechanisms controlling actin filament dynamics in nonmuscle cells. *Annu Rev Biophys Biomol Struct* **29**, 545-576 (2000). <https://doi.org/10.1146/annurev.biophys.29.1.545>
- 100 Dominguez, R. & Holmes, K. C. Actin structure and function. *Annu Rev Biophys* **40**, 169-186 (2011). <https://doi.org/10.1146/annurev-biophys-042910-155359>
- 101 Sung, M. H. & McNally, J. G. Live cell imaging and systems biology. *Wiley Interdisciplinary Reviews: Systems Biology and Medicine* **3**, 167-182 (2011).
- 102 Dominguez, R. Structural insights into de novo actin polymerization. *Current opinion in structural biology* **20**, 217-225 (2010).

- 103 Dominguez, R. Actin filament nucleation and elongation factors--structure-function relationships. *Crit Rev Biochem Mol Biol* **44**, 351-366 (2009). <https://doi.org:10.3109/10409230903277340>
- 104 Kerkhoff, E. Cellular functions of the Spir actin-nucleation factors. *Trends Cell Biol* **16**, 477-483 (2006). <https://doi.org:10.1016/j.tcb.2006.07.005>
- 105 Caldwell, J. E., Heiss, S. G., Mermall, V. & Cooper, J. A. Effects of CapZ, an actin capping protein of muscle, on the polymerization of actin. *Biochemistry* **28**, 8506-8514 (1989). <https://doi.org:10.1021/bi00447a036>
- 106 Casella, J. F., Flanagan, M. D. & Lin, S. Cytochalasin D inhibits actin polymerization and induces depolymerization of actin filaments formed during platelet shape change. *Nature* **293**, 302-305 (1981). <https://doi.org:10.1038/293302a0>
- 107 Keller, R. Cell migration during gastrulation. *Curr Opin Cell Biol* **17**, 533-541 (2005). <https://doi.org:10.1016/j.ceb.2005.08.006>
- 108 Locascio, A. & Nieto, M. A. Cell movements during vertebrate development: integrated tissue behaviour versus individual cell migration. *Curr Opin Genet Dev* **11**, 464-469 (2001). [https://doi.org:10.1016/s0959-437x\(00\)00218-5](https://doi.org:10.1016/s0959-437x(00)00218-5)
- 109 Le Clainche, C. & Carlier, M. F. Regulation of actin assembly associated with protrusion and adhesion in cell migration. *Physiol Rev* **88**, 489-513 (2008). <https://doi.org:10.1152/physrev.00021.2007>
- 110 Svitkina, T. M. & Borisy, G. G. Arp2/3 complex and actin depolymerizing factor/cofilin in dendritic organization and treadmilling of actin filament array in lamellipodia. *J Cell Biol* **145**, 1009-1026 (1999). <https://doi.org:10.1083/jcb.145.5.1009>
- 111 Xue, F., Janzen, D. M. & Knecht, D. A. Contribution of Filopodia to Cell Migration: A Mechanical Link between Protrusion and Contraction. *Int J Cell Biol* **2010**, 507821 (2010). <https://doi.org:10.1155/2010/507821>
- 112 Mejillano, M. R. *et al.* Lamellipodial versus filopodial mode of the actin nanomachinery: pivotal role of the filament barbed end. *Cell* **118**, 363-373 (2004). <https://doi.org:10.1016/j.cell.2004.07.019>
- 113 Witke, W., Sutherland, J. D., Sharpe, A., Arai, M. & Kwiatkowski, D. J. Profilin I is essential for cell survival and cell division in early mouse development. *Proceedings of the National Academy of Sciences* **98**, 3832-3836 (2001).

- 114 Braun, A. *et al.* Genomic organization of profilin-III and evidence for a transcript expressed exclusively in testis. *Gene* **283**, 219-225 (2002).
- 115 Krishnan, K., Moens, P. & Watson, K. Functional Dynamics of Human Profilin I and II: Interaction with Phosphatidylinositol (4, 5) Bisphosphate and Poly-L-Proline. (2009).
- 116 Fedorov, A. A. *et al.* X-ray structures of isoforms of the actin-binding protein profilin that differ in their affinity for phosphatidylinositol phosphates. *Proceedings of the National Academy of Sciences* **91**, 8636-8640 (1994).
- 117 Nodelman, I. M., Bowman, G. D., Lindberg, U. & Schutt, C. E. X-ray structure determination of human profilin II: A comparative structural analysis of human profilins. *Journal of molecular biology* **294**, 1271-1285 (1999).
- 118 Pandey, D. K. & Chaudhary, B. Evolutionary expansion and structural functionalism of the ancient family of profilin proteins. *Gene* **626**, 70-86 (2017).
- 119 Coumans, J. V., Davey, R. J. & Moens, P. D. Cofilin and profilin: partners in cancer aggressiveness. *Biophysical reviews* **10**, 1323-1335 (2018).
- 120 Lorente, G., Syriani, E. & Morales, M. Actin filaments at the leading edge of cancer cells are characterized by a high mobile fraction and turnover regulation by profilin I. *PLoS One* **9**, e85817 (2014).
- 121 Goldschmidt-Clermont, P. J., Machesky, L. M., Doberstein, S. K. & Pollard, T. D. Mechanism of the interaction of human platelet profilin with actin. *The Journal of cell biology* **113**, 1081-1089 (1991).
- 122 Witke, W. The role of profilin complexes in cell motility and other cellular processes. *Trends in cell biology* **14**, 461-469 (2004).
- 123 Verheyen, E. M. & Cooley, L. Profilin mutations disrupt multiple actin-dependent processes during *Drosophila* development. *Development* **120**, 717-728 (1994).
- 124 Sato, A. *et al.* Profilin is an effector for Daam1 in non-canonical Wnt signaling and is required for vertebrate gastrulation. (2006).
- 125 Ahern-Djamali, S. M. *et al.* Mutations in *Drosophila* Enabled and rescue by human vasodilator-stimulated phosphoprotein (VASP) indicate important functional roles for Ena/VASP homology domain 1 (EVH1) and EVH2 domains. *Molecular biology of the cell* **9**, 2157-2171 (1998).
- 126 Gertler, F. B., Niebuhr, K., Reinhard, M., Wehland, J. & Soriano, P. Mena, a relative of VASP and *Drosophila* Enabled, is implicated in the control of microfilament dynamics. *Cell* **87**, 227-239 (1996).

- 127 Haffner, C. *et al.* Molecular cloning, structural analysis and functional expression of the proline-rich focal adhesion and microfilament-associated protein VASP. *The EMBO journal* **14**, 19-27 (1995).
- 128 Lambrechts, A. *et al.* Profilin II is alternatively spliced, resulting in profilin isoforms that are differentially expressed and have distinct biochemical properties. *Molecular and cellular biology* **20**, 8209-8219 (2000).
- 129 Brindle, N. P., Holt, M. R., Davies, J. E., Price, C. J. & Critchley, D. R. The focal-adhesion vasodilator-stimulated phosphoprotein (VASP) binds to the proline-rich domain in vinculin. *Biochemical Journal* **318**, 753-757 (1996).
- 130 Krishnan, K. & Moens, P. D. Structure and functions of profilins. *Biophysical reviews* **1**, 71-81 (2009).
- 131 Shao, J., Welch, W. J., DiProspero, N. A. & Diamond, M. I. Phosphorylation of profilin by ROCK1 regulates polyglutamine aggregation. *Molecular and cellular biology* **28**, 5196-5208 (2008).
- 132 Fan, Y. *et al.* Stimulus-dependent phosphorylation of profilin-1 in angiogenesis. *Nature cell biology* **14**, 1046-1056 (2012).
- 133 Fan, Y. *et al.* Profilin-1 phosphorylation directs angiocrine expression and glioblastoma progression through HIF-1 $\alpha$  accumulation. *Nature cell biology* **16**, 445-456 (2014).
- 134 Shao, J. & Diamond, M. I. Protein phosphatase 1 dephosphorylates profilin-1 at Ser-137. *PLoS One* **7**, e32802 (2012).
- 135 Rizwani, W. *et al.* S137 phosphorylation of profilin 1 is an important signaling event in breast cancer progression. *PloS one* **9**, e103868 (2014).
- 136 Mouneimne, G. *et al.* Differential remodeling of actin cytoskeleton architecture by profilin isoforms leads to distinct effects on cell migration and invasion. *Cancer cell* **22**, 615-630 (2012).
- 137 Allen, A. *et al.* Actin-binding protein profilin1 promotes aggressiveness of clear-cell renal cell carcinoma cells. *Journal of Biological Chemistry* **295**, 15636-15649 (2020).
- 138 Hassan, A. A., Vitorino, M. V., Robalo, T., Rodrigues, M. S. & Sá-Correia, I. Variation of Burkholderia cenocepacia cell wall morphology and mechanical properties during cystic fibrosis lung infection, assessed by atomic force microscopy. *Scientific Reports* **9**, 16118 (2019). <https://doi.org:10.1038/s41598-019-52604-9>

- 139 Ewen-Campen, B., Comyn, T., Vogt, E. & Perrimon, N. No Evidence that Wnt Ligands Are Required for Planar Cell Polarity in *Drosophila*. *Cell Reports* **32**, 108121 (2020). <https://doi.org/10.1016/j.celrep.2020.108121>
- 140 Kooij, V. *et al.* Profilin modulates sarcomeric organization and mediates cardiomyocyte hypertrophy. *Cardiovasc Res* **110**, 238-248 (2016). <https://doi.org/10.1093/cvr/cvw050>
- 141 Khadka, D. K., Liu, W. & Habas, R. Non-redundant roles for Profilin2 and Profilin1 during vertebrate gastrulation. *Dev Biol* **332**, 396-406 (2009). <https://doi.org/10.1016/j.ydbio.2009.06.008>
- 142 Sheldahl, L. C. *et al.* Dishevelled activates Ca<sup>2+</sup> flux, PKC, and CamKII in vertebrate embryos. *The Journal of cell biology* **161**, 769-777 (2003).
- 143 Popgeorgiev, N. *et al.* The apoptotic regulator Nr2f1 controls cytoskeletal dynamics via the regulation of Ca<sup>2+</sup> trafficking in the zebrafish blastula. *Developmental cell* **20**, 663-676 (2011).
- 144 Pernier, J., Shekhar, S., Jegou, A., Guichard, B. & Carlier, M. F. Profilin Interaction with Actin Filament Barbed End Controls Dynamic Instability, Capping, Branching, and Motility. *Dev Cell* **36**, 201-214 (2016). <https://doi.org/10.1016/j.devcel.2015.12.024>
- 148 von Dassow, M. and L. A. Davidson (2011). "Physics and the canalization of morphogenesis: a grand challenge in organismal biology." *Phys Biol* **8**(4): 045002.
- 149 Martin, A. C. and B. Goldstein (2014). "Apical constriction: themes and variations on a cellular mechanism driving morphogenesis." *Development* **141**(10): 1987-1998.
- 150 Tcherkezian, J. and N. Lamarche-Vane (2007). "Current knowledge of the large RhoGAP family of proteins." *Biology of the Cell* **99**(2): 67-86.
- 151 Chesarone, M. A., *et al.* (2010). "Unleashing formins to remodel the actin and microtubule cytoskeletons." *Nature reviews Molecular cell biology* **11**(1): 62-74.
- 152 Kühn, S. and M. Geyer (2014). "Formins as effector proteins of Rho GTPases." *Small GTPases* **5**(3): e983876.
- 153 Meinke, P., *et al.* (2015). "Nucleoskeleton dynamics and functions in health and disease." *Cell Health and Cytoskeleton* **7**: 55-69.